

University of Windsor

Scholarship at UWindor

Electronic Theses and Dissertations

Theses, Dissertations, and Major Papers

1-1-2007

Engine defect detection using wavelet analysis.

Bhaskar Ray
University of Windsor

Follow this and additional works at: <https://scholar.uwindsor.ca/etd>

Recommended Citation

Ray, Bhaskar, "Engine defect detection using wavelet analysis." (2007). *Electronic Theses and Dissertations*. 6978.

<https://scholar.uwindsor.ca/etd/6978>

This online database contains the full-text of PhD dissertations and Masters' theses of University of Windsor students from 1954 forward. These documents are made available for personal study and research purposes only, in accordance with the Canadian Copyright Act and the Creative Commons license—CC BY-NC-ND (Attribution, Non-Commercial, No Derivative Works). Under this license, works must always be attributed to the copyright holder (original author), cannot be used for any commercial purposes, and may not be altered. Any other use would require the permission of the copyright holder. Students may inquire about withdrawing their dissertation and/or thesis from this database. For additional inquiries, please contact the repository administrator via email (scholarship@uwindsor.ca) or by telephone at 519-253-3000ext. 3208.

NOTE TO USERS

This reproduction is the best copy available.

UMI[®]

ENGINE DEFECT DETECTION USING WAVELET ANALYSIS

by

BHASKAR RAY

A Thesis
Submitted to the Faculty of Graduate Studies through
Electrical And Computer Engineering
in Partial Fulfillment of the Requirements for
the Degree of Master of Applied Science at the
University of Windsor

Windsor, Ontario, Canada

© BHASKAR RAY 2007



Library and
Archives Canada

Bibliothèque et
Archives Canada

Published Heritage
Branch

Direction du
Patrimoine de l'édition

395 Wellington Street
Ottawa ON K1A 0N4
Canada

395, rue Wellington
Ottawa ON K1A 0N4
Canada

Your file *Votre référence*
ISBN: 978-0-494-35003-4
Our file *Notre référence*
ISBN: 978-0-494-35003-4

NOTICE:

The author has granted a non-exclusive license allowing Library and Archives Canada to reproduce, publish, archive, preserve, conserve, communicate to the public by telecommunication or on the Internet, loan, distribute and sell theses worldwide, for commercial or non-commercial purposes, in microform, paper, electronic and/or any other formats.

The author retains copyright ownership and moral rights in this thesis. Neither the thesis nor substantial extracts from it may be printed or otherwise reproduced without the author's permission.

AVIS:

L'auteur a accordé une licence non exclusive permettant à la Bibliothèque et Archives Canada de reproduire, publier, archiver, sauvegarder, conserver, transmettre au public par télécommunication ou par l'Internet, prêter, distribuer et vendre des thèses partout dans le monde, à des fins commerciales ou autres, sur support microforme, papier, électronique et/ou autres formats.

L'auteur conserve la propriété du droit d'auteur et des droits moraux qui protègent cette thèse. Ni la thèse ni des extraits substantiels de celle-ci ne doivent être imprimés ou autrement reproduits sans son autorisation.

In compliance with the Canadian Privacy Act some supporting forms may have been removed from this thesis.

Conformément à la loi canadienne sur la protection de la vie privée, quelques formulaires secondaires ont été enlevés de cette thèse.

While these forms may be included in the document page count, their removal does not represent any loss of content from the thesis.

Bien que ces formulaires aient inclus dans la pagination, il n'y aura aucun contenu manquant.


Canada

ABSTRACT

This study is concerned with the development of a non-intrusive engine fault detection system that uses vibration signature analysis to detect and diagnose mechanical defects in internal combustion engines. Various existing engine fault detection methods are studied and a new method is developed that incorporates the use of Wavelet Packet Transform (WPT). Vibration signals are recorded using accelerometers mounted on the engine and measurements are then transformed to the crank angle domain and subsequently to wavelet domain from which the features are analyzed and compared to the vibration signatures of engines with known defects. The results from this study show that the proposed method can detect the cause of several commonly occurring mechanical defects in engines, such as defective valve lash adjusters, cam phasers, chain-tensioners and piston rod assembly related defects while also allowing for the precise identification of the faulty component(s) without the need to dismantle the engine.

DEDICATION

This work is dedicated to my parents, who have always provided me with the love and support to achieve everything possible and to Terry, who stood by me throughout my University experience and offered unrelenting support and encouragement and will always be the inspiration to all that I do in life.

ACKNOWLEDGEMENT

The author would like to express his sincere thanks to his supervisors Dr. Jimi Tjong and Dr. M. Ahmadi. Their encouragement and innovative ideas enabled me to successfully complete this thesis. The author would also wish to express his sincere appreciation to the committee members, Dr. B. Shahrrava and Dr. D. Ting for their insight and recommendations.

Special thanks go to the many members of the Ford Powertrain Engineering Research and Development group for their time, assistance and support through the course of this study. In particular, the author would like to thank Mohammed Fawzy Aly, for all the valuable advice, assistance and insights that he provided during the study. Author would also like to thank Tony Fountaine, Ted Murawski, Richard Koresky, Russell Ellwood, and Greg Maxwell for their cooperation, knowledgeable insight and technical assistance in conducting all engine testing required for completing this study.

TABLE OF CONTENTS	
ABSTRACT	iii
DEDICATION	iv
ACKNOWLEDGEMENTS	v
LIST OF TABLES	x
LIST OF FIGURES	xi
ABBREVIATIONS	xvi
CHAPTER 1: INTRODUCTION	1
1.1 Background	1
1.2 Motivation	1
1.3 Defect Detection Using NVH Indicators	5
1.3.1 Noise and Acoustic Signal	6
1.3.2 Pressure Signals	7
1.3.3 Vibration Signals	8
1.4 Research Objective	11
1.5 Thesis Outline	13
CHAPTER 2: DEFECT DIAGNOSTIC METHODS	15
2.1 Data Acquisition	15
2.2 Data Reductions and Processing	16
2.3 Algorithm for diagnosis of engine defects	16
2.3.1 Time Domain Analysis	16
2.3.1.1 Crank Angle Domain	17
2.3.1.2 Time domain averaging	19
2.3.1.3 Root Mean Square (RMS)	20
2.3.1.4 Crest Factor	21
2.3.1.5 Kurtosis	21
2.3.1.5 Variance	22

3.3.3.4 Sampling	62
3.3.4: Bruel & Kjaer Model 5974 Charge Amplifier	64
3.4 Transducer Positioning	64
3.5 Summary	67
Chapter 4: DATA ANALYSIS AND RESULTS	68
4.1 Data Processing	68
4.1.1 Transforming to Crank Angle Domain	68
4.1.1.1 Finding the Engine Speed	71
4.1.2 Resampling	72
4.1.3 Wavelet Packet Decomposition	73
4.1.3.1 Mother Wavelet	74
4.1.3.2 Level of Decomposition	77
4.1.4 Wavelet Packet Energy	78
4.2 Defect Classification	78
4.3: Engine Defects under Investigation	79
4.4 Good and Defective Engine	81
4.5 Engine Defect Vibration Signature Types	83
4.6 Engine Fault Detection System	86
4.6.1 Engine Fault Detection System Pseudo Code	89
4.7 Graphical User Interface	91
4.8: Case Studies	95
4.8.1 Case Study: Defective Right Cam Phaser	95
4.8.2 Case Study: Defective Right Chain Tensioner	99
4.8.3 Case Study: Defective Cylinder #1 Intake Lash Adjuster	103
4.8.4 Case Study: Defective Cylinder #4 Exhaust Lash Adjuster	107
4.8.5 Case Study: Cylinder #4 Bore Non-Cleanup	111
4.9 Comparison of Wavelet Analysis with Variance and STFT	114
4.10 Summary	119

Chapter 5: CONCLUSIONS AND RECOMMENDATIONS	123
5.1 Conclusions	123
5.2 Recommendations and Future Work	125
REFERENCES	126
APPENDICES	132
A: 5.4L 3V ENGINE SPECIFICATIONS	132
B: CELL#7 DYNAMOMETER SPECIFICATIONS	133
C: CHARGE-TYPE ACCELEROMETER SPECIFICATIONS	134
D: ICP-TYPE ACCLEROMETER SPECIFICATIONS	135
E: ACCELEROMETER CALIBRATOR SPECIFICATIONS	136
F: PROSIG ACQUISITION SYSTEM SPECIFICATIONS	137
G: 8-CHANNEL CHARGE AMPLIFIER SPECIFICATIONS	138
VITA AUCTARIS	139

LIST OF TABLES

Table 3.1 Accelerometer channel naming convention	67
Table 4.1 Engine RPM calculation	71
Table 4.2: Engine defects under investigation	79
Table 4.3: Defect Description and the associated fault number	80
Table 4.4: Fault Database Table	88
Table 4.5: Maximum variance for each accelerometer channels	95
Table 4.6: Fault parameters for defective right bank cam phaser	98
Table 4.7: Maximum variance for each accelerometer channels	99
Table 4.8: Fault parameters for defective right bank chain tensioner	102
Table 4.9: Maximum variance for each accelerometer channels	103
Table 4.10: Fault parameters for defective cylinder #1 intake lash adjuster	106
Table 4.11: Maximum variance for each accelerometer channels	107
Table 4.12: Fault parameters for defective cylinder #4 intake lash adjuster	110
Table 4.13: Piston position during engine cycle	113
Table 4.14: Fault database for cylinder non-cleanup defects	113
Table 4.15: Fault parameters for defective cylinder #1 intake and exhaust lash adjuster	115
Table 4.16: Fault parameters for defective right bank cam phaser	117
Table 4.17: Engine Fault Detection Summary	120
Table 4.18: Modified Engine Fault Detection Summary	121
Table 4.19: Summary of test engines and cumulative success rates	122
Table A.1: 5.4L 3V Engine Specifications	132
Table B.1: Cell#7 Dynamometer Specifications	133
Table C.1: Charge-type Accelerometer Specifications	134
Table D.1: ICP-type Accelerometer Specifications	135
Table E.1: Accelerometer Calibrator Specifications	136
Table F.1: PROSIG System Specifications	137
Table G.1: 8-Channel Charge Amplifier Specifications	138

LIST OF FIGURES

Figure 2.1:	Time domain average of vibration data. Period was taken to be the time taken by the crankshaft to rotate 720 degrees (1 engine cycle)	20
Figure 2.2:	Waterfall running variance plot for 30 engine cycles. Graph shows there is a vibration spike at 360 degrees crank angle consistently during all engine cycle.	24
Figure 2.3:	Average variance of the 30 cycles in the crank angle domain. Graph shows there is significant vibration spike at 360 degrees crank angle.	24
Figure 2.4:	Frequency response of vibration signal for a good engine and engine with a defective phaser.	29
Figure 2.5:	Order Analysis	31
Figure 2.6:	Comparison of Time, Frequency, STFT and Wavelet domain analysis.	39
Figure 2.7:	Two-channel filter bank	43
Figure 2.8:	DWT Mechanism - Filtering and Sub sampling of signal	44
Figure 2.9:	DWT decomposition tree	45
Figure 2.10:	Discrete Wavelet Transform Tree	46
Figure 2.11:	Wavelet Packet Transform Tree	46
Figure 3.1:	Illustration of test setup. A 5.4L 3V Engine and transmission are coupled with a dynamometer.	56
Figure 3.2:	Accelerometers used for the study. PCB Model 353B15 Accelerometer (left) and Bruel & Kjaer Type 4366 Accelerometer (right)	59
Figure 3.3:	Bruel & Kjaer Type 4294 Calibrator	60
Figure 3.4:	The Prosig 5600 System front view.	61
Figure 3.5:	The Prosig 5600 System rear view.	61

Figure 3.6:	Red circles show the location of accelerometers on the right side of engine (2 on the cylinder head lugs and 2 on the engine lugs)	66
Figure 3.7:	Red circles show the location of accelerometer on the left side of engine (2 on the cylinder head lugs and 2 on the engine lugs)	66
Figure 3.8:	Red circles show the location of accelerometers on the front cover (1 on each bank)	66
Figure 4.1:	CID signal (top plot) and Right Front Cover Accelerometer (bottom)	69
Figure 4.2:	CID Signal	69
Figure 4.3:	CID Signal is used as a reference for the crankshaft position	70
Figure 4.4:	Using the CID signal to find the 0 degree TDC of Cylinder #1 and transforming the time domain data into angle domain.	70
Figure 4.5:	Engine RPM tracking	72
Figure 4.6:	Data resampling each engine cycle to 7200 points	73
Figure 4.7:	Wavelet Packet Decomposition tree representation	73
Figure 4.8:	Members of the Daubechies' wavelet family (Db2 thru Db10)	75
Figure 4.9:	Impulse Response of the Db15 lowpass filter	77
Figure 4.10:	Impulse Response of the Db15 highpass filter	77
Figure 4.11:	Magnitude Response of Db1, Db5, Db10 and Db15 lowpass filters	77
Figure 4.12:	Impulse Response of the Db15 highpass filter	77
Figure 4.13:	Vibration level of good engine	81
Figure 4.14:	WPD Coefficients of vibration signal from a good engine	82
Figure 4.15:	WPD packet energy of vibration signal from a good engine	83
Figure 4.16:	Single vibration spike per engine cycle.	84
Figure 4.17:	Comparison of vibration signal from a good engine (red) and defective engine (blue) with multiple vibration spikes	85
Figure 4.18:	Waterfall Variance plot for 30 engine cycles	86
Figure 4.19:	Waterfall Variance plot for 30 engine cycles	86

Figure 4.20:	Engine Fault Detection Software Welcome Screen	91
Figure 4.21:	Options under File Menu	92
Figure 4.22:	Threshold Menu	92
Figure 4.23:	Selecting Engine Block Lug Accelerometers	93
Figure 4.24:	Selecting Cylinder Head Lug Accelerometers	93
Figure 4.25:	Selecting the Front Cover Accelerometers	93
Figure 4.26:	Running Fault Diagnostic Module	94
Figure 4.27:	Running diagnostics is finished	94
Figure 4.28:	Display results and warnings	94
Figure 4.29:	Displaying message indicating that the vibration signature recorded by the accelerometer does not match the signature of any known defect and vibration level is below threshold level hence it is a good engine.	94
Figure 4.30:	Displaying message indicating a fault is detected to be present for the particular accelerometer and it matches the signature of a known fault. The message shows the fault number along with the fault description	94
Figure 4.31:	Displaying message indicating that the energy content of the vibration signal recorded by the accelerometer is within limits of the threshold and there is no vibrations spikes are present that is over the threshold for any crank angle.	94
Figure 4.32:	Message displayed when a vibration spike is detected at crank angle(s) or wavelet packet(s) that is not in the fault database.	94
Figure 4.33:	Vibrations recorded by FCR accelerometer	96
Figure 4.34:	Running variance waterfall of FCR recorded vibrations for 40 engine cycles	96
Figure 4.35:	Wavelet packet coefficients	97
Figure 4.36:	Wavelet packet energy	98
Figure 4.37:	Vibrations recorded by FCR accelerometer	100
Figure 4.38:	Running variance waterfall of FCR recorded vibrations for 40 engine cycles	100

Figure 4.39:	Vibration amplitudes for 1 engine cycle	101
Figure 4.40:	Wavelet packet coefficients	101
Figure 4.41:	Wavelet packet energy	102
Figure 4.42:	Vibrations recorded by HeadRF accelerometer	104
Figure 4.43:	Running variance waterfall of HeadRF recorded vibrations for 40 engine cycles	104
Figure 4.44:	Vibration amplitudes for 1 engine cycle	105
Figure 4.45:	Wavelet packet coefficients	105
Figure 4.46:	Wavelet packet energy	106
Figure 4.47:	Vibrations recorded by HeadRR accelerometer	108
Figure 4.48:	Running variance waterfall of HeadRF recorded vibrations for 40 engine cycles	108
Figure 4.49:	Wavelet packet coefficients	109
Figure 4.50:	Wavelet packet energy	110
Figure 4.51:	40-Engine cycle waterfall plot for LugRR accelerometer	111
Figure 4.52:	Average variance in crank angle domain	112
Figure 4.53:	Defective Cylinder 1 intake Lash Adjuster. HeadRF Accelerometer position recorded a spike at 355 degrees CA.	116
Figure 4.54:	Defective Cylinder 1 exhaust Lash Adjuster. HeadRF Accelerometer position recorded a spike at 365 degrees CA.	116
Figure 4.55:	Defective Cylinder 1 intake Lash Adjuster. HeadRF Accelerometer position recorded a variance spike at 355 degrees CA.	116
Figure 4.56:	Defective Cylinder 1 exhaust Lash Adjuster. HeadRF Accelerometer position recorded a variance spike at 365 degrees CA.	116
Figure 4.57:	Wavelet Packet Energy at Level =4	116
Figure 4.58:	Wavelet Packet Energy at Level =4	118
Figure 4.59:	Severely defective right bank phaser. FCR accelerometer position recorded a spike at 525 degrees CA.	118
Figure 4.60:	Defective right bank phaser. FCR accelerometer position	

	recorded a spike at 525 degrees CA.	118
Figure 4.61:	Frequency response over 1 Engine Cycle (Severely defective and good phaser).	118
Figure 4.62:	Frequency response over 1 Engine Cycle (Defective phaser and good phaser)	118
Figure 4.63:	Wavelet Packet Energy at Level =4	118
Figure 4.64:	Wavelet Packet Energy at Level =4	118

ABBREVIATIONS

A	Amplitude, or cross-sectional
AC	Alternating Current
ADC	Analog-to-Digital Converter
BDC	Bottom-Dead-Centre
CID	Cylinder Indicator Signal
CWT	Continuous Wavelet Transform
DC	Direct Current
DWT	Discrete Wavelet Transform
f_s	sampling frequency
FCR	Front Cover Right-hand side
FCL	Front Cover Left-hand side
FT	Fourier Transform
FFT	Fast Fourier Transform
HeadRF	Engine Head Right Front Lug
HeadRR	Engine Head Right Rear Lug
HeadLF	Engine Head Left Front Lug
HeadLR	Engine Head Left Rear Lug
i	data index
ICE	Internal Combustions Engine
ICP	Integrated Circuit Piezoelectric
LugRR	Engine Block Right Front Lug
LugRR	Engine Block Right Rear Lug
LugLF	Engine Block Left Front Lug
LugLR	Engine Block Left Rear Lug
n	total number of samples or cycles
NVH	Noise, Vibration and Harshness
PERDC	Powertrain Engineering Research & Development Centre
RMS	Root-mean-square
RPM	Revolutions Per Minute
RV	Running Variance

S	Signal
SAE	Society of Automotive Engineers
SOHC	Single Overhead Camshaft
SNR	Signal-to-noise Ratio
STFT	Short-time Fourier Transform
T	period of measurement
TDC	Top-Dead-Centre
V_i	average variance
WPD	Wavelet Packet Decomposition
WPT	Wavelet Packet Transform
*	Complex Conjugate
\otimes	Convolution

CHAPTER 1

INTRODUCTION

1.1 Background

This study is concerned with the development of a vibration signature analysis method for the early detection and diagnosis of mechanical faults in Internal Combustion Engines (ICE). Advanced engine maintenance programs incorporate various methods for monitoring the health of engine components, helping us to check if the engine is running under its normal operating conditions. They also enable us to foresee any malfunctions or abnormal operations and diagnose if any defect is present [Ben-Ari et al, 1998]. In this document, we will first discuss briefly, existing diagnosis methods that have been researched and explored in depth by various researchers for detecting different types of defects in internal combustion engines using the engine's noise, vibration and harshness (NVH) characteristics as the primary source of parameters. We will then explore and discuss the possibility of using a different approach with the goal of detecting new faults in a more accurate and efficient way.

1.2 Motivation

The main goals of every manufacturer are to achieve high productivity at minimal cost, high customer satisfaction, innovative concepts and products, and an having efficient manufacturing and assembly process [Tjong, 1992]. In a production environment, having an in-process testing system that is capable of detecting and diagnosing manufacturing and assembly defects is much more efficient than testing products upon completion of

their assembly. Such systems play a vital role for the company as it greatly increases productivity, customer satisfaction and help reduce scrap cost.

As such, in any modern engine-manufacturing environment, such online engines monitoring diagnostic system are present on the assembly line. These test stations are generally known as “cold test” and “hot test” stands. Engines are tested several times at different stages of its assembly process at these test stations, which are usually capable of detecting and diagnosing many manufacturing related engine defects. These in-process test stations subject the engine to a number of rigorous tests and check for missing components, certain machining related defects or other assembly defects. They also provide monitoring of important parameters such as torque, oil/coolant cavity leaks, cylinder pressure, crankshaft balance, fuel rail pressure, integrity of the engine harness and all electronics sensors and the proper functionality of the electronic control unit. If at any stage of the manufacturing process, an engine is diagnosed to have a fault, then it is routed to a repair bay on the assembly line where it receives careful inspection and is repaired if possible or is otherwise scrapped. These test stations can detect defects early in the process, thereby reducing downtime and repair costs that would be incurred if the engine were to be disassembled after complete assembly. It is desirable that all defects in the engine are detected during these in-process tests. However, as good as these tests stands may be, they are not able to detect 100% of the defects due to the fact that the internal combustion engine is a highly complicated machine with hundreds of moving components. Furthermore, some engine defects are detectable only after being completely assembled and are subjected to certain operating conditions, such as running at a specific

engine speed (revolutions per minute or rpm) or at specific operating engine load or oil temperature. In addition to these different operating conditions, the defect may only show up intermittently and may not be present at all times. Since it is not feasible to subject the engines to all test operating conditions in a manufacturing environment, sometimes, defective engines do get shipped out with its defect undetected.

These defective engines can then only be detected after the entire vehicle has been fully assembled and is test-driven at the Body and Assembly (B&A) plants, at the dealership, or following a customer complaint due to excessive noise or vibration from the engine after the vehicle has been sold. In many of these cases, if such “noisy” engines are identified, they are usually exchanged with a new one as per warranty and the total cost of the engine replacement and repair easily exceeds the cost of a new engine by a few times. Considering that a typical engine manufacturer is capable of producing roughly 500,000 engines a year, even if a small percentage of the total number of engines produced contains some undetected defects, it can potentially cause the manufacturer to incur high cost due to replacing these engines after the vehicles are fully assembled. Most of these engines that are replaced due to abnormal noise or vibration have some mechanical defects. These defects are mainly due to the presence of faulty components that can be easily replaced, and the engine repaired, if the cause is identified correctly. Repairing these engines usually involves partial disassembly that can be performed in vehicle at the dealership or at the B&A plants, thereby drastically reducing the cost of the full engine replacements.

There are several conventional ways to diagnose these engines at the B&A plants or at the dealerships. The most common is by auditory assessment. In general, if a noise is concentrated in a narrow bandwidth, or has a very rapid rise time or is intermittent or irregular, it is deemed “noisier” than if it remains steady. An experienced inspector or mechanic usually performs these assessments by listening to the sound level and frequency variations of the abnormal engine noise to identify the mechanical defects inside engine. Words like “tick”, “knock”, “rattle”, “whine”, “chatter”, “whistle”, “hiss”, “clunk” are often used to describe these defects. Another method that is used in conjunction with the auditory assessment is to isolate the noise to a particular cylinder by disconnecting the fuel injectors or spark plugs to stop the combustion process in each cylinder. Though these methods are often simple and fast, the judgment is subjective to the listener and is prone to errors. Furthermore, these methods are inconsistent due to the effect of ambient condition or the physiological state of the inspector himself. This is especially true when the abnormal noise is on the borderline of acceptability.

Product and design engineers use a more scientific approach to diagnose these defects by using various NVH indicators for detection. But these methods are mostly used as experiments in a laboratory setting and not at B&A plants or dealerships. There are many applications in industry such as monitoring of rotating machines that have repetitive signals, which are generally periodic, where NVH characteristics are used for fault detection. However, it is difficult to use many of these standard techniques to analyze measurements from internal combustion engines because its signals contain both periodic components as well as random component that are generated by friction and mechanical

impact inside the engine. The various vibration analysis methods that are used for such defect detection are, for example, time domain averaging, order analysis, spectral analysis etc. The details and merits of these methods are discussed in Chapter 2. While some of these methods are effective in detecting certain defects, they are not in cases of others, especially the ones of interest to us in this study. As a result, more effective techniques are required to better analyze NVH measurements and detect engine faults more reliably. Hence there is a need to develop and implement a practical, standardized, cost effective and non-intrusive diagnostic system that can perform diagnosis, detect and identify any defects in these engines that have been installed in a vehicle without complete dismantling of the engine being necessary. Such a system should not only detect faulty engines but should also have the capability to diagnose which specific component(s) are defective so they can be replaced and the engine repaired. It will reduce the amount of time and effort required to manually detect the defect and will also help maintain a constant quality standard which will ultimately lead to better quality, increased customer satisfaction, greater sales, a better reputation and ultimately leading to greater profit for the company.

1.3 Defect Detection Using NVH Indicators

The noise and vibration generated by a faulty engine is complex in nature. The analysis must decompose the data in such a way that the fault recognition process can be concentrated on those attributes of the signal that is most representative of the faults to be diagnosed, avoiding inclusion of contaminated, redundant and insignificant components

of the signals. The NVH indicators that are used to detect engine defects that result from abnormal mechanical impacts or from the combustion process are

- i) Noise signals or sound pressure levels
- ii) Pressure signals
- iii) Vibration signals

1.3.1 Noise and Acoustic Signal

Sound measurement is one of the oldest techniques to detect machine defects. Almost thirty years ago, Chung et al [1979] of General Motors Research Laboratories developed a cross-spectral method of measuring sound intensity to perform a detailed mapping of engine noise, noise source ranking and also calculate total engine sound power with reasonable accuracy. Noise or acoustic signals are measured using microphones or sound intensity measurement, as done by several researchers such as Tjong [Tjong, 1992], Jonuscheit [Jonuscheit, 2000] and Leitzinger [Leitzinger, 2002]. Jonuscheit used sound intensity measurements to determine noise sources in engines by using two overhead microphones to measure sound pressure in a production environment [Jonuscheit, 2000]. Leitzinger performed a survey using different indicators and transducers such as microphones, accelerometers and vibrometers to detect engine defects. Leitzinger reported that microphones produce inconsistent results and were unable to detect defects he investigated. He also concluded that the most reliable transducers were accelerometer and laser doppler vibrometers [Leitzinger, 2002]. The advantage of using microphone to measure sound pressure is that it is quite easy to take and that it provides non-contact measurements. The main disadvantage of sound measurement is that it has to be acquired

in a suitable and controlled environment such as a semi-anechoic chamber or an enclosure that will attenuate unwanted noise signals.

Biedl suggested quantifying the vibration of components through noise measurements such as SAE-J1074 test. SAE-J1074 is a test using microphones that measures the noise radiation pattern at one-meter distances surrounding the engine and is usually done in a semi-anechoic chamber. He states SAE-J1074 was optimal in developmental work when defining the amount of noise reduction required to meet target specifications. He concluded that only by point-to-point acceleration measurements is the only way to accurately describe a vibrating system [Beidl et al, 1999].

1.3.2 Pressure Signals

Pressure measurements for engines are generally taken in the vicinity of the combustion chambers to measure in-cylinder pressure variations as done by Chandroth [Chandroth et al, 1999 (2), (3)], and Rizzoni [Rizzoni et al, 1994]. It can also be used for measuring pressures in the intake, exhaust manifold or oil gallery as done by Bryant [Bryant et al, 1992]. Bryant of Ford Motor Company, who hold several US patents in the area of engine testing and diagnostics, developed a novel method where he monitored multiple indicators such as crankcase air pressure, intake and exhaust manifold pressures, oil pressure, torque to diagnose defects such as missing or broken components in engine. He later successfully implemented his fault detection system in the cold test stands at the Ford Cologne Engine Plant in Germany. In a separate study, Bruce Bryant developed another novel method where he monitored exhaust pressure to detect misfire of individual

cylinders in real time. For each engine cycle the pressure signal is sampled and digitized and fed as an input vector for a pattern classifier that then discriminates between firing and misfiring cylinders based on the predetermined internal coefficients of a trained classifier. Sharkey performed a study where an engine fault diagnosis system was developed using multiple sensors such as acoustic, vibration and in-cylinder pressure signal traces to detect leaking intake and exhaust valves and defective fuel injectors. The signal characteristics were then fed to a trained ANN (Artificial Neural Network), which discriminated each class of data [Sharkey et al, 2000]. In another study, Chandroth used vibration and in-cylinder pressure signals from a diesel engine to detect engine defects [Chandroth et al, 1999 (1), (2)].

1.3.3 Vibration Signal

Vibration analysis techniques are fairly common in industry. It is used frequently as a fault detection and diagnostic tool to detect malfunctioning rotating machines such as electric motors, turbines, compressors as shown by Tamaki, [Tamaki et al, 1994] and other researchers. Vibrations produced by rotating machines are usually repetitive signals that are more or less periodic in nature. Vibration analysis is also used as a part of preventive maintenance programs to detect defects such as bearing failure [Heng et al, 1998], excessive wear or structural damage and to predict failures. This is done by monitoring the changes in the levels of machine vibration. These vibration tests often enable us to identify the faults early in the maintenance process without having to dismantle the machine. Mitchell [Mitchell, 1981] and Eshleman [Eshleman, 1995] performed studies on correlation between abnormal operations and the pattern of the

vibration spectrum exhibited by the machine. They used it to identify various types of defects in rotating machines such as bearing wear, misalignment and tolerances related defects.

All machines vibrate because they are mechanical systems with moving components and comprise an elastic system that oscillates in response to excitations [Ben-Ari et al, 1998]. Every machine has their specific characteristic modes of vibrations that can be distinguished during normal operating conditions. Each of the modes is characterized by its spectrum and a distinguished pattern of relative amplitudes that is dependent on its mass, system stiffness, fitting tolerances, friction levels, and other parameters typical to the system [Ben-Ari et al, 1999]. When a machine malfunctions, it causes the excitation forces to vary and thus changes its system characteristics and hence the vibration signature of the system. This change can then be detected and distinguished from normal conditions by using appropriate vibration monitoring and analysis method. These vibration-monitoring techniques have been mostly applied to relatively simple rotating machines that consist of a relatively small number of moving parts and the movement of these components is relatively smoother. Several researchers such as Ben-Ari [Ben-Ari et al, 1998, 1999] and Modgil [Modgil et al, 2004] for example, noted that in many cases, there exist a direct one-to-one relationship between the cause of the defect and the frequency content and amplitude of the vibration signature.

In recent times, these vibration analysis applications have been also applied to complicated devices that incorporate large number of moving parts for e.g. reciprocating

machines, gearboxes [Miller, 1999], transmissions [Biqing et al, 2004] and [Tumer et al, 2002], and also in a small number of applications involving internal combustions engines as done by Tjong [Tjong, 1992, 1993], Bryant [Bryant et al, 1992], Chandroth [Chandroth et al, 1999 (1), (2)], Samimy [Samimy et al, 1996], Ghosh [Ghosh et al, 1991], Mingzan [Mingzan et al, 2003]. The reason for the low number of industrial applications can be attributed to the complex nature of the working principles of internal combustion engines coupled with the fact it contains large number of moving parts. Fault detection in Internal combustion engines often requires the understanding of the dynamic and chemical processes taking place inside an engine, which are difficult to model accurately noted Chandroth [Chandroth et al, 1999 (1)].

Combustion and inertial forces, in-cylinder pressure variations and mechanically induced structural resonance are the cause of vibrations in engines [Preide]. Tjong [Tjong, 1992] categorized the generation of noise and vibration by a faulty engine into three areas

- i) Impact between components due to incorrect clearance between valve train, gears, connecting rod, pistons and bearings etc. The impact usually results in an impulse generated vibration occurring at fixed crankshaft angle(s).
- ii) Imbalance in rotating components of the engine such as crankshaft, camshaft (s), balance shaft, gears. This results in vibration that is harmonic at low orders of the engine rotation.
- iii) Abnormal combustion due to incorrect ignition timing, incorrect valve opening etc.

Engine vibration signals are measured in the form of surface borne acceleration with accelerometers attached on the outside of the engine as shown by Tjong [Tjong, 1992], Leitzinger [Leitzinger, 2002], Daws, [Daws, 2002] or as velocity signals that is measured using vibrometers such as with laser doppler vibrometers as shown by Leitzinger [Leitzinger, 2002]. Biedl studied vibrations generated by an engine by using a scanning laser vibrometers. He concluded that the results gave a good overview of the entire vibration behavior of an engine side but he recommended using point-to-point surface measurements using accelerometers for accurate data. The reason being, laser performs a non-contact measurement and the accuracy of such measurement results mainly depends on surface reflectivity and measurement angles. Any variation of the angles and reflectivity and would yield a skewed vibratory response [Beidl et al, 1999]. Tjong [US Patent 5821412] found a novel method to diagnose mechanical anomalies in internal combustion engines using vibration amplitudes at various crank angle position and implemented it in the cold test and hot test stands in a manufacturing environment.

1.4 Research Objectives

Our main goal is to develop a system that can diagnose and identify defects in engines by performing non-intrusive tests, so we can repair it without having the need to remove the faulty powertrain from the vehicle. The defects under study result in abnormal mechanical impacts in engines due to faulty components.

Sound level measurements using microphones has to be acquired in a controlled environment such as inside a semi-anechoic chamber hence it is not feasible in our case

as we aim to detect engine defects in the field. Pressure measurements are already performed at various stages of the cold test in the manufacturing line and can help detect missing components but can not detect all malfunctioning components in the engine. In-cylinder pressure measurements can indicate if any combustion related problems are present but it is also impractical to carry out in the field, as it requires cylinder heads that are instrumented with pressure transducers. Also, a majority of the studies that have been performed in the area of engine defect detection investigates ways to detect combustion knock in an engine as done by Thomas [Thomas et al, 1996], Molinaro [Molinaro et al, 1992, Konig, [Konig, 1996] and Rizzoni [Rizzoni et al, 1993]. Combustion knock is caused by irregular combustion and generates pressure oscillations in the cylinder. The placement and designs of valves, spark plugs, fuel injection ports and additive contents in fuel are factors causing the existence of combustion knock. Detection of combustion knock is not the focus of this study. The main interest in this project is detection of faulty components present inside the engine using vibration characteristics of good and faulty engines and the way in which the results are processed in order to extract the relevant data and identify the fault. The engines we are interested in diagnosing are the ones that have mechanical faults and have already passed through cold test stands without the fault being caught.

Therefore, for this study, vibration is used the only indicator for detection of engine defects. Vibration signal is directly related mechanical operations within the engine and contain valuable information of the health of different engine valve train or combustion chamber components. This information could be used to identify various engine faults

and can help prevent catastrophic failures in future. For the proposed application, using vibrometers is highly impractical due to limitation in space in the engine compartment of the vehicle. Hence, we will use piezoelectric accelerometers to measure vibration. Also, these vibration transducers are relatively small and a large number of them can be used if necessary at different locations to capture localized vibration. The piezoelectric accelerometers are the most commonly used transducer for vibration measurements because of its relatively small size, low cost, robustness and usability over a wide frequency range.

In order to successfully meet the objective of this study there are a number of goals that have to be met and they are

- i. Select data acquisition equipments and appropriate transducers for engine vibration detection and also determine optimal measurement locations that exhibit good vibration characteristics.
- ii. Collect sufficient amount of data from both good engines and engines with different types of defects.
- iii. Develop a standardized test and fault diagnosis algorithm that can successfully detect faulty components.

1.5 Thesis Outline

The remainder of this thesis is structured as follows: *Chapter 2* discusses all state-of-the-art diagnostic methods for engine fault detection using NVH parameters, such as various

time, frequency and joint time-frequency domain techniques, and their theoretical background.

Chapter 3 discusses the experimental setup, all test conditions, key concepts for data acquisition, testing and data acquisition equipment used for this study and their specifications.

Chapter 4 discusses different steps of the defect detection method, data analysis and processing steps, implementation of the algorithm, brief overview and description of the graphical user interface (GUI) that has been developed and test results for detection of different engine faults and case studies.

Chapter 5 concludes the thesis and recommendations are provided for future work and development.

CHAPTER 2

DEFECT DIAGNOSTIC METHODS

This chapter describes the fault detection and diagnostic process and all state-of-the-art machine fault diagnostic techniques based on time, frequency, and joint time-frequency domain, using various NVH indicators that are currently used in the industry. The theory behind these methods is discussed along with their various advantages and disadvantages that each method poses. The chapter concludes with description of the proposed method that is used in this study to detect faulty engines as well as to identify the cause of the fault.

There are three main steps to the fault detection process of an internal combustion engine. They are data acquisition, data reduction and processing and finally algorithm for diagnosis of defects.

2.1 Data Acquisition

The first step in the defect detection process is data collection. It involves determining which types of and how many sensors should be used, the measurement locations, and type of hardware that should be used for data acquisition. Also, we need to identify sources of variability in the data acquisition process and with the system and these must be minimized as much as possible.

2.2 Data Reductions and Processing

This is done to selectively and systematically choosing the acceptable data and to eliminate from the measured vibration signals different kinds of noise such as mechanical noise due to vibration, electrical noise due to improper grounding of the data acquisition system or irregularities in the power supply, electromagnetic noise from ambient radiation and communication waves, electronic noise in the instrumentation etc. This process is usually based on knowledge gained by individuals directly involved with the data acquisition.

2.3 Algorithm for diagnosis of engine defects

A variety of data analysis techniques are available and used to detect and identifying engine defects through the use of NVH measurements. A brief review of many of these techniques is provided in the following section. Traditional techniques can be broadly divided in to three categories: time based and frequency based and joint time-frequency based. Time-Frequency analyses techniques are the most recommended methods as noted by Yen as they are suitable for analyzing non-stationary signals such as vibrations generated by mechanical impacts [Yen et al, 1999 (1), 2000].

2.3.1 Time Domain Analysis

Time domain analysis of vibration signals is one of the simplest and cheapest fault detection approaches. This analysis is performed usually by examining some statistical parameters related to the time domain vibration signal. Various time domain statistical parameters have been used as trend parameters to detect the presence of any defects. The

most used ones are Standard Deviation, RMS, Crest factor and Kurtosis. Usually greater values of these parameters indicate presence of a fault. By comparing these statistical parameters from vibration signal to the normal values calculated using vibrations from “good” machines, the presence of a defect and its severity can be detected. This approach has been widely used in detecting bearing damages. Heng [Heng et al, 1998] and Martin [Martin et al, 2004] reported in their studies that Kurtosis, Crest factor and skew values of the vibration signals can be used for detection of bearing faults at early stages in their development. Their results confirmed that these statistical methods could be used to identify different types of defects present in bearings.

However, analysis of engine noise and vibration in time domain is usually not performed, since raw time data is difficult to comprehend and provides little or no useful information. Therefore, in almost all cases, post processing of time domain data is performed in order to present the data in a form that will provide more detailed information regarding frequencies, amplitudes, crank angles etc.

2.3.1.1 Crank Angle Domain

Internal combustion engines operate in a cyclic manner hence the most common analysis that is performed is converting the time domain signal to crank angle domain. Daws reported that analysis of data in the crankshaft angle domain is very logical and useful because it allows one to correlate any observed signal abnormalities with specific points and events in the engine cycle [Daws, 2002]. Analysis in this domain requires that

crankshaft or camshaft position is also acquired simultaneously so vibration signals can be synchronized to engine cycle when analyzing the data.

Some typical processing methods that may be performed in time domain are time domain averaging or calculation of the statistical parameters such as RMS noise and vibration amplitudes [Bruel & Kjaer, 1982], Kurtosis, Crest Factor, Variance analysis etc. These parameters can give an indication of the noise or vibration level present based solely on one value. Once computed, it can be compared to see if it falls within an acceptable range and thus we can use it to discriminate between good or bad parts.

As such almost all researchers use the crank angle domain approach when analyzing displacement or vibration data of an engine and further post processing are usually performed on the crank angle domain data. Alvey used crank angle domain method with vibration measurements to detect defects in engines in a production line for cold start and hot start tests. He successfully identified certain defects through these on-line tests by comparing with a database of defect signatures in the angle domain [Alvey et al, 2005]. Tjong discussed and utilized this method as well and he incorporated variance analysis method in conjunction with crank angle domain data to identify various engine faults [Tjong et al, 1993]. Other authors such as Leitzinger also used acceleration versus crank angle to display the vibration generating events at particular moments in the engine cycle [Leitzinger, 2002]. Szczepanski extensively used the angle domain to display displacement, velocity and acceleration data and he was able to identify the valve-

opening, closing and seating acceleration at constant and sweeping speeds [Sczepanski, 2004].

2.3.1.2 Time domain averaging

Time domain averaging is a process in which the recorded vibration signal in ensemble averaged over the rotational period of interest. After a large number of averages are taken, the resulting signal becomes nearly periodic. If the raw vibration signal is represented as a continuous signal $s(t)$, then the linear averaging operation is given by Equation 2-1

$$\bar{s}(t) = \left(\frac{1}{N} \right) \sum_{m=0}^{N-1} s(t - mT) \quad (2-1)$$

where T is the rotational period and N is the number of averages.

This technique is effective in suppressing signals that are not periodic within the averaging period and it helps reducing noise in the signal. This method can be used for detection of faults that occur consistently at a certain instance of the engine cycle. Internal combustion engines operation on a cyclical basis, therefore, all of the events that occur can be matched to a position in the cycle. However, there are several drawbacks for this method. First, it is not effective in the detection of semi periodic process. Second, good noise reduction requires many averages and long signal lengths. Also, any variability in shaft speed will require a variable sampling rate. Therefore, these time domain methods possess only minimal diagnostic capabilities needed for identifying engine defects.

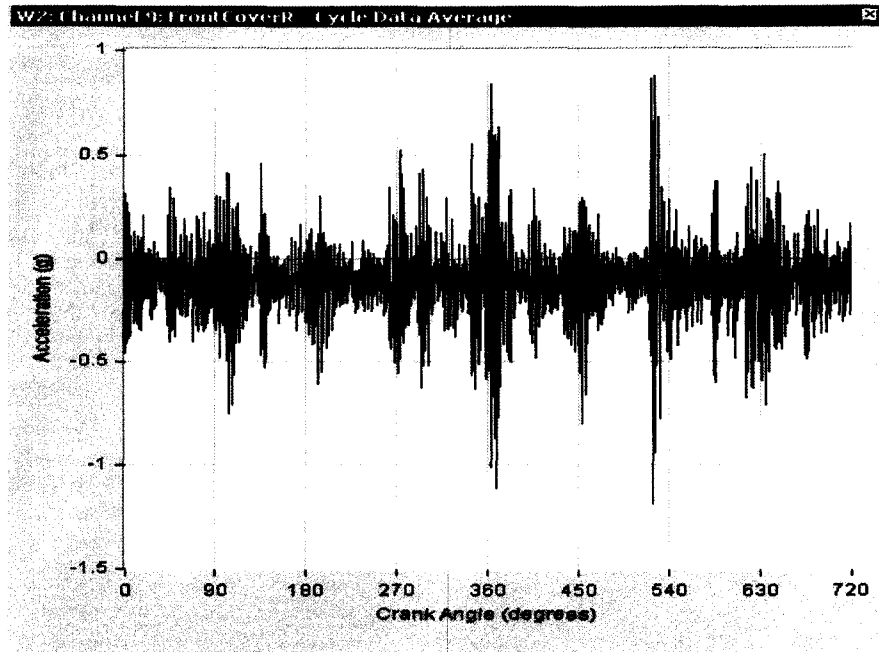


Figure 2.1: Time domain average of vibration data. Period was taken to be the time taken by the crankshaft to rotate 720 degrees (1 engine cycle).

2.3.1.3 Root Mean Square (RMS)

The simplest approach to measuring defects in the time domain is using the root-mean-square (RMS) approach, which provides a measure of the power content in the vibration signature. The RMS of a signal x , can be defined as

$$x_{rms} = \sqrt{\frac{1}{N} \sum_{n=1}^N x_n^2} \quad (2-2)$$

where x_{rms} = signal RMS value

$x_n = n^{\text{th}}$ data sample

N = Total number of data samples

Monitoring the RMS of the vibration in time domain is most widely practiced defect diagnostic method being used in the industry. It is simple to implement and the results are easy to interpret. It is mostly used in monitoring of simple machines and machine components. The RMS value is usually compared to a pre-determined threshold and if it

exceeds the threshold, it is an indication of presence of a defect. However, since it generates a single valued number, it can only indicate whether the machine or the component being monitored is good or bad and provides no information about signal characteristics that may indicate specific defects.

2.3.1.4 Crest Factor

The Crest Factor of a waveform is defined as the ratio of the peak amplitude of the input signal to its RMS level. Hence it is a dimensionless quantity.

$$CrestFactor = \frac{x_{peak}}{x_{rms}} \quad (2-3)$$

Modgil used crest factor as one of the statistical indicator for vibration diagnostics of engines and reported that the crest factor value should lie between 2 and 6. He found that a value greater than 6 indicates that the data exhibits significant non sinusoidal signal content [Modgil et al, 2004].

2.3.1.5 Kurtosis

Kurtosis is another statistical indicator that is widely when performing vibration analysis in time domain. Kurtosis is a measure of the "peakedness" in the data and emphasizes high amplitude deviation in the signal from the normal level. The definition of Kurtosis (K) is

$$K = \frac{\int_0^T [x(t) - \mu_x]^4 dt}{T\sigma^4} \quad (2-4)$$

where, x is the signal

μ_x = signal mean

T = duration of the signal

σ = signal standard deviation

A perfect random vibration has a kurtosis value of 3 whereas a vibration signal with kurtosis value of greater than 3 implies the signal has peaks. Higher kurtosis means more of the variance is due to infrequent extreme deviations, as opposed to frequent modestly sized deviations. Using kurtosis of the vibration signal data in time domain has been widely used for defect detection purposes. Martin showed that it could be used in bearing fault detection with great success [Martin, 1995]. Calculating the kurtosis value very useful in detecting faults when the impacts are only intermittent but it cannot provide diagnostic information about specific faults when the machine and its vibration signature is complex.

2.3.1.6 Variance

This is a statistical method that is commonly used in conjunction with the crank angle domain analysis when analyzing vibration signatures for internal combustion engines. Leitzinger [Leitzinger, 2002] and Tjong [Tjong, 1992, 1993] showed that the calculations for variance analysis can be represented by three mathematical steps as shown below:

1. Calculating the Ensemble Average which is the average of the amplitudes at each crankshaft angle and can be represented by Equation 2-5 as shown below:

$$\bar{x}_i = \frac{1}{N} \sum_{j=1}^N x_{j,i} \quad (2-5)$$

Where: \bar{x}_i = ensemble average

n = total number of cycles,

$x_{j,i}$ = the amplitude of the i^{th} cycle at j^{th} crank angle, as j goes from 0 to 720° .

2. Calculate Running Variance (RV) represented by Equation 2-6

$$\begin{aligned} RV_{j,i} &= (x_{j,i} - \bar{x}_i)^2 \\ RV_{j,i} &= (x_{j,i} - x_i)^2 \end{aligned} \quad (2-6)$$

Where: $RV_{j,i}$ = running variance of the i^{th} cycle at crank angle j .

3. Average Variance V_i can then be represented by Equation 2-7:

$$V_i = \frac{1}{n} \sum_{j=1}^n RV_{j,i} \quad (2-7)$$

Where: V_i = average variance.

Variance analysis is a useful tool for extracting semi-periodic components from a set of data. This type of analysis is useful in attenuating amplitudes of normal occurring data values to a low level in order to better observe and exaggerate the semi-periodic component of the signal. As well, since the variance process squares all data, all values are positive which makes developing the diagnostic algorithm easier.

This analysis is best used in the angle domain where the vibrating phenomenon is consistently repeated over every engine revolution and can be related to a particular crankshaft angle. The variance analysis has also been shown to be accurate in representing the phenomenon that repeats semi-periodically during engine cycles. These semi-periodic amplitudes may be attenuated over many averaged cycles; however, through variance analysis these amplitudes are effectively maintained. Figure 2.2 and Figure 2.3 shows the waterfall running variance plot and the average variance plot for a

defective engine respectively. There is a vibration spike of varying magnitude is occurring at a crank angle of around 360 degrees consistently for all engine cycles.

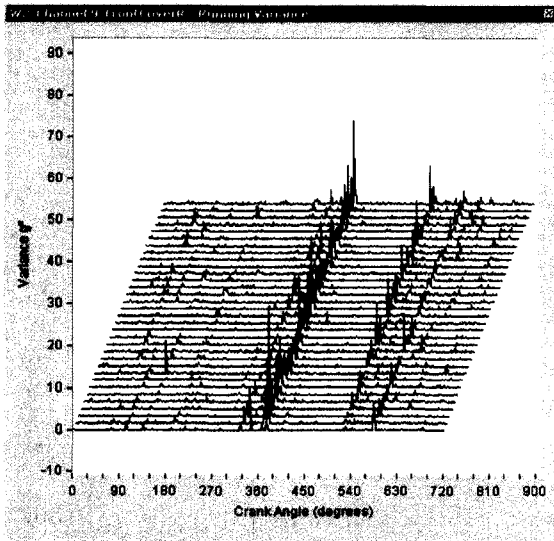


Figure 2.2: Waterfall running variance plot for 30 engine cycles. Graph shows there is a vibration spike at 360 degrees crank angle consistently during all engine cycle.

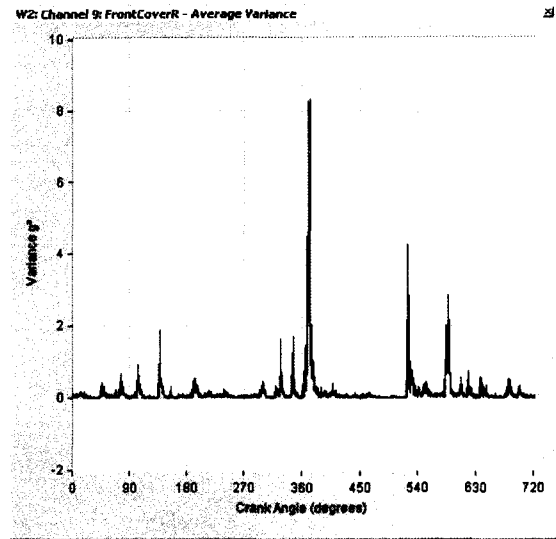


Figure 2.3: Average variance of the 30 cycles in the crank angle domain. Graph shows there is significant vibration spike at 360 degrees crank angle.

Tjong has used this method extensively and showed that engine defects can be detected using the variance analysis. Due to cyclic operation of an internal combustion engine, vibration spikes should occur at relatively constant crankshaft positions from cycle to cycle. Moreover, where they occur and how many times per cycle can determine to which cylinder the defect is related to and further possibly identifying the nature of the fault itself [Tjong, 1992]. Using this method we can find out at what crank angle (engine cycle location) the vibration impulse is occurring and then relate it to a particular event in its cycle. The main drawback for this, using this method we can only narrow down the possible causes of defects and not be definitive about the specific defect.

2.3.2 Frequency Domain Analysis

Frequency based methods are also popular techniques for analyzing the vibration signals. Most times machine defects are characterized by certain impulses that occur at particular frequencies or have components at known harmonics. Hence, an effective diagnosis method is to analyze the vibration signals in its frequency domain. Usually, a baseline level is first created that represent the normal operating conditions. Then any abnormal conditions in machines are then diagnosed by monitoring the trend and by comparing to the baseline data. We can calculate the dominant frequencies or orders associated with the machine fault and use it for defect identification. This method has been used successfully for most cases of machinery diagnostics.

There are several frequency domain analysis techniques that are widely used in the area of vibration analysis of rotational machines, such as the

- i. Discrete Fourier Transform (DFT) or more commonly the Fast Fourier Transform (FFT)
- ii. Order domain analysis
- iii. Cepstrum analysis

2.3.2.1 Fast Fourier Transform

Fast Fourier Transform (FFT) is possibly the most widely used signal analysis technique, used in the industry for data analysis. This approach is used based on the notion that the spectral content, rather than the vibration amplitude, is the key to determining the

machine condition. Therefore, instead of analyzing vibration directly in the time domain, the FFT of the vibration signal is analyzed.

Fourier transform decomposes a time based signal into a complex exponential functions of different frequencies and can be represented by Equation 2-8 in its continuous form.

$$X(f) = \int_{-\infty}^{\infty} x(t)e^{-2j\pi ft} dt \quad (2-8)$$

where t stands for time, f for frequency, $x(t)$ the signal in time domain and $X(f)$ the signal in frequency domain. The inverse of the transform is given by Equation 2-9.

$$x(t) = \int_{-\infty}^{\infty} X(f)e^{2j\pi ft} df \quad (2-9)$$

This analysis is based on the notion that any regular periodic function and certain non-periodic functions with finite integral can be expressed as a sum of trigonometric functions in an infinite time framework [Bogges and Narcowich, 2001]. In Equation 2-8, the original signal $x(t)$ is multiplied with an exponential term $e^{-2j\pi ft}$ or $\cos(2\pi ft) + j\sin(2\pi ft)$ i.e. a sine and cosine term of frequency f and then integrating over all times. The value of $X(f)$ depends on whether or not $x(t)$ has a dominant frequency component at frequency f . If $x(t)$ contains a dominant frequency f , then $X(f)$ will be large and if it does not contain frequency f , then $X(f)$ will be zero. Since the integration is from minus infinity to plus infinity, it does not matter where in time the component with frequency f appeared and hence it does not impact the result of the integration. Thus, as Politis notes, the Fourier transform gives a unique representation of the signal in the frequency domain and provides information about which frequencies appear in the signal but not about the time instants in which these frequencies are encountered [Politis 2003].

The most useful form of the transform when used with real, digitally sampled data is the Discrete Fourier Transform. It essentially replaces the integral transform with a finite version. Equations 2-10 and 2-11 can represent the forward and inverse transform respectively.

$$G(k) = \frac{1}{N} \sum_{n=0}^{N-1} g(n) e^{-j \frac{2\pi kn}{N}} \quad (2-10)$$

$$g(n) = \sum_{k=0}^{N-1} G(k) e^{j \frac{2\pi kn}{N}} \quad (2-11)$$

The calculation of DFT involves computation of a large number of complex multiplications in order to generate a useful frequency spectrum. This is a computationally exhaustive process and often not practical when performing real time analysis. For this reason, an algorithm has been developed, known as the Fast Fourier Transform (FFT), which that performs an efficient or fast implementation of the DFT by greatly reducing the number of computations. FFT is widely employed in signal processing and related fields to analyze the frequencies and used in a wide variety of applications, from digital signal processing to solving partial differential equations to algorithms for quickly multiplying large integers.

Taking the FFT of the signal gives us the spectrum in the frequency domain. The spectrum presents information indicating the level of the vibration at particular frequencies. Thus all major frequency components and their amplitudes can be identified and be used for trending and fault detection purposes. The frequency identifies the source of the fault and the amplitude identifies the severity. As the faults start to develop in

machine components, the vibration spectrum peaks at the defect frequency and its harmonics that is associated with the faulty element. As the severity of the damage increases, the corresponding amplitudes of the peaks in the power spectrum increase. Often times, the Auto Power Spectrum is used to identify key frequency components in the spectrum. Auto Power Spectrum is computed as shown in Equation 2-12

$$AutoPowerSpectrum(x) = \frac{FFT(x)FFT^*(x)}{n^2} \quad (2-12)$$

where x is the input time-domain signal and n is the number of points in the signal.

Fourier has been used extensively in vibration analysis to detect machine defect. Siedlitz used the frequency domain to distinguish between resonant and non-resonant motion in machines. However he concluded that in order to use Fourier transform with vibration signal, the event must be periodic [Siedlitz, 1990]. Ghosh have used this method to detect combustion knock in internal combustion engines [Ghosh et al, 1991]. Boubal mentions combustion knock induces resonance as stationary waves that have fundamental frequencies around 6 kHz. This frequency is depended on geometry of the combustion chamber. He recommends high pass filtering the signal with a cut off frequency of 5 kHz to eliminate all frequency components below because they derive from noise related to the working of the engine and not related to combustion knock [Boubal 2000].

This method works great when used in applications involving simple machines such as detecting faulty bearing as done by Staszewski [Staszewski et al, 1999] and by Eren [Eren et al, 2002], or to detect broken rotor bar etc as shown by Yazici [Yazici et al, 1999]. But it becomes almost impossible to distinguish the fault imposed peaks when the

signal to noise ratio is low and the vibration spectrum has a large number of frequency components due to complexity of the system.

Nurhadi investigated the correlation between the vibrations measured by accelerometers mounted on an engine with engine components being the source for the excitations. The engine was motored by an electric motor with its spark plug removed cancelled compression and combustion. Such a setup removed a lot of unwanted frequencies from the data [Nurhadi et al, 1993]. Suh investigated valvetrain dynamics of an engine and concluded that the standard Fourier transform was not well suited for such applications as it was non-stationary response. He recommended using other techniques such as Wavelet transform, Wigner-Ville Distribution and Short-Time Fourier Transform (STFT) instead. This transform is suitable for analyzing stationary signals and not a suitable tool for the analysis of non-stationary signals such as vibration signatures generated by mechanical faults in an engine as it mostly consists of transients [Suh, 2002].

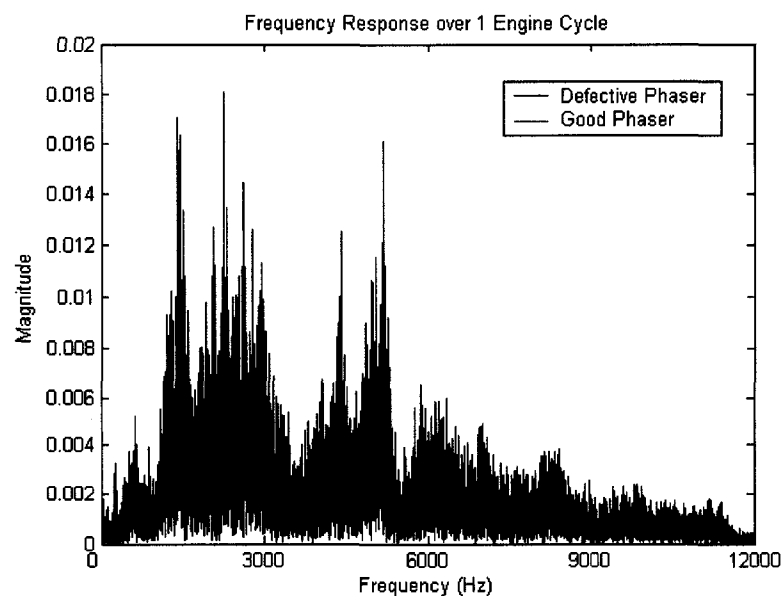


Figure 2.4: Frequency response of vibration signal for an engine with good and defective phaser.

Figure 2.4 shows the plot of FFT of a good and defective engine over 1 engine cycle. While difference may be observed in the case of extremely severe case of defective engines, no obvious difference can be seen in the frequency representation of the two signals for this case. Hence more intense frequency domain analysis has to be pursued in order to discover the independent frequency content of each defective valvetrain components. Also, this analysis does not provide us with any time-related data. Without a time-relation the physical meaning of the frequency results would still be insignificant when analyzing vibration signals generated by an engine.

2.3.2.2 Order Analysis

Another frequency domain analysis technique that is also often performed on vibration data acquired from rotational machines is the Order Tracking Analysis. An NVH order is a sinusoidal phenomenon at a frequency that is a fixed multiple of the rotation speed of the rotating source producing the phenomenon [Ford: Basic Order Tracking for NVH, 2003]. These phenomena are usually described by

- a) Order number
- b) Type of phenomena such as force, displacement or pressure etc.
- c) The rotating source such as tire, engine or fan etc.

For example, a 3rd order tire force variation is a sinusoidal force at three times the rotation frequency of the tire producing the force. In the case of engine, orders are referenced to crankshaft rotation speed. Thus a 2nd order engine phenomena means that it occurs at twice the crankshaft rotation frequency. The main difference between order analysis and conventional frequency domain analysis is that the resulting spectrum is a

function of order (harmonics of rotational speed) as opposed to a function of frequency (i.e. Hz).

Order analysis is a useful tool to use in the analysis of engine noise and vibration where the primary interest is in the behavior of the harmonic orders of the crankshaft speed especially when taking measurements over a range of engine speed in order to analyze the vibration characteristics of an engine [Mercer, 2007]. The rotating and reciprocating components in the engine produce a variety of forces and couples. These tend to increase with the square of the engine speed (rpm). Order tracking is the process of determining the amplitude of these sinusoids as the rotation speed varies with the main goal being to identify the dominant orders [Bruel and Kjaer, 1982]. The waterfall plot in the Figure 2.5 shows the graphical representation of the analysis where the symbol f_1 stands for the basic rotation frequency, f_n for the frequency of the n^{th} order. If the rotation is characterized by an RPM value then:

$$f_1 = RPM/60 \quad (2-13)$$

$$f_n = n f_1 \quad (2-14)$$

$$n = f_n / f_1 \quad (2-15)$$

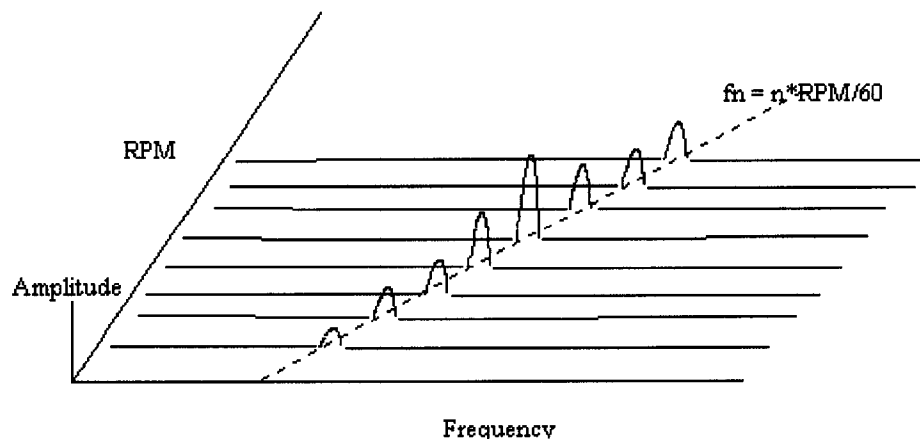


Figure 2.5: Order Analysis

The main concept behind order analysis is that the sampling rate during data acquisition is synchronized with the rotation speed of the crankshaft in order to lock the sampling locations to constant crankshaft angles. Thus even if the speed changes, the sampling will still occur at the same shaft angles and the frequency content of the signal will be a function of order. This can be achieved either by attaching an encoder to the crankshaft during data acquisition to record the shaft positions. Fourier transform is then applied on the data to transform it into order domain and the result of Fourier analysis is then the amplitude of sine waves at fixed multiples of the basic rotation frequency, that is to say the amplitudes of the orders.

From the order analysis, we are able to identify certain issues in engines related to engine balance, firing, cylinder to cylinder variation, deflections of the block or bearing supports, deflections of the crank, alternator imbalance and fan imbalance, crankshaft bending, unequal exhaust or intake runners etc. among many other phenomena [Ford: Basic Order Tracking for NVH, 2003]. Also, in their research, Blough have discussed the strengths and weaknesses of various order tracking analysis methods [Blough et al, 1999]. However this method does not give any information about any faulty components that we are interested in nor does it pin point to the cause of mechanical defect present in the engine.

2.3.2.3 Cepstrum Analysis

Cepstrum is defined as the power spectrum of the logarithm of the power spectrum and is represented in dB scale. It reduces multiple harmonic components to a single component

and can detect of periodicity with the spectrum of the given signal or harmonic and sideband components within the signal. It is used in the analysis of complex signals that contains multiple harmonics and hence it is used in many rotational machine related applications such as detection of bearings [Van Dyke et al, 2001] and gearbox defects [Dimaggio et al, 2000]. Toshihiko used cepstrum analysis to successfully detect misfire in internal combustion engines [Toshihiko et al, 1997].

Dimaggio showed that the cepstrum method can not only detect abnormal vibration characteristics, but can also provide insight into the nature of a defect [Dimaggio et al, 2000]. Zheng investigated fault detection in rotor machinery and concluded that the cepstrum method is effective in recovering excitations to transient components from vibration signals dominated by harmonic components. They developed a method for recovering excitations causing multiple transient signal components from vibration signals, especially from rotor vibration signals to detect faults like fatigue cracks in rotors and rubbing between rotors and stators or between rotors and seals [Zheng et al, 2001].

2.3.3 Time-Frequency Analysis

Analyzing data in either time or frequency domain shows signal characteristics in their respective domains only. All data acquisition is done in time domain. When data is analyzed in time domain it gives no spectral information and when time domain signal is transformed to the frequency domain the detailed information about the time domain is lost. Therefore these methods have their limits. Also, with respect to frequency domain analysis, we must take note that the results of the Fourier transform are only valid for

stationary signals as noted by various researchers such as Goumas [Goumas et al, 2002] and Yen [Yen et al, 2000]. Natural phenomena are usually nonlinear and the majority of the signals have changing frequency contents. For example, the vibrations caused by the valvetrain of the engine contain non-stationary transients as they contain short periodic impulsive components that are produced by impacts between components. In stationary signals, all frequency components that are present in the signal exist throughout the entire duration of the signal. In non-stationary signal the frequencies can change or appear for short duration as it happens in vibration signal of a defective engine. Fourier transform can be used for non-stationary signals, if we are only interested in what spectral components exist in the signal, but not interested at what time or interval they occur. However, if this information is needed, then Fourier transform is not the right transform to use. Vibration signal from complex machines such as an internal combustion engines contains both periodic components as well as random component that are generated by such items as friction and impact of mechanical components in the engine. As a result, more effective techniques are required in order to better analyze noise and vibration measurements and to more reliably detect engine defects.

Therefore, a different approach has been developed where a signal is mapped to a function of both time and frequency. This method is called Time-Frequency Analysis. As the name suggests the main advantage of time-frequency domain techniques is the use of both time and frequency domain information thus allowing for the investigation of the transient features such as impacts in a vibration signal [Suh, 2002], [Yen et al, 2005]. A number of time-frequency domain techniques have been proposed including Short-time

Fourier Transform (STFT), Wigner-Ville Distribution (WVD) and the Wavelet Transform (WT). Suh recommended using these techniques for analyzing vibration signature of complex rotating machines where the signal to noise ratio is low and a large number of frequency components are present for defect diagnosis purposes [Suh, 2002].

2.3.3.1 Short Time Fourier Transform

Short-time Fourier Transform (STFT) method is a revised version of the Fourier Transform (FT) and it was developed to overcome the limitations of FT in analyzing non-stationary signals. Several researchers have chosen this method over the traditional FT to diagnose and detect machine faults. Yazici reported using the spectrogram from the STFT to form feature vectors for bearing fault detection with high accuracy [Yacizi et al, 1999].

The STFT of a signal $x(t)$ can be defined by Equation 2-16 as

$$G(f, \tau) = \int_{-\infty}^{\infty} [x(t) \otimes g(t - \tau)] e^{-j2\pi ft} dt \quad (2-16)$$

where $g(t)$ is the window function. The only difference between the FT and STFT is that the signal is divided up into small segments. It uses windows to zoom into small portions of the non-stationary signals and treats it as a stationary signal during at windowed instant and performs Fourier Transform on it to analyze their local frequency spectrum [Cohen]. In the next step, the window is shifted to a new location, multiplied with the product and then taking the FT of it. And this procedure is followed, until the end of the signal is reached. Through this transformation, the STFT converts the signal from the time domain into time-frequency plane (f, τ) .

The main problem with STFT is that there is a tradeoff between time and frequency resolution. The time frequency resolution of the STFT is determined by the window function $g(t)$. When the window is small, it gives good time resolution, but poor frequency resolution and when the window is large, it gives poor time resolution but good frequency resolution. When the window is infinite, it is same as Fourier Transform. Hence, if good localization in time is desired, then a narrow window in the time domain has to be chosen. However, if good frequency localization is desired, a narrow window in the frequency domain has to be chosen. But once the window function $g(t)$ is defined, the time and frequency resolution is fixed. This is the reason several researchers such as Yen [Yen et al, 1999 (1) (2), 2000, 2005], Goumas [Goumas et al, 2002], Djurovic [Djurovic et al, 1999] have suggested using other Time-Frequency analysis techniques such as Wavelet Analysis or time-frequency distribution techniques such as Wigner-Ville Distribution for analysis of vibration data of complex machines.

2.3.3.2 Time-Frequency Distribution

Other popular time-frequency analysis techniques include the Wigner-Ville Distribution (WVD) and the Choi-Williams Distribution (CWD). These methods have been reviewed in several papers for analysis of non-stationary signals to diagnose defects in machines. Konig [Konig, 1996] and Samimy [Samimy et al, 1994, 1996] have used Cross Wigner-Ville Distribution to detect combustion knocks in engines from both vibration and in-cylinder pressure signal signature. Samimy used WVD to observe engine knock from vibration impulses as an energy distribution is both time and frequency domain [Samimy et al, 1996]. Boubal used smoothed version of the WVD to detect engine knock from

pressure signals. He reported that the representation of a signal with knock using such a distribution shows both the non-stationary character of the signal as well as the clear dependence of the resonance frequency values with respect to time [Boubal, 2000]. Using this technique, we can express the values of the resonance frequencies as a function of crank angle.

There are two main problems with these distributions that have been reported by Tafreshi [Tafreshi et al, 2002]. They are 1) cross-terms that are produced in the transform because of bilinear (quadratic form) and 2) aliasing, which causes a frequency component to be duplicated at a distance π . Zheng introduced an alias-free exponential time-frequency distribution as a remedy these problems [Zheng et al, 1999].

2.3.3.3 Wavelet Analysis

Wavelet Transform (WT) is another powerful time-frequency analysis technique that is increasingly being used in the industry for analysis of non-stationary signals such as vibration signature monitoring of machine. Wavelet analysis can represent a signal in terms of a set of basis functions and thus can describe a signal on various levels of resolutions or scales corresponding to different frequency bands. In this section we will provide a review of the fundamentals of the Wavelet Transform (WT). We then extend it to describe the Continuous Wavelet Transform (CWT) and Discrete Wavelet Transform (DWT) and finally Wavelet Packet Transform (WPT). This background is essential and helps us make the necessary connections between wavelets and filter banks since all our work uses the fast filter bank implementations of the WPT as its foundation. The filter

bank implementations of the WT and WPT are also referred to as the fast WT (FWT) and fast WPT (FWPT), respectively.

2.3.3.3.1 Overview of Wavelet Transform

Wavelets analysis is a natural extension of Fourier analysis techniques such as Fourier Transform (FT) and Short-time Fourier transform (STFT) [Daubechies 1992]. It was developed, as an alternative to STFT to over come the latter's resolution problems as discussed in the previous section. Wavelet analysis is essentially multi-resolution. It decomposes a signal using different window size at different scales – it uses small window size for higher scales or low frequencies and a large window size for lower scale or high frequency components. This allows us to capture both high frequency and low frequency information of the signal.

A wavelet, also means a small wave, is a function that decreases quickly towards zero at both ends. We can control the shape of the function using dilation and shifting it using translation to capture a localized event. One particular characteristic of this transforms is its ability to detect hidden details of waveforms that may otherwise go unnoticed. This is especially useful in machinery vibration monitoring where it is important to detect impulse-like transients in the signal.

One important advantages of this method over STFT is that it provides multiple resolution in time and frequency, which is important for analyzing transient signals containing both high and low frequency components. WT provides good resolution in the

frequency domain at low frequencies and good resolution in the time domain at high frequencies [Polikar 2003].

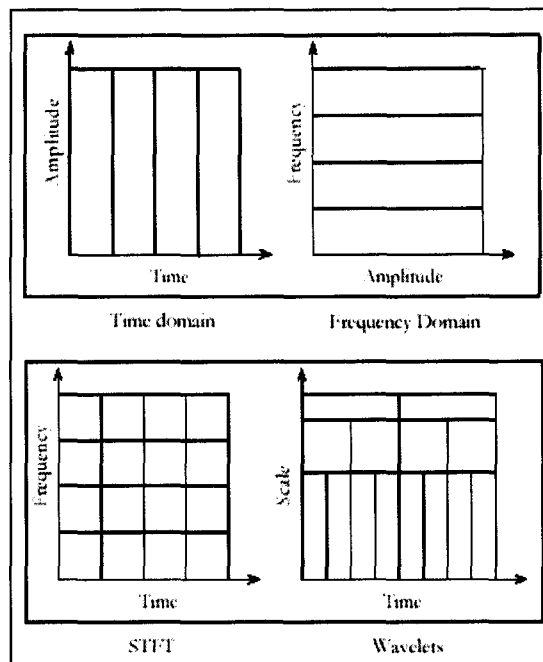


Figure 2.6: Comparison of Time, Frequency, STFT and Wavelet domain analysis.

Figure 2.6 graphically illustrates the multiresolution property of WT and also compares it with time, frequency and STFT. Time and frequency domain analyses provide information only in their own domain. For STFT, the time-frequency resolutions are determined by the width of the analysis window, which once selected is fixed for the entire analysis, i.e., both time and frequency resolutions are constant. Therefore the time-frequency plane consists of squares in the STFT case. In the case of wavelet analysis, the widths and heights of the boxes change but the area is constant. Each box represents an equal portion of the time-frequency plane, but giving different proportions to time and frequency. For low scales, (i.e. high frequencies), the width of the boxes is short which indicated that the time resolution gets better. At the same time, the heights of the boxes increase, i.e., the frequency resolution gets poorer. At higher scales (i.e. low frequencies),

the heights of the boxes are shorter which corresponds to better frequency resolutions but their widths are longer indicating poor time resolution since there is more ambiguity regarding the value of the exact time. Therefore, it shows wavelets provide good resolution in time domain for higher frequencies and good resolution in frequency domain for lower frequencies.

2.3.3.3.2 Continuous Wavelet Transform (CWT)

Wavelets are a natural extension of the Fourier analysis [Daubechies 1992]. A wavelet is small wave whose energy is concentrated in time. As reviewed in section 2.3.2.1 Fourier transform decomposes a time based signal into to complex exponential functions of different frequencies and can be represented by Equation 2-17.

$$X(f) = \int_{-\infty}^{\infty} x(t)e^{-2j\pi ft} dt \quad (2-17)$$

where t stands for time, f for frequency, $x(t)$ the signal in time domain and $X(f)$ the signal in frequency domain.

The continuous wavelet transform is an integral transform, in which a signal is represented in terms of a family of time and frequency localized basis functions and is defined as follows:

$$W(\tau, s) = \frac{1}{\sqrt{|s|}} \int_{-\infty}^{\infty} w(t) \cdot \psi^* \left(\frac{t - \tau}{s} \right) \cdot dt \quad (2-18)$$

So we can see that, the term $e^{-j2\pi ft}$ in Equation 2-17 is replaced by the wavelet bases $\psi_{\tau,s}(t)$ to decompose the signal into the time-scale domain, where

$$\psi_{(\tau,s)}(t) = \frac{1}{\sqrt{|s|}} \psi\left(\frac{t-\tau}{s}\right) \quad (2-19)$$

τ is the translation parameter and s is the scale or the dilation parameter. τ and s are both real values. In order to detect the characteristics of a signal, we compare it to a given scaled and time-shifted elementary functions. This representation is called wavelet analysis and the elementary function, $\psi(t)$, is also known as a mother wavelet. A wavelet basis is a set of linearly independent functions constructed from a single mother wavelet with a scale and translation parameter. Polikar notes that unlike a Fourier transform, a wavelet transforms' basis functions are localized in both time and frequency. Since the basis function is localized in time, it is necessary to translate them in time in order to cover the entire domain. Then, since the wavelet is localized in frequency, it is necessary to scale them in time and shifting them in frequency. Thus, the continuous wavelet transform is computed by changing the scale of the analysis window, shifting the window in time, multiplying by the signal, and integrating over all times [Polikar, 1999].

The $1/\sqrt{s}$ is an energy normalization term that makes the wavelets of different scales have same amount of energy. A wavelet needs to satisfy certain conditions to correctly represent signals and for the inverse transform to exist. First a wavelet must integrate to zero

$$\int_{-\infty}^{\infty} \psi(t) \cdot dt = 0 \quad (2-20)$$

All wavelets are band pass filters. Additionally, the wavelet must be an admissible function. Which is to say, it must have finite energy and satisfy the equation

$$\int_{-\infty}^{\infty} \frac{|\psi(w)|^2}{|w|} \cdot dw < \infty \quad (2-21)$$

There are infinitely many wavelets in the sense that any function concentrated in time can serve as an analyzing function. There are many wavelets that have been developed for various applications to best suit several problems in science and engineering related to transient, time-variant, or non-stationary phenomena. This gives the method a great flexibility. The most commonly used ones are namely, Haar, Daubechies, Morlet, Biorthogonal, Mexican hat etc. Which wavelets work best for fault diagnostics is a question that many authors have asked and is a subject of ongoing research. Ideally, we would like to match the wavelet to the physics of the problem as such different wavelets are suited for different types of applications and they are all unique in nature. It all depends on what type of signal we have and what signal features exactly we are looking for.

2.3.3.3 Discrete Wavelet Transform (DWT)

The idea behind Discrete Wavelet Transform (DWT) is the same as it is in the CWT where a time-scale representation of a digital signal is obtained but is considerably easier to implement. Implementation of the DWT is usually carried out using the multi-resolution analysis (MRA) method. The idea of MRA is to decompose the input signal using a two-channel filter bank followed by subsequent downsampling process. Filters of different cutoff frequencies are used to analyze the signal at different scales.

The signal is passed through a series of half band highpass filters to analyze the high frequencies, and it is passed through a series of half band lowpass filters to analyze the low frequencies. Figure 2.7 represents the filtering mechanism using a two-channel filter bank. The input signal, S , is filtered using is a low pass and a high pass filter to generate the coefficients of A and D respectively.

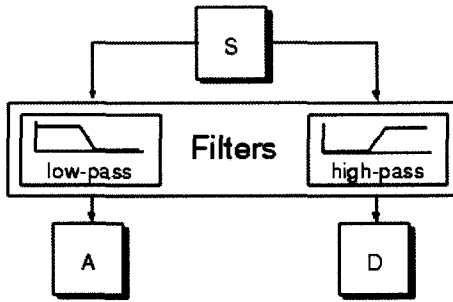


Figure 2.7: Two-channel filter bank [Matlab]

Once the filtering of signal is achieved, the scale can be changed by downsampling operations. The downsampling process in essence reduces the sampling rate by removing some of the samples of the signal thereby changing the scale.

Figure 2.8 is schematic representation of the DWT mechanism where $g[n]$ and $h[n]$ represent the impulse response of a highpass (or wavelet) filter and lowpass (or scaling) filter respectively. The discrete filters $g[n]$ and $h[n]$ are quadrature mirror filters associated with the scaling function and the mother wavelet function [Daubechies, 1992].

The highpass and lowpass filters are related by Equation 2-22

$$g[N - 1 - n] = (-1)^n \cdot h[n] \quad (2-22)$$

where N is the filter length.

The procedure starts with passing the input signal, s , through both filters. Filtering a signal corresponds to the mathematical operation of convolution of the signal with the impulse response of the filter. The convolution operation in discrete time is defined as follows:

$$s[n] * h[n] = \sum_{k=-\infty}^{\infty} s[k]h[n-k] \quad (2-23)$$

During filtering, the half band lowpass filter removes all frequencies that are above half of the highest frequency in the signal and this constitutes the coefficients of A (approximation). Similarly the half band highpass filter removes all the low frequencies and computes the coefficients of D (detail). Half band filtering removes half of the frequency content, hence it can be interpreted as losing half of the information. Therefore, the resolution is halved after the filtering operation.

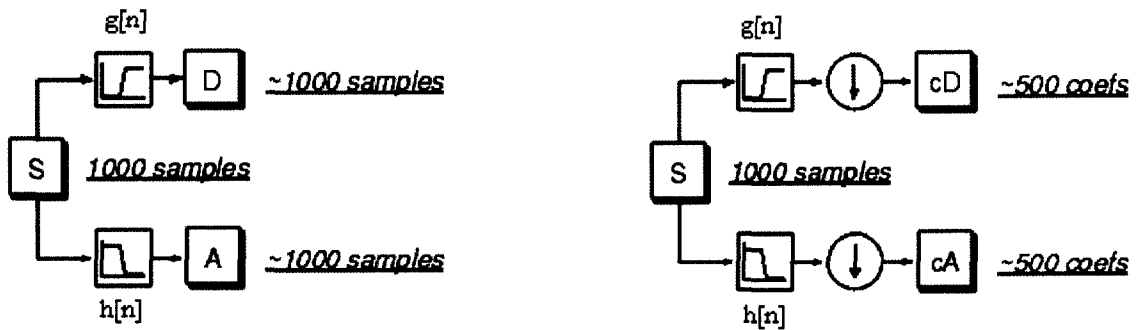


Figure 2.8: DWT Mechanism - Filtering and Sub sampling of signal [Matlab]

After passing the signal through the half band filters, the sequence A and D contain only half the original frequency information. Therefore, half of the samples can be eliminated according to the Nyquist's criteria. So, in the second step of the process, A and D is downsampled by 2 since half of the number of samples are redundant and the coefficients

of cA and cD are computed. This downsampling process doubles the scale. Equation 2-24 and 2-25 can be used to represent the DWT process.

$$cA = s_{low}[k] = \sum_n s[n] * h[2k - n] \quad (2-24)$$

$$cD = s_{high}[k] = \sum_n s[n] * g[2k - n] \quad (2-25)$$

The decomposition process can be iterated, with successive approximations (i.e. low frequency part) being decomposed in turn, so that one signal is broken down into many lower resolution components. This is called the wavelet decomposition tree (Figure 2.9).

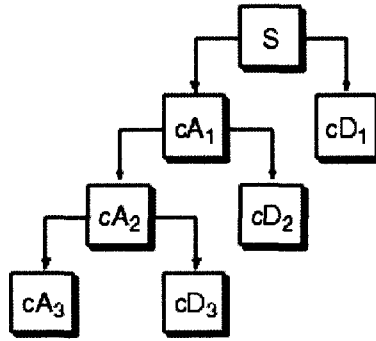


Figure 2.9: DWT decomposition tree [Matlab]

At every level, this decomposition halves the time resolution since only half the number of samples now characterizes the entire signal and doubles the frequency resolution, since the frequency band of the signal now spans only half the previous frequency band.

Since the analysis process is iterative, in theory it can be continued indefinitely. In reality, the decomposition can proceed only until the individual details consist of a single sample or pixel. Thus DWT transforms the original signal vector into a new vector, which is filled sequentially with wavelet coefficient of the different levels. These are the signal characteristics that can be used as features for classification purposes.

2.3.3.3.4 Wavelet Packet Analysis (WPT)

The Wavelet Packet Transform (WPT) is an extension of the discrete wavelet transform. The decomposition of a signal is carried out in the same way as in DWT (Figure 2.8) by simple cascade filtering using two analysis filters and then downsample by a factor of two, giving us two new sequences. Figure 2.9 and 2.10 shows the schematic of a DWT tree and WPT tree/node structure respectively. In case of DWT, only the low frequency part is decomposed in subsequent levels but for WPT, both high and low frequency parts are decomposed.

The same set of two filters are used, a low-pass filter, whose impulse response is denoted by $h[n]$ and its mirror version which is a high-pass filter whose impulse response is denoted by $g[n]$. This process is iterated over and over again on the newly created sequences and this result in a uniform decomposition in frequency subbands, which covers the interval extending from 0 Hz up to half the sampling rate f_s adopted in digitizing the input signal. The newly created sequences are called WPT coefficients. This filter bank based implementation method is also referred to as the fast WPT (FTPT)

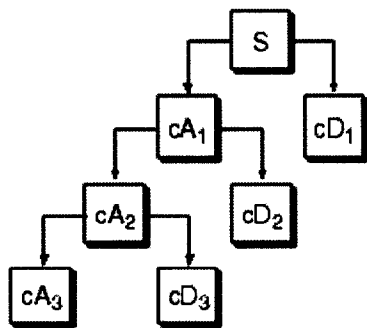


Figure 2.10: Discrete Wavelet Transform Tree [Matlab]

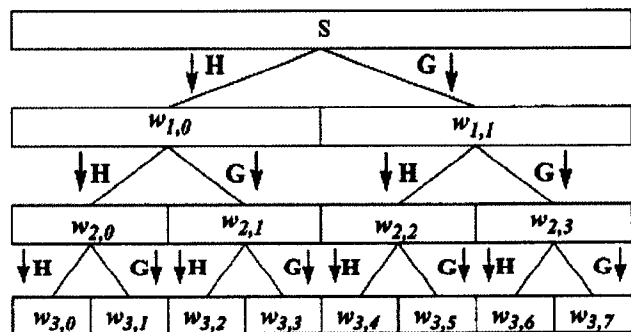


Figure 2.11: Wavelet Packet Transform Tree

Figure 2.11 shows the wavelet packet node representation of a level-3 complete tree basis. It represents each wavelet packet as a node where, a wavelet packet, $W_{j,k}$ is a function of two indices: j denoting the depth or the number of level of decomposition within the transform and k the position of each node. If we want to split a wavelet packet node at level j and position k into two nodes at level $j+1$ and positions $2k$ and $2k+1$, we will get the following two wavelet packets,

$$w_{j+1,2k}(t) = \sum_{n=0}^{N-1} h[n]w_{j,k}(2t - n) \quad (2-26)$$

and

$$w_{j+1,2k+1}(t) = \sum_{n=0}^{N-1} g[n]w_{j,k}(2t - n) \quad (2-27)$$

This allows the WPT to have more than one basis function (or wavelet packet) at a given scale whereas DWT has one basis at each scale other than at the last level where it has two. The set of wavelet packets collectively make up the complete family of possible bases hence more feature vectors. Also, if needed, we have the flexibility to form other bases from existing bases by taking linear combinations of the bases. Another advantage that WPT provides over DWT is that WPT has better frequency resolution in higher frequencies. DWT only decomposes the low frequency portion of the signal thus it faces difficulties in discriminating between signals having close high-frequency components. This flexibility of a rich collection of abundant information with arbitrary time-frequency resolution allows extraction of features that combine stationary and non-stationary features. As a result WPT is increasingly becoming the chose of analysis techniques when analyzing vibration signals as noted by Yen (Yen, 1999 (1), (2), 2000, 2005].

2.3.3.4 Applications of Wavelet Analysis in Vibration Monitoring

Although only recently, wavelet analysis has been investigated in several studies dealing with fault detection of machines from analysis of the vibration signals generated by the machine. Yen provides a good overview in the application of wavelet analysis of in the area of vibration monitoring of machines. Several traditional methods such as Fourier Transform and STFT were presented and a new method based on Wavelet Packet Transform (WPT) is introduced as an alternative means of extracting time-frequency information from vibration signature. He proposed the use of node energy from wavelet packets as a more robust signal feature for classification of defects in helicopter gearbox, instead of using the wavelet coefficients itself [Yen et al, 1999 (2), 2000]. Eren used WPT for detecting bearing faults in motor [Eren et al, 2002]. Staszewski also investigated bearing defect detection using the variance of the wavelet coefficients [Staszewski et al, 1999].

Goumas presented a new method for extracting features from vibration signals in the wavelet domain and use them for classification of washing machines into three distinct classes. Vibration signals were decomposed to wavelet vectors using discrete wavelet transform with Daubechies (Db4) (Daubechies [1992]) wavelet being the mother wavelet. Several statistical parameters such as sample variance, mean, maximum and minimum values were then calculated from the wavelet coefficients and these were used as feature vectors. Several distance classifiers were then investigated for classification purposes and an optimum solution was suggested [Goumas et al, 2002].

Applications of the WT for feature extraction from vibration signals for fault detection and diagnosis of internal combustion engines remain relatively few. Most common application of WT relating to engines is detection of combustion knock from pressure and vibration signal of the engine. Yang performed a study on misfire detection using momentary crankshaft speed [Yang et al, 1999]. Tafreshi investigated use of wavelet packet transform to detect combustion knock in a single cylinder engine in an experimental setting [Tafreshi et al, 2002]. Mingzan investigated use of wavelet packet transform of the vibration signal to classify three different modes of wear in valves in a diesel engine. Three level of decomposition was used to create eight wavelet packet vectors and the energy of these vectors were calculated and used for classification [Mingzan et al, 2003].

Chandroth conducted a study to classify diesel engine faults from vibration signals. The faults investigated were leaking inlet/exhaust valve and blocked/poorly atomizing injector. The vibration signal in the crank angle domain was decomposed using discrete wavelet transform using Db8 [Daubechies, 1992] as the mother wavelet. Instead of using data for complete engine cycle (0 – 720 degrees of crank angle), only a quarter of the cycle (0 – 180 degrees of crank angle), which correspond to the power stroke of the piston, was considered and decomposed to 8 levels. Principal Component Analysis was then used to classify the feature vectors to their respective classes [Chandroth et al, 1999 (1)]. In a separate study, Chandroth also used in-cylinder pressure measurements as the input signals and successfully classified the same defects to their respective classes. In this analysis, the pressure data was decomposed to 12 levels using orthogonal wavelet

transform with the 4th order Daubechies' wavelet, Db4 [Daubechies, 1992], as the mother wavelet. Variance of the wavelet vectors was used to classify the results to different classes [Chandroth et al, 1999 (2), (3)]. This application also illustrates that the choice of the wavelet depends on the application on hand.

2.5 Advantages of wavelet analysis over other methods

Wavelet analysis holds several advantages over other methods discussed in the previous sections. Wavelet analysis retains both time and frequency information of the signals. Thus it has the advantage of having information about an extra dimension that neither variance analysis nor FFT has as they all analyze signals in just one dimension i.e. either time (crank angle) or in frequency domain.

As a result, while variance analysis of vibration data in crank angle domain can detect the vibration impulse occurring due to mechanical impacts of faulty components at particular crank angles (engine cycle position), it does not contain any frequency information of those impacts hence can not distinguish between two events if they can take place at the same time in a engine cycle. Whereas, if whose two events have different frequency content, wavelet analysis is able to distinguish between the two events. Thus using variance analysis, we can only narrow down the possible causes of defects and not be definitive about the specific defect while wavelet analysis has the added dimensionality and can precisely detect the source of defect.

The same extra dimension also gives wavelet analysis an extra edge over FFT. The frequency content of the signal is a vital indicator of defect since most machine defects are characterized by certain impulses that occur at particular frequencies or have components at known harmonics. FFT provides information about which frequencies appear in the signal but not about the time instants (crank angle) where these frequencies are encountered. Internal combustion engines operate in a cyclical basis hence the time information is critical and can be used to discriminate between two different defects that have the similar frequency content but occurs at different time in the engine cycle. Furthermore, vibration signals generated by an engine contain both periodic components as well as random components that are generated by such items as friction and impact of mechanical components in the engine. As such they contain a large number of frequency components due to complexity of the engine and are essentially nonstationary and not periodic which is the assumption of Fourier transform. In stationary signals, all frequency components that are present in the signal exist throughout the entire duration of the signal. In non-stationary signal the frequencies can change or appear for short duration as it happens in vibration signal of a defective engine. Fourier transform is suitable for analyzing stationary signals and not a suitable tool for the analysis of non-stationary signals such as vibration signatures generated by mechanical faults in an engine as it mostly consists of non stationary transients such as short periodic impulses that are produced by impacts between components. Hence Fourier analysis does not work well in analyzing vibration signal of a defective engine as also illustrated by figure 2.4.

Short-time Fourier transform uses a fixed sized window to find the frequency content of the windowed instant. The main problem with STFT is that there is a tradeoff between time and frequency resolution. The time-frequency resolution of the STFT is determined by the window function. Hence, if good localization in time is desired, then a narrow window in the time domain has to be chosen and if good frequency localization is desired, a narrow window in the frequency domain has to be chosen. Whereas wavelet analysis can represent a signal in terms of a set of basis functions and thus can describe a signal on various levels of resolutions or scales corresponding to different frequency bands. Wavelet analysis decomposes a signal using different window size at different scales – it uses small window size for higher scales or low frequencies and a large window size for lower scale or high frequency components. This allows us to capture both high frequency and low frequency information of the signal. Another advantage of wavelet analysis over STFT is that the basis function of STFT is still sines and cosines but in the case of wavelet analysis we have the option of choosing the wavelet basis function that works best for the application on hand. Once we choose this function, also called the mother wavelet, we can control the shape of it using dilation and then shift it using translation to capture localized events and thus detect hidden details of waveforms that may otherwise go unnoticed. This is especially useful in machinery vibration monitoring where it is important to detect impulse-like transients in the signal.

2.6 Proposed Engine Fault Detection Method

Our goal is to detect and diagnose mechanical defects in engine from vibration signatures of the engine. In this study, a method based on wavelet packet decomposition (WPD) is

proposed to process and analyze vibration signals of internal combustion engines. This method allows for diagnosis and detection of defective components inside the engine without dismantling it. Vibration signals of both good and defective engines are recorded using accelerometers from different locations on the engine during its normal operations. Measuring vibration from different locations on the engine yields localized vibration data from all parts of the engine. These vibration waveform measurements are then transformed to the crank angle domain and subsequently to wavelet packets using WPD from which features are extracted and analyzed for defects. Since internal combustion engines operate in a cyclical manner, transforming all time domain data to crank angle domain helps us to correlate any unusual vibration phenomena to a particular events of the engine cycle such as valve or piston position. Wavelet packets are used since they can produce narrower and improved frequency resolutions while also retaining time information of the original signal, and hence also the crankshaft angle information. The wavelet packet transform is used to decompose the vibration signals into several frequency bands. Wavelet packet energy is then computed and is used as the main indicator to discriminate between good and bad engines. The packet energy is compared with an energy threshold that is established from taking vibration measurements of good engines. If an engine in question is found to be defective, based on the threshold, we then attempt to classify the fault type based on the three parameters:

- **Wavelet Packet** - provides the frequency bandwidth information of the fault
- **Crank Angle** – provides information about the location of the fault with respect to the engine cycle

- ***Dominant Accelerometer*** - indicates the general area on the engine where the defect is located

Detailed step-by-step description of the defect detection process is given in *Chapter 4:*

Data Analysis and Results.

2.7 Summary

In this chapter, we first briefly discuss the various steps involved in any machine fault detection process. All state-of-the-art data processing techniques that are used in the area of machine fault detection are discussed starting with time domain and then frequency domain and finally joint time-frequency analysis. A brief theoretical background and the merits and demerits of each method are discussed. Along with the above, an overview of applications of each method is also discussed citing various researchers who have successfully implemented these techniques for their applications of interest. We also establish the need to use time-frequency analysis such as wavelet transform when analyzing vibration data from complex machines such as an internal combustion engine as this domain yields better results for non-stationary signals such as vibrations generated by mechanical impacts. The chapter concludes with a brief description of the proposed method based on WPD that is developed during this study to detect and identify cause of mechanical defects in engines.

CHAPTER 3

EXPERIMENTAL DETAILS

This study was undertaken to detect several commonly occurring engine faults. In this chapter we will discuss the test set up, the testing equipments and the test conditions that were used for the study.

3.1 Engine Test Setup

The engine model chosen for this study is the single overhead cam (SOHC) eight-cylinder (V8) 5.4-litre three-valve (3V) engine. Detailed specification of the engine can be found in *Appendix A: 5.4L 3V Engine Specification*. The tests were conducted in the semi-anechoic chambers in the engine dynamometer laboratory at the Ford Powertrain Engineering Research & Development Center (P.E.R.D.C.) to ensure no outside noise levels affected the vibration response of the system. In order to accurately re-create the vibration characteristics of an engine inside a vehicle, the test setup included the powertrain system: consisting of the engine, clutch and transmission assembly; Front End Accessory Drive (FEAD) subsystem: consisting of the fan belt, power-steering pump, alternator and compressor; powertrain mounts and mount brackets that are used in the vehicle. This is done to simulate in vehicle condition as close as possible.

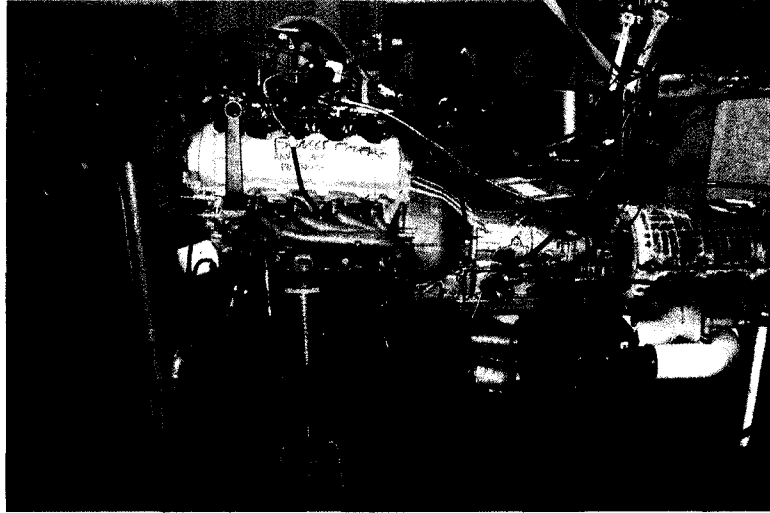


Figure 3.1: Illustration of test set up. A 5.4L 3V Engine and transmission is coupled with a dynamometer.

To ensure consistency, all engines were tested using the same setup and under the controlled conditions of an engine dynamometer test cell. The specifications of the cell are listed in *Appendix B: Cell#7 Dynamometer Specifications*.

3.2 Operating Conditions

Engine vibration characteristics depend on lot of engine operating conditions such as engine speed (rpm), load and engine oil and coolant temperature. These factors associated with this testing were considered when setting up these experiments. All engines were run under neutral idle conditions which is ~600rpm for the 5.4L 3V engine. Temperature is also an important factor in measuring engine vibration because different component of the engine tend to distort, warp, expand or contract depending on the operating temperature of the engine. This may result in insufficient or excessive clearances than normal and cause it to vibrate. The engine cooling water and the oil temperature was controlled to be between 180-190°F. This provided a “hot” idling condition. Problematic engine noise is usually most prominent under these conditions.

3.3 Acquisition Equipments

The main equipments that were used are vibration transducers and a data acquisition system. In addition to these, there were other accessories that were needed in order for the accelerometers to function properly and also for verification purposes such as a charge amplifier and a transducer calibrator respectively. The following section will give a detailed description of the transducers and accessories used in the study. A listing of all transducers and accessories specification is listed in Appendices C through G.

3.3.1 Transducers

The transducers used for the measurement of vibration are piezoelectric accelerometers. Bruel & Kjaer [Bruel & Kjaer, 1982] and Licht [Licht et al, 1987] describe the theory and application relating to this type of transducer. A piezoelectric accelerometer main consists of three parts, the accelerometer base, the piezoelectric elements and a series of seismic masses. Licht provides a general representation of piezoelectric accelerometers [Licht et al, 1987].

The piezoelectric element is usually placed between the accelerometer base and the seismic mass and it acts as spring. The seismic masses vibrate with the same magnitude and phase as the accelerometer base. When the accelerometer is subjected to an excitation, the seismic mass exerts a force on the piezoelectric elements that is equal to the product of their mass and acceleration ($\text{Force} = \text{Mass} \times \text{Acceleration}$). This causes the piezoelectric elements to produce a charge that is proportional to the acceleration and thus the acceleration of the surface the accelerometer is attached to is measured.

Piezoelectric accelerometer is the transducer of choice because of its relatively small size, durability, low cost, wide frequency range, good measurement stability and good linearity. There are two types of piezoelectric accelerometers that are most commonly used. They are the charge output type accelerometers and internally amplified accelerometer also called the Integrated Circuit Piezoelectric (ICP) type accelerometers. Charge output sensors are high output impedance, piezoelectric sensors (without built-in electronics) that typically require external charge or voltage amplifier for signal conditioning. ICP type sensors are low output impedance sensors that contain built in integrated circuits to convert the charge signal to voltage and they require a constant current power supply.

3.3.1.1 Bruel & Kjaer Type 4366 Accelerometer

This is a charge type piezoelectric accelerometer that requires a charge amplifier to convert its output charge signals to voltage. It requires low noise cabling due to its high impedance output. It can withstand high temperatures and is quite durable and robust under harsh environment. Hence this accelerometer is used in locations on the engine where it gets really hot from radiations from the exhaust manifold. Also the sensitivity and the frequency range of this accelerometer is optimum for measuring engine vibration. The detailed specification of this accelerometer is given in *Appendix C: Specifications of Bruel & Kjaer Type 4366 Accelerometer*.

3.3.1.2 PCB Model 353B15 Accelerometer

This is an Integrated Circuit Piezoelectric (ICP) type accelerometer that is used for moderate temperature range application. It cannot withstand high temperatures due to the microelectronics built into the accelerometer itself. Low noise cabling is not necessary to obtain clean signal due to its low impedance output. This accelerometer is used in locations on the engine where it does not get very hot. Also the sensitivity and the frequency range of this accelerometer is optimum for measuring engine vibration. The detailed specification of this accelerometer is given in *Appendix D: Specifications of PCB Model 353B15 Accelerometer*. Figure 3.2 shows the picture of both types of accelerometer used in this study.

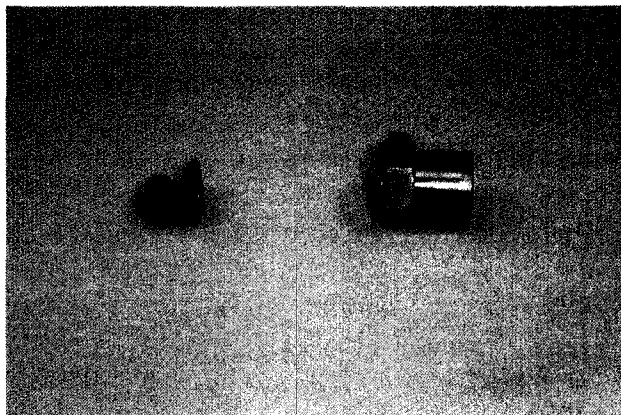


Figure 3.2: Accelerometers used for the study: PCB Model 353B15 accelerometer (left) and Bruel & Kjaer Type 4366 accelerometer (right)

3.3.2 Transducer Calibrator

All accelerometers are calibrated using a Bruel & Kjaer Type 4294 Calibration Exciter. This is done to ensure data consistency and the calibration of the accelerometers. Accelerometers can be threaded onto the calibrator, or attached onto it by means of wax or glue. The calibrator produces a reference sinusoidal acceleration of 10m/s^2 rms at a

frequency of 1000 rad/s or 159.2 Hz. (See *Appendix E: Specifications for Calibration Exciter*).

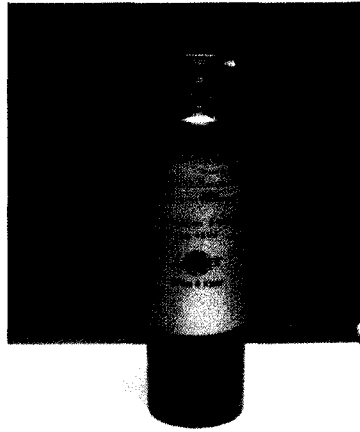


Figure 3.3: Bruel & Kjaer Type 4294 Calibrator

3.3.3 Data Acquisition System

The data acquisition system used in the study is the Prosig 5600 System. It is a 16-bit data acquisition system. Each Prosig 5600 unit has a maximum of 8 analog input channels. Hence two Prosig 5600 units were used as stacked to give us a total of 16 channels. This system is user friendly and has a WindowsTM based interface to control the setup and acquisition parameters. The accelerometer output is an analog voltage, which is converted to a discrete signal by Analog-to Digital Conversion (ADC) and stored in PC so it can later be processed and analyzed. The 16-bit ADC card of this system can support maximum sampling frequency of 100 kHz per channel with a resolution of 0.3 μ V. The detailed acquisition system specifications are summarized in *Appendix F: PROSIG5600 System Specifications*.

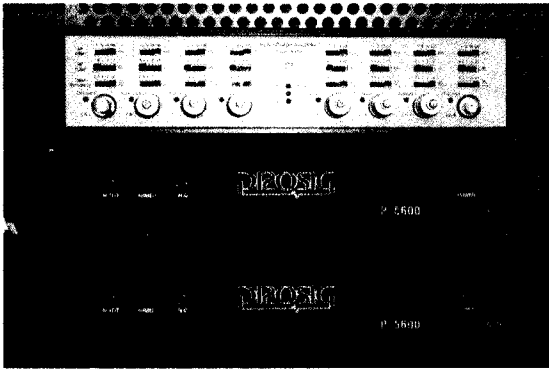


Figure 3.4: The Prosig 5600 System front view.



Figure 3.5: The Prosig 5600 System rear view.

Some of the particularly important parameters and concepts that are involved in this ADC process include anti-aliasing filtering, signal coupling, quantization and sampling frequency.

3.3.3.1 Anti-aliasing Filtering

During data acquisition input analog signals is passed through a low-pass hardware filter before the signal is sampled and recorded. The front-end of the Prosig 5600 data acquisition system has a built in anti-aliasing filter that automatically adjusts the cut-off frequency of this low pass filter based on the selected sampling rate to ensure that the aliased frequencies are not digitized. A low-pass filter with cut-off frequency 13107 Hz was used during all acquisitions.

3.3.3.2 Signal Coupling

ICP transducers require a supply of constant current in order to operate but this creates a DC voltage. Charge-type transducers generate a charge that is amplified by a charge amplifier, and this charge amplifier also adds a DC offset to the measured signal.

Therefore AC coupling was applied to all signals acquired in this study to remove any DC offset caused by the transducers.

Each signal was allowed to stabilize for about ten seconds during data is collected. This was done to allow enough time to charge the accelerometers and to allow the high-impedance data acquisition system circuitry to completely ground. Also, care is taken to ensure all data acquiring equipment is properly grounded.

3.3.3.3 Quantization

The accelerometer output is an analog voltage, which is converted to a discrete signal by the 16-bit Analog-to Digital Converter (ADC) of the Prosig System. This process is known as quantization. This is done by dividing the amplitude range of the system into a number of discrete levels. For instance, an N-bit ADC would allow for 2^N quantized levels. Therefore, the 16-bit ADC would be broken down into 2^{16} or 65536 levels. Since the system has maximum full-scale input range of $-10V$ to $+10V$, it can be divided up into 2^{16} levels thereby allowing for a resolution of $300\mu V$. The system also has an adjustable gain of 1 to 1000. Therefore at a gain of 1000, the system has a maximum resolution of $0.3\mu V$.

3.3.3.4 Sampling

The output of any transducer is a continuously varying voltage. The ADC of the system samples this analog signal and stores them as discrete values. Sampling is a process by which the continuous analog signal is multiplied by a unity amplitude discrete valued

sampling function resulting in a discrete time signal where the values are equally spaced in time, Δt . The sampling frequency, f_s is defined as:

$$f_s = \frac{1}{\Delta t} \quad (3-1)$$

where Δt is the time spacing between samples

Setting the proper sampling frequency is one of the most important parameter of any data acquisition as it determines what signal characteristics will be accurately recorded and not. The sampling frequency should be set high enough to capture the maximum frequency component of interest that is in the signal. Shannon sampling theorem states that the sampling rate should be at least twice the highest frequency (f_{max}) present in the signal in order to properly reproduce this analytic signal.

$$f_s \geq 2f_{max} \quad (3-2)$$

f_{max} is also known as Nyquist frequency. If the sampling frequency is less than the Nyquist frequency, then the frequency components that are more than $\frac{1}{2}$ the sampling frequency will be not be recorded accurately due to an error referred to as aliasing. Aliasing allows frequencies that are higher than the Nyquist frequency to be falsely reflected back into lower frequencies and causes the analog signal to not be accurately reproduced. Most data acquisition systems cannot sample fast enough to fully prevent aliasing errors. To account for this error usually hardware based anti-aliasing lowpass filter is used.

The bandwidth we are interested in is 0-10000Hz. The sampling rate chosen for our study is 32768Hz i.e. 32768 samples were recorded per channel per second. The data

acquisition time was set to 8 seconds to ensure data for enough engine cycle is collected. This acquisition length yielded 262,144 samples per channel.

3.3.4: Bruel & Kjaer Model 5974 Charge Amplifier

An eight-channel charge amplifier was required for data acquisition since we used charge type piezoelectric accelerometers. Charge amplifier converts an input charge signal from the accelerometer into an output voltage to be sent to the data acquisition system for recording. This amplifier allowed direct dial-in of transducer sensitivity in the range of 0.1-10pC per unit acceleration. Detailed specifications of the charge amplifier can be found in *Appendix G: 8-Channel Bruel & Kjaer Model 5974 Charge Amplifier Specifications*.

3.4 Transducer Positioning

Vibration signals are recorded during normal engine operations using accelerometers mounted on the engine at strategic locations where it exhibits good NVH response characteristics. A total of ten accelerometers are used for all engines tested. These are mounted on different locations on the engine since we want to capture the vibration characteristics of the whole engine. Apart from the ten accelerometers, data is also acquired for an additional channel to record the engine speed (rpm) and also the engine cycle position. This is achieved by taking the signal trace for of the engine Cylinder Identification (CID) sensor. The 5.4L 3V engines have two CID sensors, one for each of left and right bank. The CID sensor connector is located on the top portion of the front cover so it was easily accessible in the vehicle. It is a non-contact electromagnetic sensor

that detects the position of the camshaft angle and generates a 5 sinusoidal pulse for each engine cycle. Thus the engine speed (rpm) can be calculated from it and this data can be used for analysis purposes to convert the data from the time domain into the angular domain.

Of the ten accelerometers, four accelerometers are mounted on the engine block with one on each of the manufacturing lugs available on the block: right front lug, right rear lug, left front lug and left rear lug. The aim is to capture all vibrations emanating from bottom part of the engine such as piston, connecting rod related phenomena.

Four accelerometers are mounted on the cylinder head with one on each of the manufacturing lugs available: right front lug, right rear lug, left front lug and left rear lug. This is done to capture all vibrations originating from the cylinder head such as valve tick, lash adjuster, phaser etc. related phenomena.

Since measurements were taken primarily on the locating lugs of the engine, each of the 4 locations on the block and the head will account for information regarding 2 cylinders. Charge type accelerometers are used on all locations on the block and cylinder head so that they can withstand the heat from the exhaust manifold. Figure 3.6 and Figure 3.7 shows the accelerometer locations on the right side and the left side of the engine respectively.

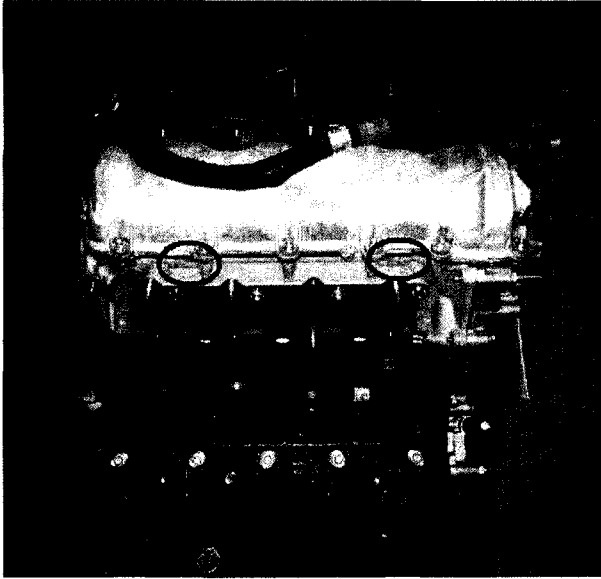


Figure 3.6: Red circles show the location of accelerometers on the right side of engine (2 on the cylinder head lugs and 2 on the engine lugs)

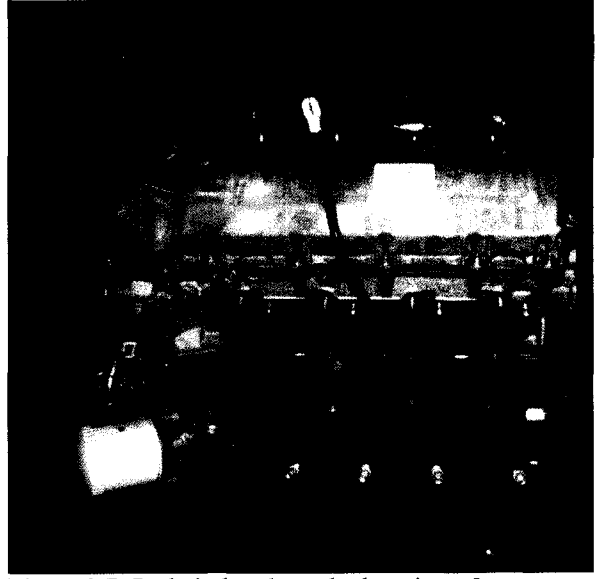


Figure 3.7: Red circles show the location of accelerometer on the left side of engine (2 on the cylinder head lugs and 2 on the engine lugs)

Two ICP type accelerometers are mounted on the front cover. This is done to capture all vibrations emanating from front of the engine such as phaser or chain tensioner related phenomena. Figure 3.8 shows the locations of the accelerometers on the front cover.

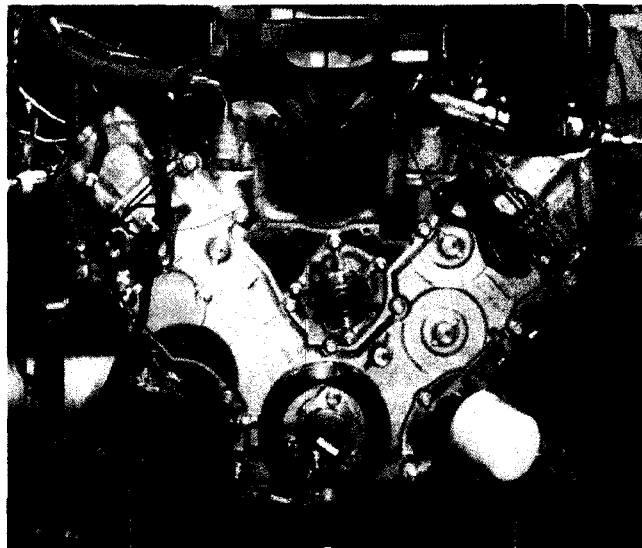


Figure 3.8: Red circles show the location of accelerometers on the front cover (1 on each bank)

These locations are also accessible inside the engine compartment of the vehicle and they are flat making it easy to attach the accelerometers. All of the accelerometers were

mounted using screw-mounted into a brass base and glued to the surface of the engine using extremely strong Loctite super glue. In this study, we will identify these accelerometers with the following naming convention as in Table 3.1:

Channel Name	Accelerometer Location
LugRF	Right Front Engine Block Lug
LugRR	Right Rear Engine Block Lug
LugLF	Left Front Engine Block Lug
LugLR	Left Rear Engine Block Lug
HeadRF	Right Front Cylinder Head Lug
HeadRR	Right Rear Cylinder Head Lug
HeadLF	Left Front Cylinder Head Lug
HeadLR	Left Rear Cylinder Head Lug
FCR	Right Front Cover
FCL	Left Front Cover

Table 3.1: Accelerometer channel naming convention

3.5 Summary

In this chapter, we provide a detailed description of the experimental set up. We determine which types of and how many sensors should be used, where the sensors are going to be placed and which types of hardware should be used for data acquisition. We develop a standard test to ensure that every test is carried out in the same way to reduce variability in data. Sources of variability in the data acquisition process and with the system are identified and minimized as much as possible. Care is taken to reduce any measurement error by eliminating different kinds of noise such as mechanical noise due to vibration, electrical noise due to improper grounding of the data acquisition system or irregularities in the power supply, electromagnetic noise from ambient radiation etc. from the measured vibration signals. We also discuss key data acquisition concepts such as anti-aliasing filtering, signal coupling, quantization and sampling frequency.

CHAPTER 4

DEFECT DETECTION METHOD AND RESULTS

This chapter describes in detail, the defect detection method that was developed, data analysis the results that were obtained during the course of the study. Our goal is to detect and diagnose mechanical defects in engine from vibration signatures of the engine. Vibration signals are recorded during normal engine operations using ten accelerometers mounted on the engine at different locations on the engine. The vibration waveform measurements are then transformed to the crank angle domain and subsequently to the wavelet packets domain from which the features are analyzed for defects.

4.1 Data Processing

There are three main data processing steps that are performed on each set of signal. They are

- i. Transforming Data to Crank Angle Domain
- ii. Data Resampling
- iii. Wavelet Packet Decomposition

4.1.1 Transforming to Crank Angle Domain

The first step of data processing is transforming all time domain data to crank angle domain, as this will help us to correlate any unusual vibration phenomena to a particular events of the engine cycle such as valve or piston position. This is possible as we acquire the signal trace for of the engine Cylinder Identification (CID) sensor simultaneously

with all other accelerometer channels. Figure 4.1 shows the time domain trace for the CID signal and an accelerometer channel.

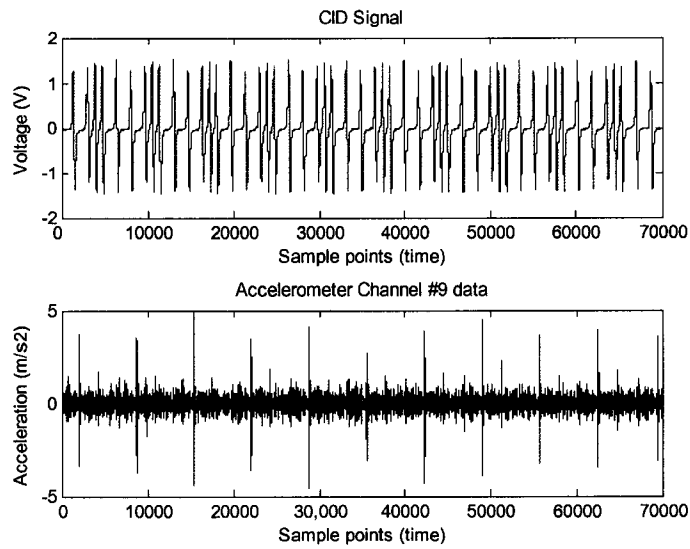


Figure 4.1: CID signal (top plot) and Right Front Cover Accelerometer (bottom)

The CID signal consists of five sinusoidal pulses - 4 equally spaced and 1 odd pulse per engine cycle i.e. 720 degrees of the crank angle. Figure 4.2 shows a zoomed in plot of the CID signal.

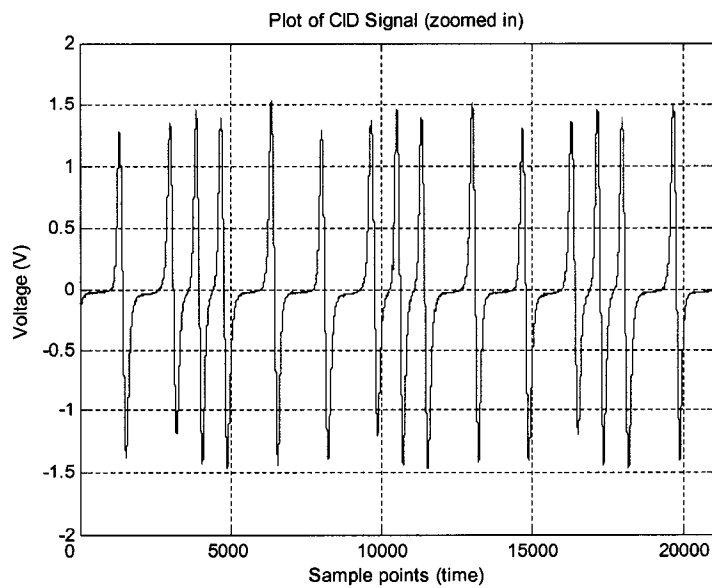


Figure 4.2: CID Signal

Figure 4.3 shows the CID signal and the vibration response recorded by an accelerometer with each engine cycle segments showed in red boxes. The zero crossing of the odd pulse of the CID signal can be used as a reference to 10 degrees after top-dead-center (ATDC) of Cylinder #1 of the engine. Consequently, using this CID signal we can find the zero degree of crankshaft position and divide the time domain data for each accelerometer channels into individual engine cycles as shown in Figure 4.4.

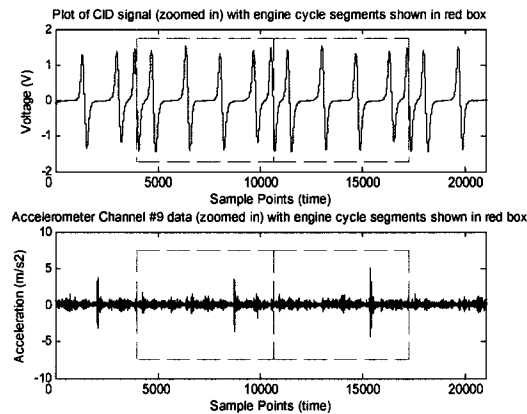


Figure 4.3: CID Signal is used as a reference for the crankshaft position

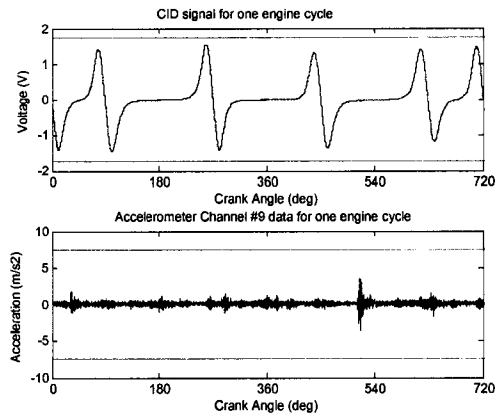


Figure 4.4; Using the CID signal to find the 0 degree TDC of Cylinder #1 and transforming the time domain data into angle domain.

4.1.1.1 Finding the Engine Speed

Since we know the sampling frequency and number of samples taken in between engine cycles, we can also compute the engine speed from the CID signal. Table 4.1 and Figure 4.5 shows this in a table and graph respectively.

CID peak index (sample #)	Number of data samples taken at sampling frequency (Fs) = 32768 for every 90 degrees of Camshaft rotation or 180 degrees of Crankshaft rotation	Seconds/ crank shaft rotation	Engine RPM
1299			
2964	1665	0.0999	601
4632	1668	0.1001	600
6297	1665	0.0999	601
7946	1649	0.0989	607
9574	1628	0.0977	614
11223	1650	0.0990	606
12894	1671	0.1003	599
14546	1651	0.0991	606
16180	1635	0.0981	612
17836	1656	0.0993	604
19519	1683	0.1010	594
21194	1675	0.1005	597
22853	1658	0.0995	603
24529	1676	0.1006	597

Table 4.1 Engine RPM calculation

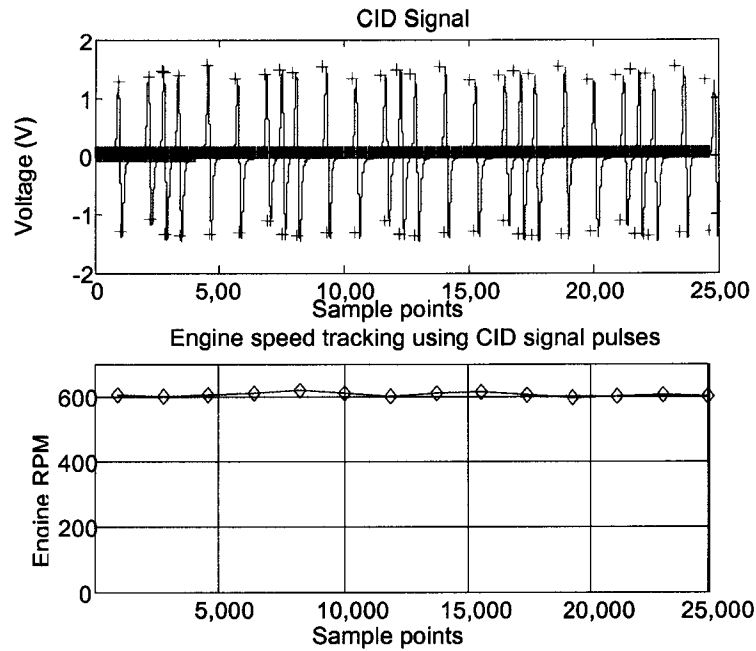


Figure 4.5: Engine RPM tracking

4.1.2 Resampling

The next step of data processing is to resample each trace so that they have same number of points i.e. all signals are have the same length. This is necessary since the engine speed varies from cycle to cycle. (Refer to Table 4.1 and Figure 4.5). Data for every engine cycle for all ten accelerometers is therefore resampled (Figure 4.6) so that each cycle has equal number of points. Each cycle is resampled to 7200 data points. Hence this is the signal length. The number 7200 was chosen to give us 10 sample points per crankshaft degree.

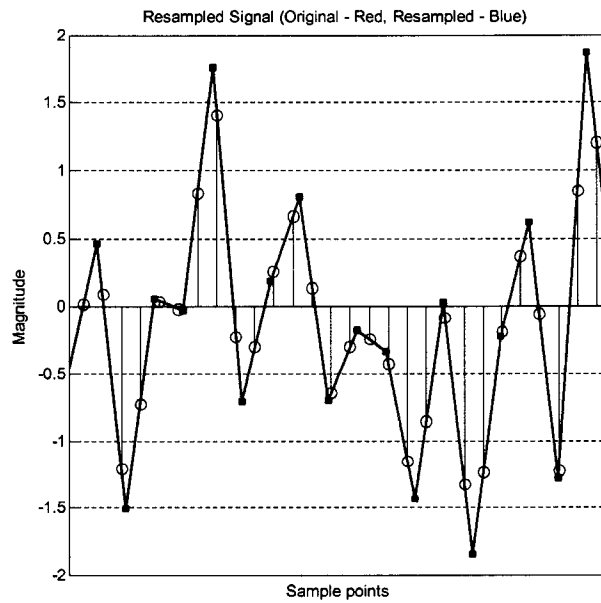


Figure 4.6: Data resampling each engine cycle to 7200 points

4.1.3 Wavelet Packet Decomposition

In previous section, we have discussed that the time domain data gets converted into crank angle domain and broken down further into smaller segments of data representing each engine cycle i.e. 0-720° crank angle (CA). This is done for all 10 accelerometer channels. Furthermore, each of these segments is resampled so that they contain the same number of data point. Wavelet Packet Decomposition of these resampled segments is carried by simple cascade filtering using two analysis filters, a lowpass and a highpass.

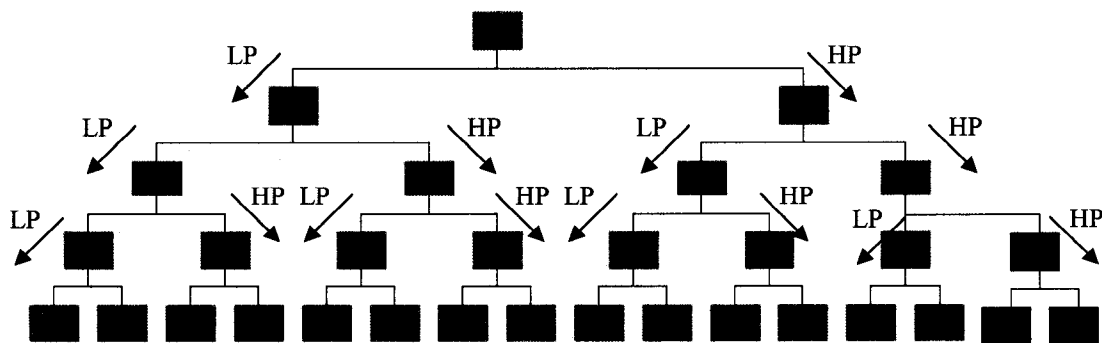


Figure 4.7: Wavelet Packet Decomposition tree representation

The WPD decomposition tree is shown in Figure 4.7 where “A” represents the original signal. At each level of decomposition, the signal is convolved with the impulse response of the halfband LP and HP filters. The result is then subsequently downsampled by a factor of 2 i.e. every other coefficient is ignored. At every subsequent level of decomposition, the vectors are called B_n , C_n , D_n , E_n , F_n , and so on where n represents the position of the wavelet packet. Thus the wavelet vector names at level 1 are B_1 and B_2 and at level 2 are C_1 , C_2 , C_3 and C_4 and so on. This naming order is similar to the conventional $W_{j,k}^n$ nodal representation of the WPD tree and is used as these names are easier to comprehend and makes it easy to work with in our application. Thus so far, in this feature extraction method, we have decomposed a signal from each engine cycle from accelerometers into several wavelet packets.

There are two parameters that we need to decide on before executing the WPD algorithm.

They are

- i. Choosing the mother wavelet
- ii. Determining the number of levels of decomposition

4.1.3.1 Mother Wavelet

There are quite a few mother wavelets available in the literature, such as Morlet wavelet, Mexican hat wavelet, Meyer wavelet, biorthogonal wavelets, the Daubechies wavelets etc. Detailed description about the Daubechies family of mother wavelets can be found in references [Daubechies, 1992]. Each of these mother wavelets possesses unique properties and is suitable for different applications. Ideally, we would like to match the

wavelet to the physics of the problem and it all depends on what type of signal we have and what signal features could be extracted. For vibration related applications Daubechies' family of wavelets is the most widely used when executing DWT and WPT. The Morlet wavelet is the most common in literature when computing CWT.

Daubechies [Daubechies, 1992] developed a family of compactly supported orthonormal mother wavelets based on the solution of a dilation equation. These wavelets have no explicit expression except for Db1, which is the Haar wavelet. The names of the Daubechies family wavelets are written as DbN, where N is the order. Figure 4.8 shows nine members of the family Db2 through Db10:

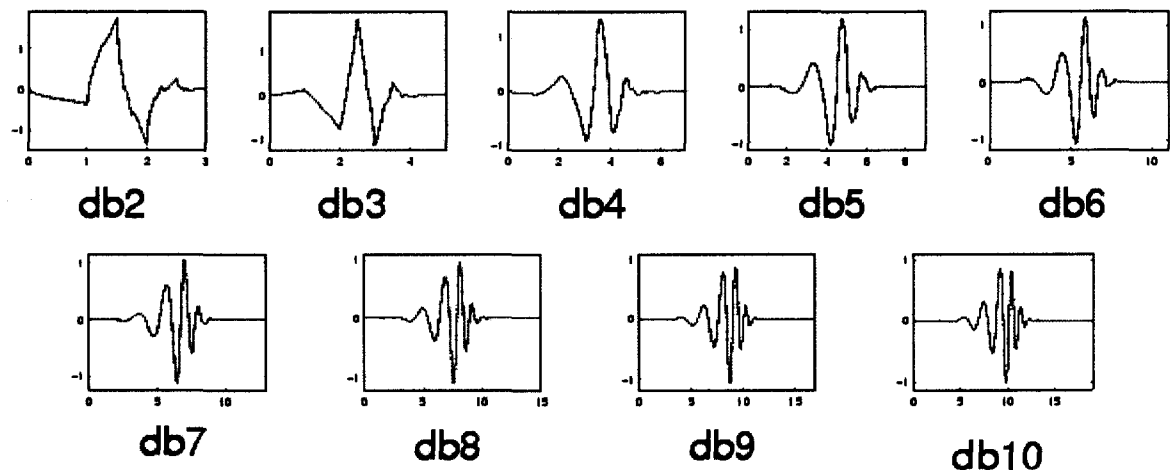


Figure 4.8: Members of the Daubechies wavelet family (Db2 thru Db10) [Matlab]

To capture the time domain abnormalities due to condition change, for example, impulses in the vibration signal caused by impact of faulty components in engines, the wavelet must have good performance on time localization. One important property of the Daubechies' wavelets is that they are compactly supported which is necessary in detecting features from vibration signals. The importance of having a compact support is

that when it is convolved with the signal, we get a localized rather than globalized result. As a result, these wavelets can detect impulse transients hidden in the vibration signal.

The Daubechies' family of wavelets has been extensively used in vibration analysis since its wavelet coefficients capture the maximum amount of the signal energy. Various researchers have used Db4 to Db20 for velocity and vibration signatures but generally higher order wavelets are used when analyzing vibration data as it captures signal characteristics very well. The shape of the wavelets does not change much as we go higher up in order. Db20 has about the same shape as Db5 but with many more oscillations in its tail on both sides. Also, these wavelet bases have a property called orthogonality which means they are completely independent of each other and thus can be added to in any sequence. One advantage of choosing higher order mother wavelets is it provides better frequency resolution. Figure 4.11 and 4.12 shows the magnitude response for the LP and HP filters derived from Db1, Db5, Db10 and Db15. Therefore we can see Db15 has the sharpest roll off and Db1 the least.

On the other hand, the disadvantage of choosing filters with better frequency resolution is that they tend to cause more blurring in the time domain. This blurring may or may not be a problem depending on what we do with the signal. Ultimately, a balance must be achieved between the need to have better frequency isolation and the need of better time resolution. For our applications Db15 is chosen as the mother wavelet because it is compactly supported in the time domain and is sharply localized in the frequency

domain. Figure 4.9 and 4.10 show the impulse response of the halfband LP and HP filters corresponding to Db15 wavelet.

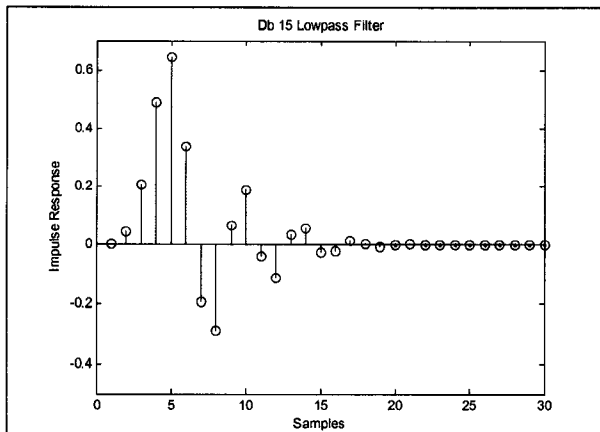


Figure 4.9: Impulse Response of the Db15 lowpass filter

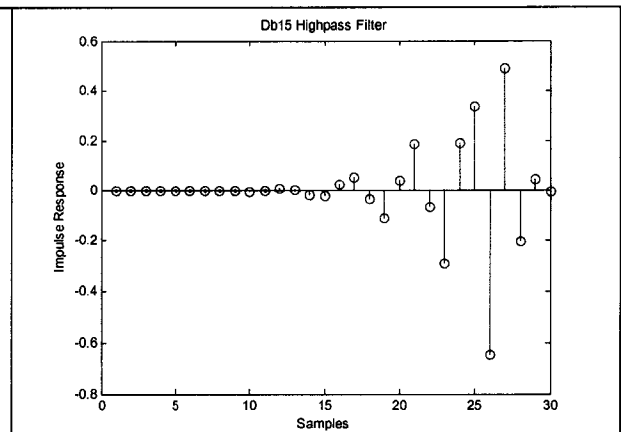


Figure 4.10: Impulse Response of the Db15 highpass filter

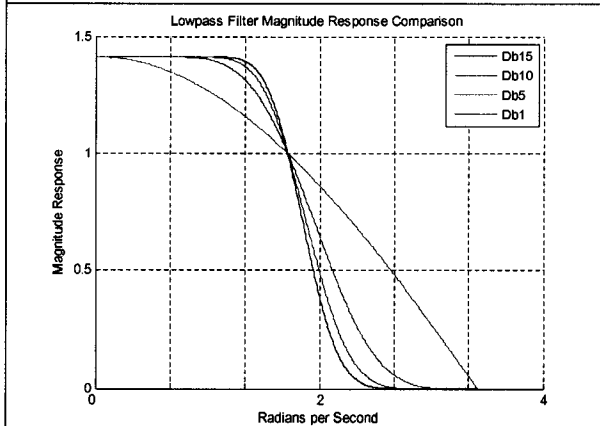


Figure 4.11: Magnitude Response of Db1, Db5, Db10 and Db15 lowpass filters

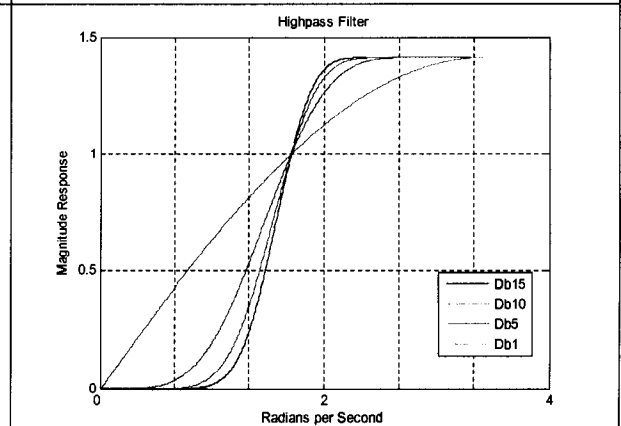


Figure 4.12: Magnitude Response of the Db15 highpass filter

4.1.3.2 Level of Decomposition

Determining of the decomposition level is the other critical issue in the WPT feature extraction process. Generally speaking, as the number of decomposition level is increased, the frequency bandwidth of each wavelet vector decreases. Therefore we gain frequency resolution. Thus, the more levels we decompose the more precisely we can determine the energy concentration of defect as the narrow band is more capable to catch changes. However, at each subsequent decomposition level the time resolution gets

halved. The time information from the WPD data is very important in our application as it represents crank angle. Due to the cyclical operating principle of the engine, a lot of engine defects usually occur at or very close to the same crank angle. This crank angle information can be related to engine events and this helps us in narrowing down the cause of defects. Hence we do not want to lose too much time resolution. Also, we do not want the decomposition level to be too high, as it may not provide any additional information from further decomposition although it will use a lot more processing time. For our application, we will use a decomposition level of 4 as it is found to be adequate for discrimination purposes for the defects under study.

4.1.4 Wavelet Packet Energy

After the vibration signals are decomposed using WPD, the energy of each wavelet vector is computed. This is done by squaring all coefficients of the wavelet packets and the results are then used as features for classification.

4.2 Defect Classification

A threshold is established from taking vibration measurements of good engines and this value is used to discriminate between a good and defective engine. If the engine in question is found to be defective, based on the threshold, we then attempt to classify what type of fault based on the three parameters

- ***Wavelet Packet*** as it provides the frequency bandwidth information of the fault
- ***Crank Angle*** – provides information about location of the fault with respect to engine cycle

- **Dominant Accelerometer** - indicates the general area of the engine where is defect is located

4.3: Engine defects under investigation

In this study, we will attempt to detect several commonly occurring mechanical defects a 5.4L 3V engine caused by 1) Lash Adjuster, 2) Cam Phaser, 3) Chain-tensioner, 4) Piston-Rod Wristpin and 5) Non-cleanup of Bore. The aim is to not only identify if an engine is good or bad but also to determine which is the faulty component so the engine can be repaired by replacing. There are 44 different defects that we want to identify –

- 24 Lash Adjusters (16 for Intake Valves and 8 for Exhaust Valves),
- 2 Cam Phasers (1 each for Right and Left Bank),
- 2 Chain-Tensioners (1 each for Right and Left Bank),
- 8 Piston/Rod (1 per Cylinder) and
- 8 Bore Non-cleanup (1 per cylinder).

Table 4.2 provides a summary of location of all 44 defects.

Defects	Total #	Locations							
		1 int	2 int	3 int	4 int	5 int	6 int	7 int	8 int
Lash Adjusters	16	1 int	2 int	3 int	4 int	5 int	6 int	7 int	8 int
	8	1 exh	2 exh	3 exh	4 exh	5 exh	6 exh	7 exh	8 exh
Phasers	2	Right Bank	Left Bank						
Chain Tensioners	2	Right Bank	Left Bank						
Piston/Rod	8	Cyl 1	Cyl 2	Cyl 3	Cyl 4	Cyl 5	Cyl 6	Cyl 7	Cyl 8
Non-Cleanup	8	Cyl 1	Cyl 2	Cyl 3	Cyl 4	Cyl 5	Cyl 6	Cyl 7	Cyl 8
	44								

Table 4.2: Engine defects under investigation

In order to discriminate between different defects, each type of defect is made associated with a fault number. Table 4.3 provides a summary of the different fault numbers.

Defect Description	Fault #	Defect Description	Fault #
Cylinder#1 Intake Rear Lash Adjuster	1	Cylinder#8 Intake Front Lash Adjuster	23
Cylinder#1 Intake Front Lash Adjuster	2	Cylinder#8 Exhaust Lash Adjuster	24
Cylinder#1 Exhaust Lash Adjuster	3	Right Bank Cam Phaser	25
Cylinder#2 Intake Rear Lash Adjuster	4	Left Bank Cam Phaser	26
Cylinder#2 Intake Front Lash Adjuster	5	Right Bank Chain Tensioner	27
Cylinder#2 Exhaust Lash Adjuster	6	Left Bank Chain Tensioner	28
Cylinder#3 Intake Rear Lash Adjuster	7	Cylinder #1 Piston/Rod	29
Cylinder#3 Intake Front Lash Adjuster	8	Cylinder #2 Piston/Rod	30
Cylinder#3 Exhaust Lash Adjuster	9	Cylinder #3 Piston/Rod	31
Cylinder#4 Intake Rear Lash Adjuster	10	Cylinder #4 Piston/Rod	32
Cylinder#4 Intake Front Lash Adjuster	11	Cylinder #5 Piston/Rod	33
Cylinder#4 Exhaust Lash Adjuster	12	Cylinder #6 Piston/Rod	34
Cylinder#5 Intake Rear Lash Adjuster	13	Cylinder #7 Piston/Rod	35
Cylinder#5 Intake Front Lash Adjuster	14	Cylinder #8 Piston/Rod	36
Cylinder#5 Exhaust Lash Adjuster	15	Cylinder #1 Non Cleanup	37
Cylinder#6 Intake Rear Lash Adjuster	16	Cylinder #2 Non Cleanup	38
Cylinder#6 Intake Front Lash Adjuster	17	Cylinder #3 Non Cleanup	39
Cylinder#6 Exhaust Lash Adjuster	18	Cylinder #4 Non Cleanup	40
Cylinder#7 Intake Rear Lash Adjuster	19	Cylinder #5 Non Cleanup	41
Cylinder#7 Intake Front Lash Adjuster	20	Cylinder #6 Non Cleanup	42
Cylinder#7 Exhaust Lash Adjuster	21	Cylinder #7 Non Cleanup	43
Cylinder#8 Intake Rear Lash Adjuster	22	Cylinder #8 Non Cleanup	44

Table 4.3: Defect Description and the associated fault number

4.4 Good and Defective Engine

A good engine can be defined as one that functions properly, has no usual levels of vibration or vibration spikes and has no audible knock. Figure 4.13 shows the vibration level of a good engine.

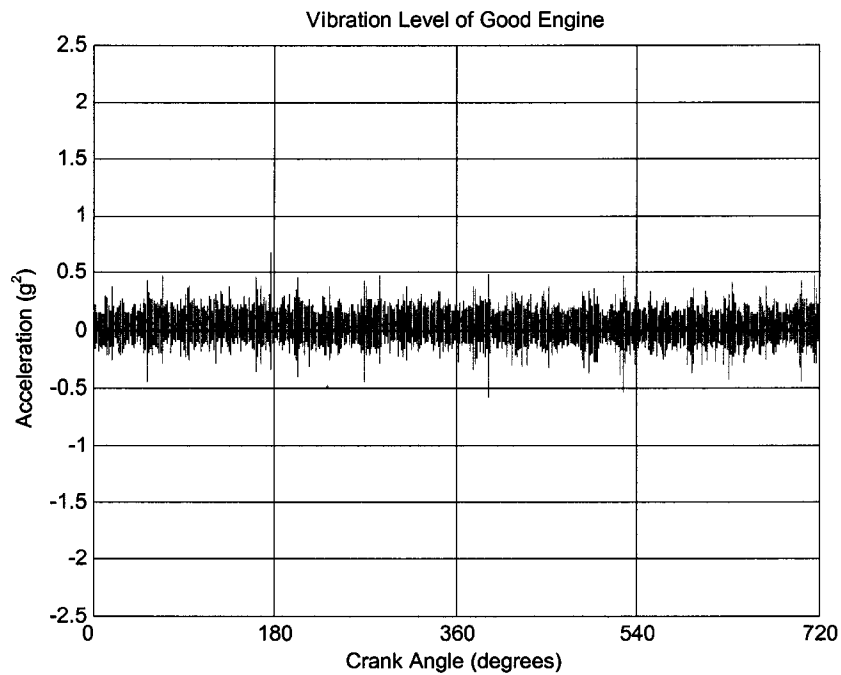


Figure 4.13: Vibration level of good engine

A total of 30 good engines were tested and the normal vibration level of a good engine was established. The amplitude of vibration from a good engine ranges from $-1.0g^2$ to $+1.0g^2$.

Figure 4.14 shows the wavelet packet coefficients of vibration signal from a good engine at decomposition level = 4.

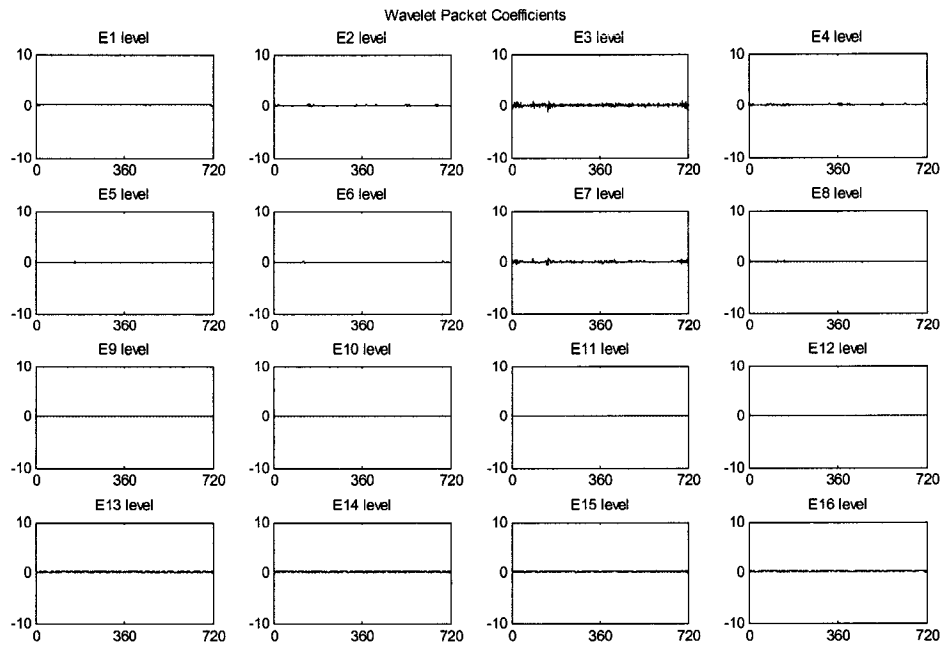


Figure 4.14: WPD Coefficients of vibration signal from a good engine

Figure 4.15 show WPD packet energy of the same signal, which is computed by taking the square of the coefficients. Squaring the coefficients also helps in suppressing the noise level in the vibration signal as it is within a range of ± 1 . Also, from these results, the threshold value that we will use to differentiate between good engine and defective engine is determined to be 5.

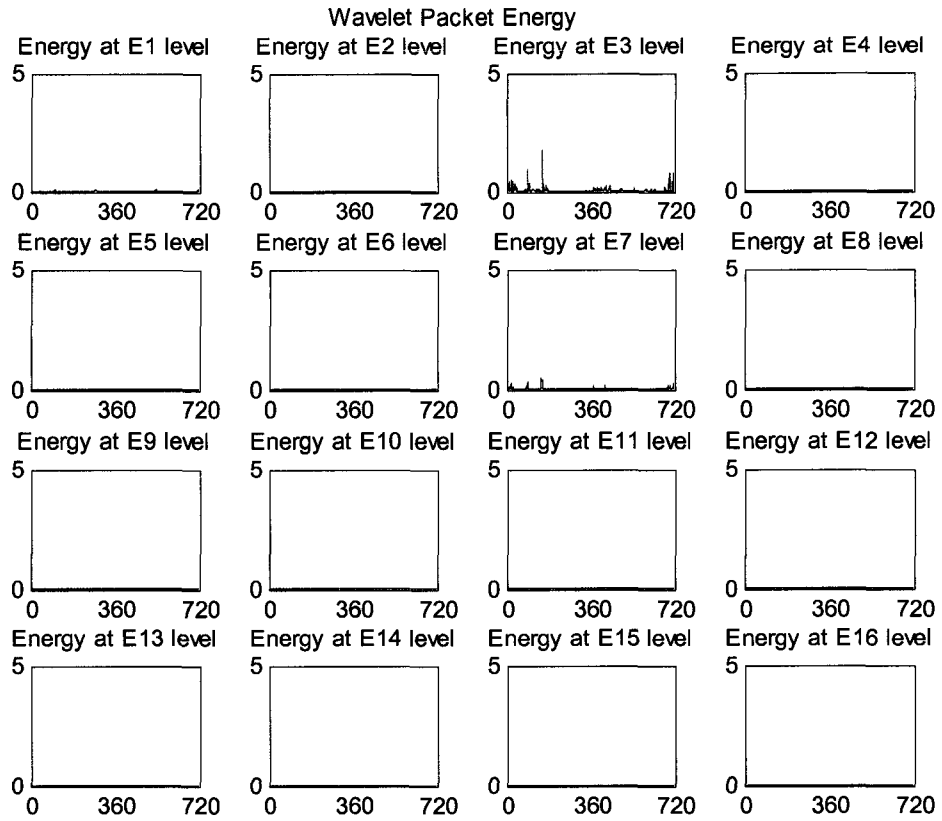


Figure 4.15: WPD packet energy of vibration signal from a good engine

4.5 Engine Defect Vibration Signature Types

Engine defects vibration signatures are usually of two kinds – single vibration spike per engine cycle (Figure 4.16) or multiple vibration spikes (Figure 4.17). Defective cam phasers and lash adjusters usually result in single spikes where as a defective chain tensioner or cylinder non-cleanup results in multiple vibration spikes per engine cycle.

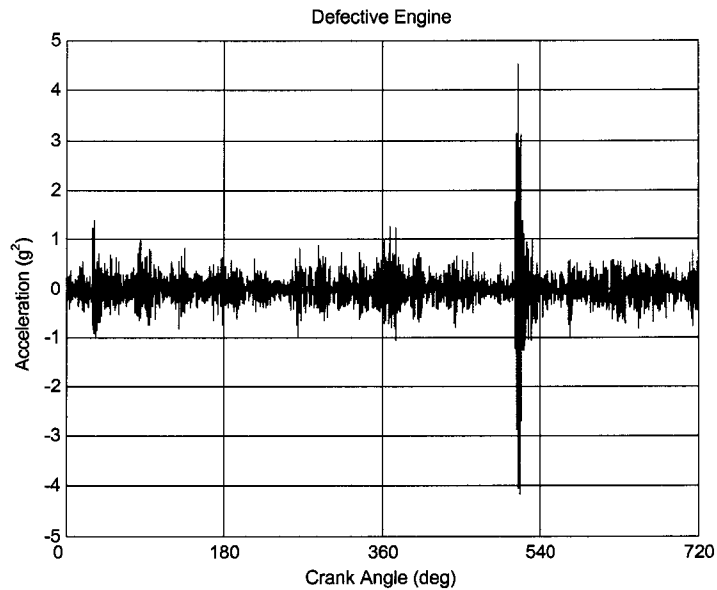


Figure 4.16: Single vibration spike per engine cycle.

Figure 4.16 shows the overlay of the vibration signal of a good and defective engine from the same transducer location (LugLF). The defective engine has bottom end knock and has multiple vibration spikes resulting from impacts between components and they occur at different crank angles. It is evident from the graph that the vibration magnitude of the defective engine is much higher when defects are present. Defective chain-tensioner, non-cleanup and piston slap may cause multiple vibration spikes per engine cycle.

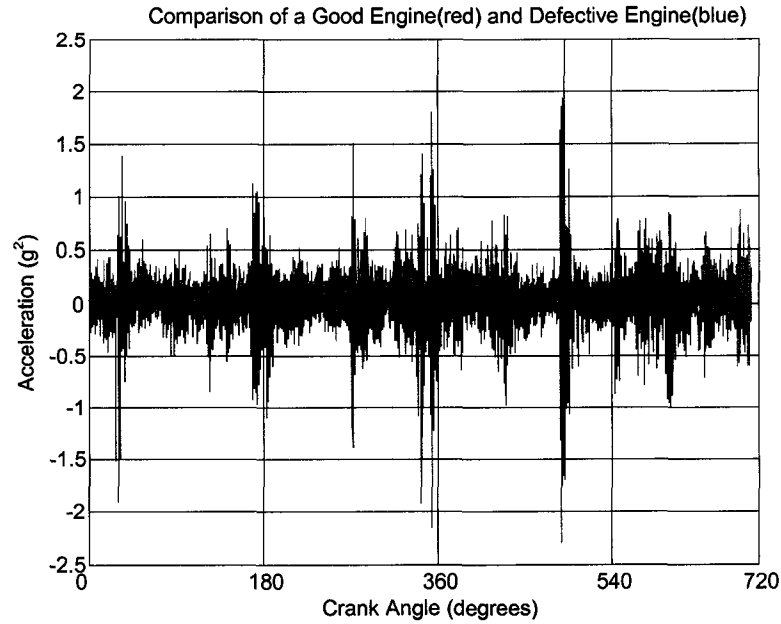


Figure 4.17: Comparison of vibration signal from a good engine (red) and defective engine (blue) with multiple vibration spikes.

The defect may also show up intermittently or may be present consistently at every engine cycle. Figure 4.18 shows a waterfall variance plot of vibrations resulting from a defective lash adjuster. The vibration spikes are consistently present at every engine cycle, occurring at approximately the same crank angle. Figure 4.19 shows a waterfall variance plot of vibration resulting from a piston wrist pin. We can see that the vibration spikes are only occurring intermittently.

To process every single engine cycle for all accelerometer will yield a lot of redundant information. This is especially true in the case of defective lash adjuster as the defect is present in every cycle. So a more efficient way to find the defect is to calculate the energy of each engine cycle and pick the cycle with the highest energy and is decomposed using WPD for feature extraction. This in essence will cut down the computation time drastically and still yield the same result.

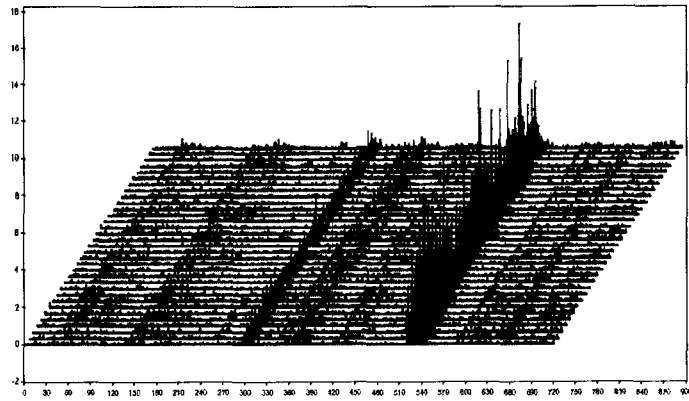


Figure 4.18: Waterfall Variance plot for 30 engine cycles

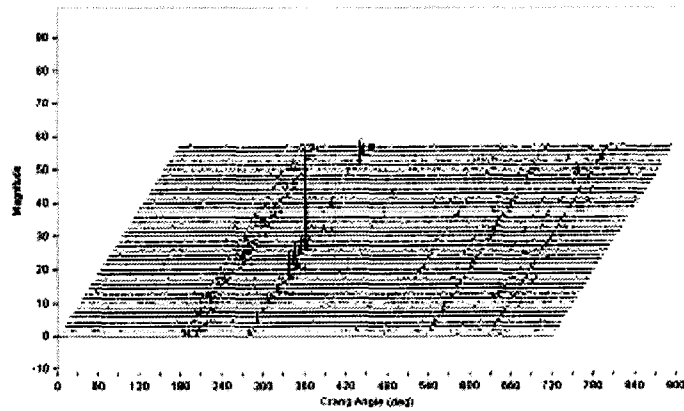


Figure 4.19: Waterfall Variance plot for 30 engine cycles

4.6 Engine Fault Detection System

A total of 30 cases of each type of known defect are tested under the same operating condition. The data from these engines with each type of fault is used to build a fault database (Table 4.4). Each fault is mapped to a 3D space comprising of the wavelet packet(s), crankshaft angle and dominant accelerometer identification. The selected wavelet packets only include those packets whose energies are affected by the presence of the fault of interest. The crank angle values represent where these faults roughly

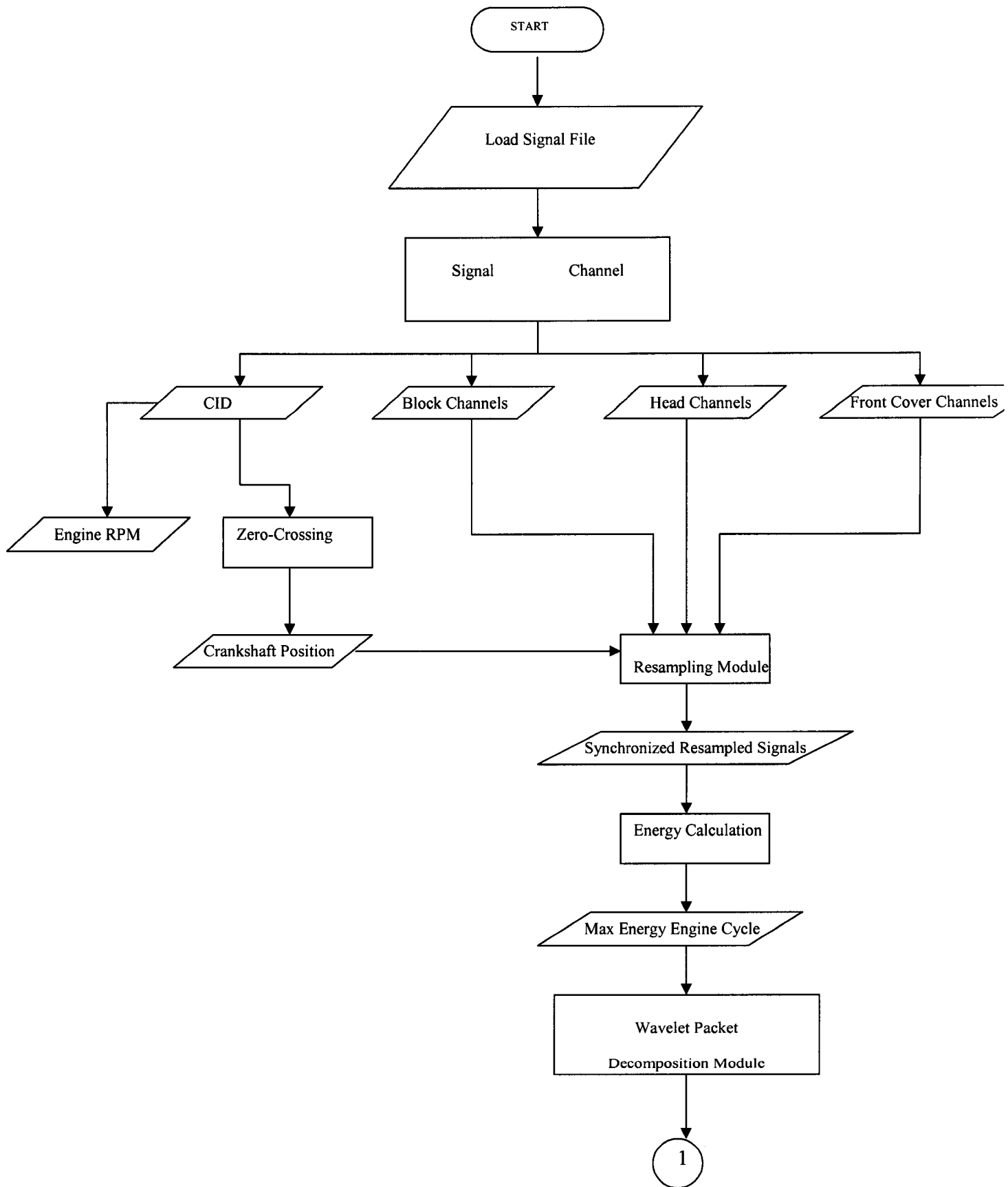
occurs with reference to the crankshaft angle. A tolerance of +/- 10 degrees of crank angle is used when analyzing any test signals. The accelerometer ID indicates where the fault is localized within the engine. Two most dominant accelerometers are chosen that have the highest average variance and best represent the fault. Of these two accelerometers, data for only one engine cycle from the most dominant accelerometer is decomposed using WPD. Only the proximity information from the second accelerometer is used. It comes into play only when there is a tie in the decision making process regarding the fault number, based on the information from the fault database. A Matlab based Graphical User Interface (GUI) is developed to detect and diagnose fault. This program runs fault diagnosis on the engine vibration signal, extract all necessary information that is needed to detect the fault, compares with the fault database and generates the fault description and code. If the program finds a spike greater than the fault threshold and is not in the database, it generates a warning message. If no abnormal vibration spikes are present in the data, engine is declared to be good. Section 4.6.1 shows the pseudo code flowchart for the Engine Fault Detection System.

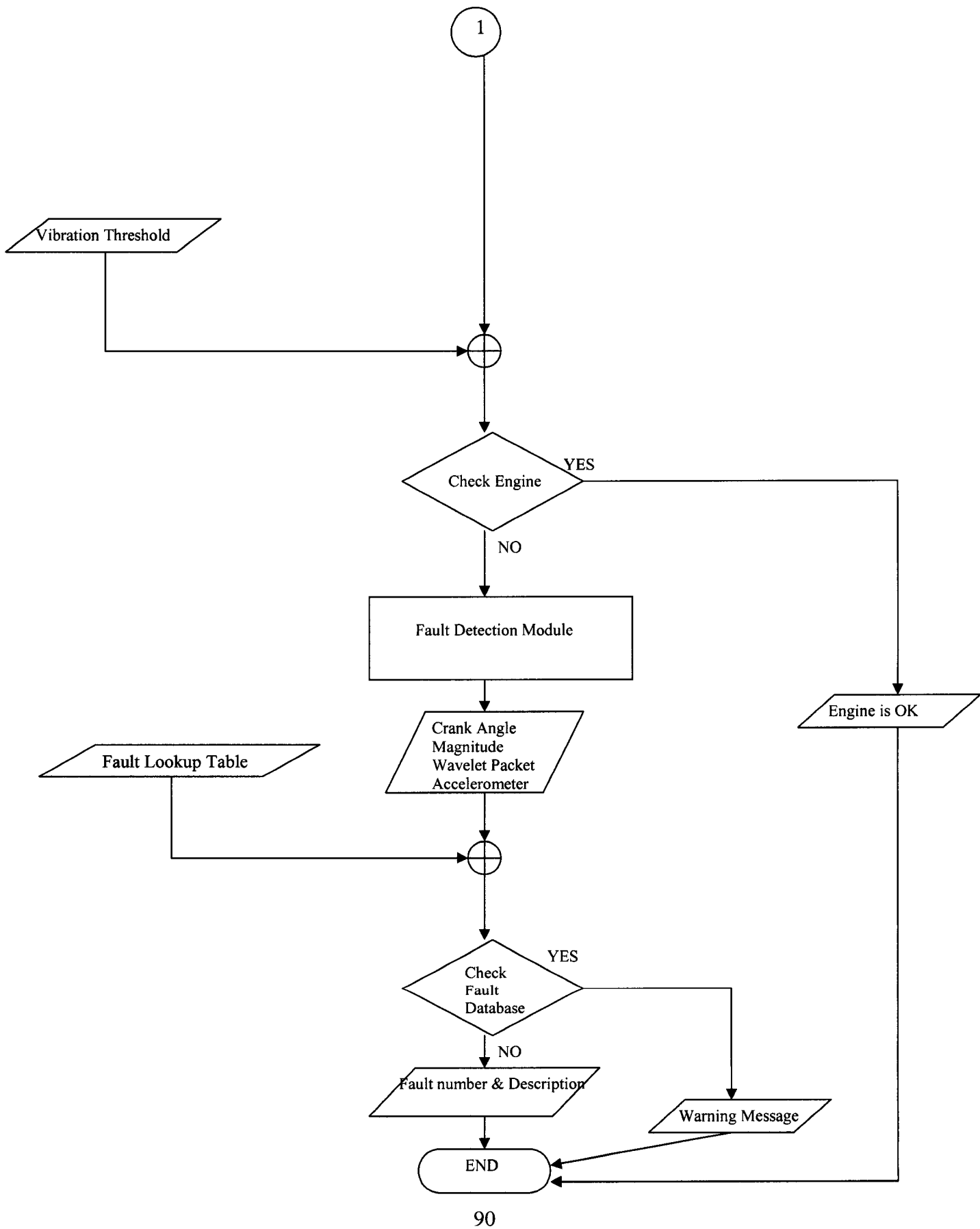
Fault Description	Fault #	Accelerometer		Fault Crank		Dominant Wavelets		
		Most Dominant (A)	2nd Most Dominant (B)	Angle +/- 10 Degrees		Packets in (A)		
Cylinder#1 Intake Rear LA	1	HeadRF	FCR	580	360	E3	E4	-
Cylinder#1 Intake Front LA	2	HeadRF	FCR	580	360	E3	E4	-
Cylinder#1 Exhaust LA	3	HeadRF	FCR	370	100	E13	E14	-
Cylinder#2 Intake Rear LA	4	HeadRF	HeadRR	140	620	E2	E4	-
Cylinder#2 Intake Front LA	5	HeadRF	HeadRR	140	620	E2	E4	-
Cylinder#2 Exhaust LA	6	HeadRF	HeadRR	370	650	E13	E14	-
Cylinder#3 Intake Rear LA	7	HeadRR	HeadRF	680	440	E2	E4	-
Cylinder#3 Intake Front LA	8	HeadRR	HeadRF	680	440	E2	E4	-
Cylinder#3 Exhaust LA	9	HeadRR	HeadRF	470	200	E13	E14	-
Cylinder#4 Intake Rear LA	10	HeadRR	HeadRF	390	180	E3	E4	-
Cylinder#4 Intake Front LA	11	HeadRR	HeadRF	390	180	E3	E4	-
Cylinder#4 Exhaust LA	12	HeadRR	HeadRF	200	640	E13	E14	-
Cylinder#5 Intake Rear LA	13	HeadLF	FCL	330	70	E3	E4	-
Cylinder#5 Intake Front LA	14	HeadLF	FCL	330	70	E3	E4	-
Cylinder#5 Exhaust LA	15	HeadLF	FCL	100	550	E5	E13	-
Cylinder#6 Intake Rear LA	16	HeadLF	HeadLR	230	690	E3	E4	-
Cylinder#6 Intake Front LA	17	HeadLF	HeadLR	230	690	E3	E4	-
Cylinder#6 Exhaust LA	18	HeadLF	HeadLR	20	460	E13	E5	-
Cylinder#7 Intake Rear LA	19	HeadLR	HeadLF	60	530	E2	E4	-
Cylinder#7 Intake Front LA	20	HeadLR	HeadLF	60	530	E2	E4	-
Cylinder#7 Exhaust LA	21	HeadLR	HeadLF	540	270	E14	E13	-
Cylinder#8 Intake Rear LA	22	HeadLR	HeadLF	490	250	E3	E4	-
Cylinder#8 Intake Front LA	23	HeadLR	HeadLF	490	250	E3	E4	-
Cylinder#8 Exhaust LA	24	HeadLR	HeadLF	270	30	E13	E14	-
Right Bank Cam Phaser	25	FCR	HeadRF	520	45	E6	E8	-
Left Bank Cam Phaser	26	FCL	HeadRF	660	150	E6	E8	-
Right Bank Chain Tensioner	27	FCR	LugRF	-	-	E7	-	-
Left Bank Chain Tensioner	28	FCL	LugLF	-	-	E7	-	-
Cylinder #1 Piston/Rod	29	LugRF	LugRR	10	370	E5	E6	-
Cylinder #2 Piston/Rod	30	LugRF	LugRR	280	640	E5	E6	-
Cylinder #3 Piston/Rod	31	LugRR	LugRF	100	460	E7	E8	-
Cylinder #4 Piston/Rod	32	LugRR	LugRF	370	10	E7	E8	-
Cylinder #5 Piston/Rod	33	LugLF	LugLR	460	100	E5	E6	-
Cylinder #6 Piston/Rod	34	LugLF	LugLR	550	910	E5	E6	-
Cylinder #7 Piston/Rod	35	LugLR	LugLF	190	550	E7	E8	-
Cylinder #8 Piston/Rod	36	LugLR	LugLF	660	300	E7	E8	-
Cylinder #1 Non Cleanup	37	LugRF	LugRR	-	-	-	-	-
Cylinder #2 Non Cleanup	38	LugRF	LugRR	-	-	-	-	-
Cylinder #3 Non Cleanup	39	LugRR	LugRF	-	-	-	-	-
Cylinder #4 Non Cleanup	40	LugRR	LugRF	-	-	-	-	-
Cylinder #5 Non Cleanup	41	LugLF	LugLR	-	-	-	-	-
Cylinder #6 Non Cleanup	42	LugLF	LugLR	-	-	-	-	-
Cylinder #7 Non Cleanup	43	LugLR	LugLF	-	-	-	-	-
Cylinder #8 Non Cleanup	44	LugLR	LugLF	-	-	-	-	-

*LA = Lash Adjuster

Table 4.4: Fault Database Table

4.6.1 Engine Fault Detection System Pseudo Code





4.7 Graphical User Interface

This section provides a brief description of the user-friendly Matlab based Graphical User Interface (GUI) that has been developed for analysis of data. The name of the program is called Engine Fault Detection Software (EFDS). The following screen shots of the program are provided along with the steps to run the diagnosis on the vibration data from any engine.



Figure 4.20: Engine Fault Detection Software Welcome Screen

There is a menu bar available with menus such as *File*, *Threshold*, *Load Input Signals*, *Fault Diagnostics Module*, *Results* and *Help*.

Under the **File** Menu, the following options are available:

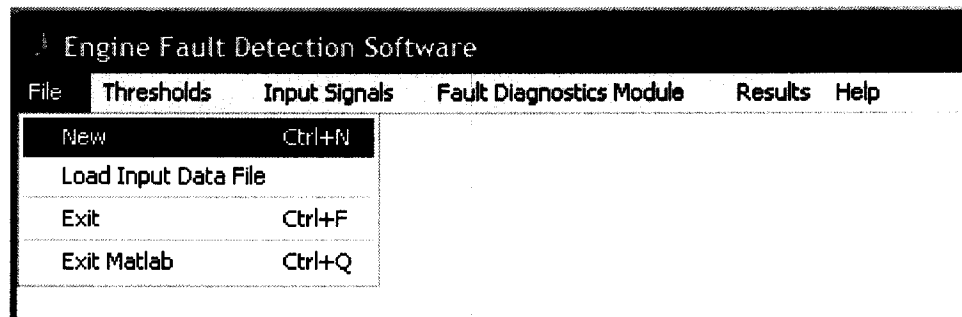


Figure 4.21: Options under File Menu

- **New** – To start a new analysis for engine. This clears the memory and initializes all variables that are necessary to run any analysis.
- **Load Input Data File** - Lets the user to select and load the data file containing the 10 channels of vibration signals of an engine that was collected using Prosig 5600 Data Acquisition System. Upon loading the file, program automatically converts the time domain data to crank angle domain and resample data for all channel and for each engine cycle.

Threshold – lets user enter threshold value of features to be used to distinguish between Good or Defective Engine

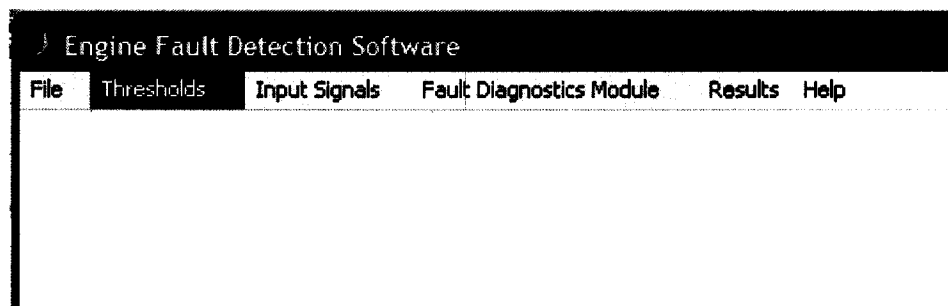


Figure 4.22: Threshold Menu

Input Signal menu lets user select the accelerometer to run the fault diagnostic module on. There are 10 accelerometers: 4 Engine Block Lugs, 4 Cylinder Head Lugs and 2 Front Cover.

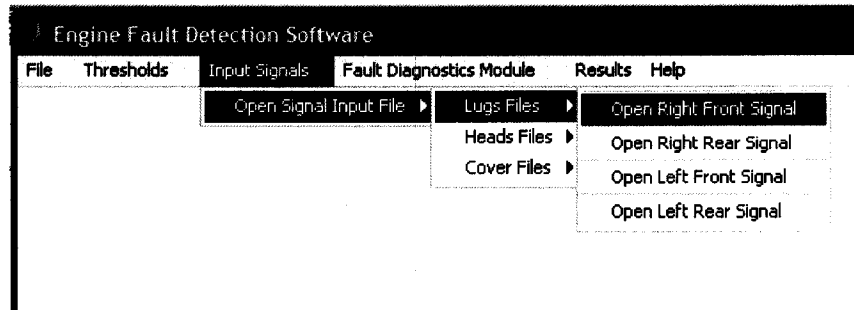


Figure 4.23: Selecting Engine Block Lug Accelerometers

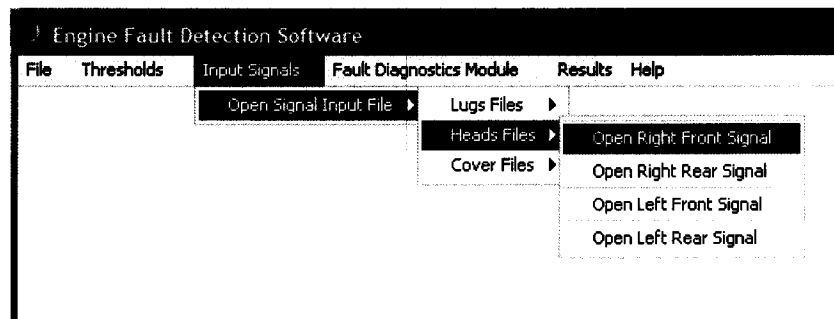


Figure 4.24: Selecting Cylinder Head Lug Accelerometers

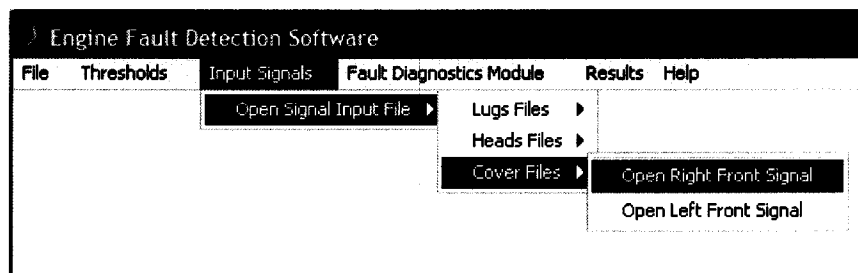


Figure 4.25: Selecting the Front Cover Accelerometers

Upon selecting the signal, the wavelet packet tree is computed on the engine cycle that has the highest energy content. This way user has the option to select and view results for the accelerometer of interest and it also cuts down on the computation time drastically.

Fault Diagnostics Module menu runs the diagnostics on the engine to detect any possible defect. After the diagnostics are done, a message is displayed that results are ready to be viewed.

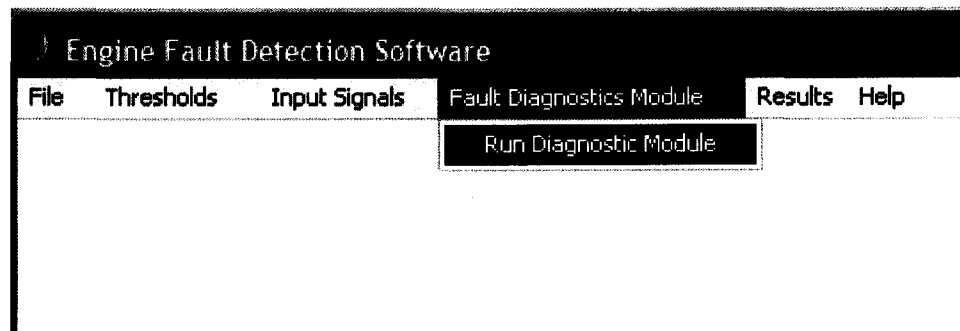


Figure 4.26: Running Fault Diagnostic Module



Figure 4.27: Running diagnostics is finished

All results such as fault codes and possible warning can be viewed after the diagnostics are done.

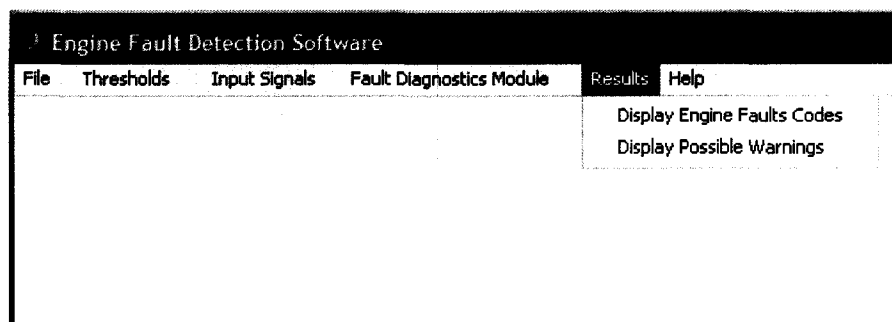


Figure 4.28: Display results and warnings

Results will display the appropriate diagnostics messages indicating good engines or if any possible faults or warning flags detected



Figure 4.29: Displaying message indicating that the vibration signature recorded by the accelerometer does not match the signature of any known defect and vibration level is below threshold level hence it is a good engine.



Figure 4.31: Displaying message indicating that the energy content of the vibration signal recorded by the accelerometer is within limits of the threshold and there is no vibrations spikes are present that is over the threshold for any crank angle.



Figure 4.30: Displaying message indicating a fault is detected to be present for the particular accelerometer and it matches the signature of a known fault. The message shows the fault number along with the fault description



Figure 4.32: Message displayed when a vibration spike is detected at crank angle(s) or wavelet packet(s) that is not in the fault database.

4.8: Case Studies

In this section, we will discuss the results from case studies of different defects present in engines.

4.8.1 Case Study 1: Defective Right Cam Phaser

Vibrations from a defective right cam phaser is best detected by the right front cover accelerometer (FCR). Hence it is the most dominant accelerometer followed by the HeadRF accelerometer. The maximum variance values for all accelerometer for the engine in case study is given in Table 4.5.

Accelerometer	Maximum Variance
FCR	8
HeadRF	2.8
HeadRR	1.6
FCL	1.3
HeadLF	0.8
HeadLR	0.8
LugRF	0.4
LugLR	0.3
LugRR	0.2
LugLF	0.2

Table 4.5: Maximum variance for each accelerometer channels

The time domain data from FCR and the waterfall plot of running variance for 40 engine cycles for the engine is shown in Figure 4.33 and Figure 4.34 respectively.

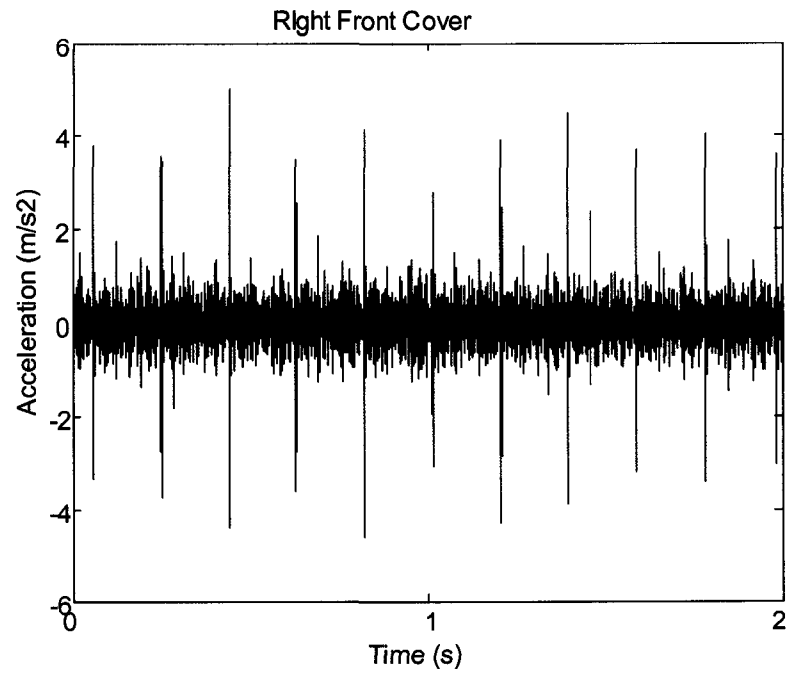


Figure 4.33: Vibrations recorded by FCR accelerometer

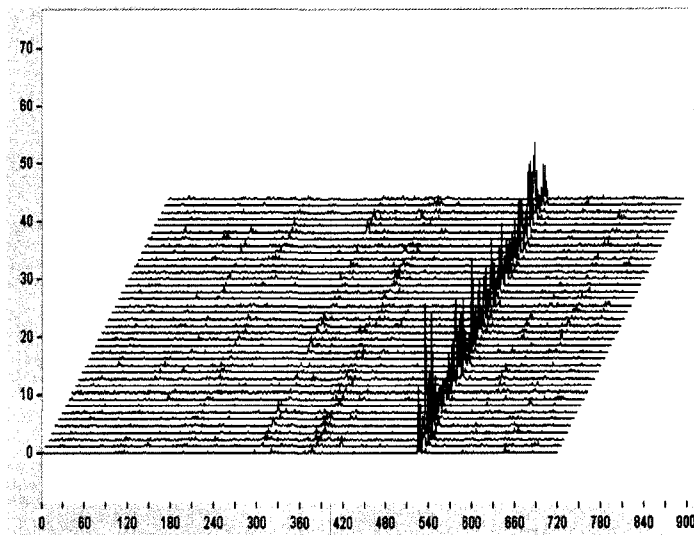


Figure 4.34: Running variance waterfall of FCR recorded vibrations for 40 engine cycles

We can see that the engine has a vibration spike occurring consistently for all engine cycles at approximately 515 degrees crank angle. The engine cycle with the maximum energy content is chosen and decomposed using WPD. The wavelet packet coefficients

and packet energies for all packets at level 4 are shown in Figure 4.35 and Figure 4.36 respectively.

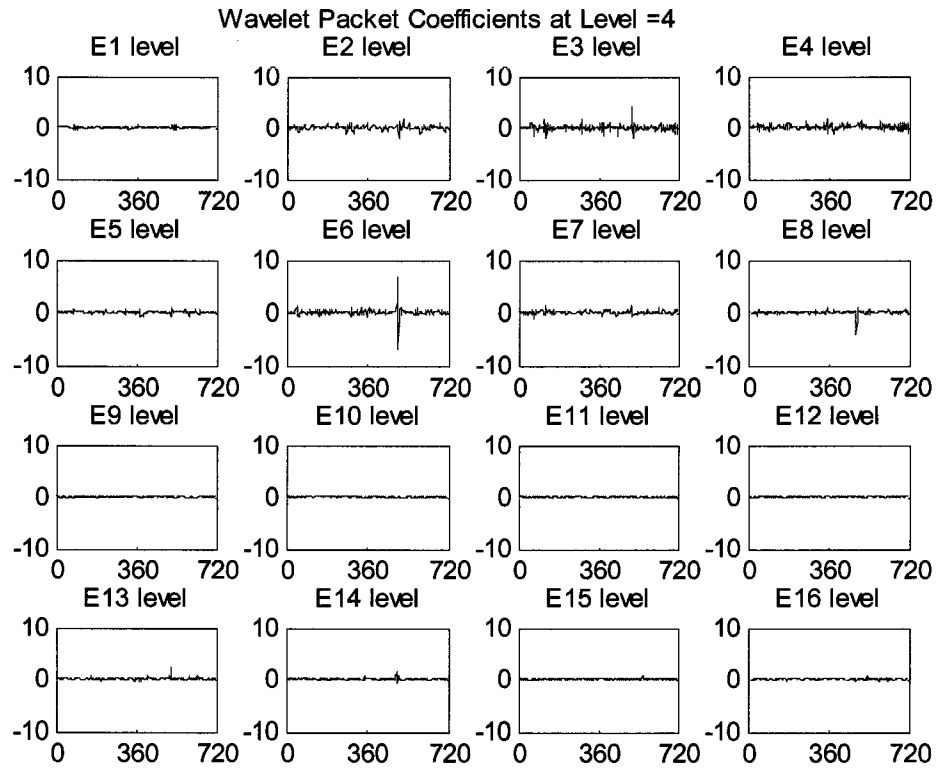


Figure 4.35: Wavelet packet coefficients

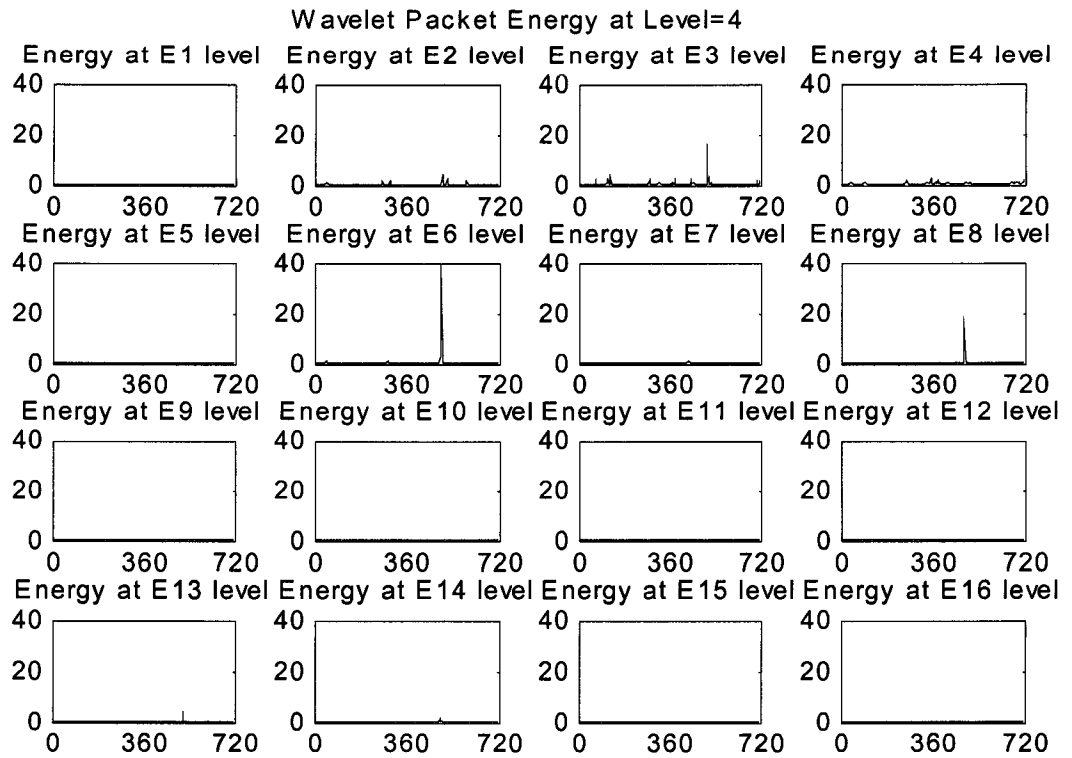


Figure 4.36: Wavelet packet energy

We can see from Figure 4.36 that most of the energy of the vibration generated by the fault is in the frequency bandwidth of E6 wavelet packet. There is also some energy in wavelet packets E8 and E3. The fault threshold for all engines is set at 5, which was established from vibration levels of good engines. Levels E6 and E8 clearly exceeds the set fault threshold. Furthermore, The vibration spike occurs at 515 degrees crank angle, which is within the 520 degrees +/-10 degrees tolerance level of a known defect. Therefore the defect corresponds to Fault #25 (Right Bank Cam Phaser) in the fault database (Table 4.6)

[REDACTED]								
Right Bank Cam Phaser	25	FCR	HeadRF	520	45	E6	E8	-

Table 4.6: Fault parameters for defective right bank cam phaser

4.8.2 Case Study 2: Defective Right Chain Tensioner

The vibrations from a defective right chain tensioner is best picked up by the right front cover accelerometer (FCR). Hence it is the most dominant accelerometer followed by the LugRF accelerometer. The maximum variance values for all accelerometer for the engine in case study is given in Table 4.7.

Accelerometer	Maximum Variance
FCR	9
LugRF	5.1
FCL	3.2
LugRR	1.6
HeadRF	0.9
HeadRR	0.8
HeadLF	0.8
HeadLR	0.3
LugLR	0.2
LugLF	0.2

Table 4.7: Maximum variance for each accelerometer channels

The time domain data and the waterfall plot of running variance for 40 engine cycles for the engine is shown in Figure 4.37 and Figure 4.38 respectively.

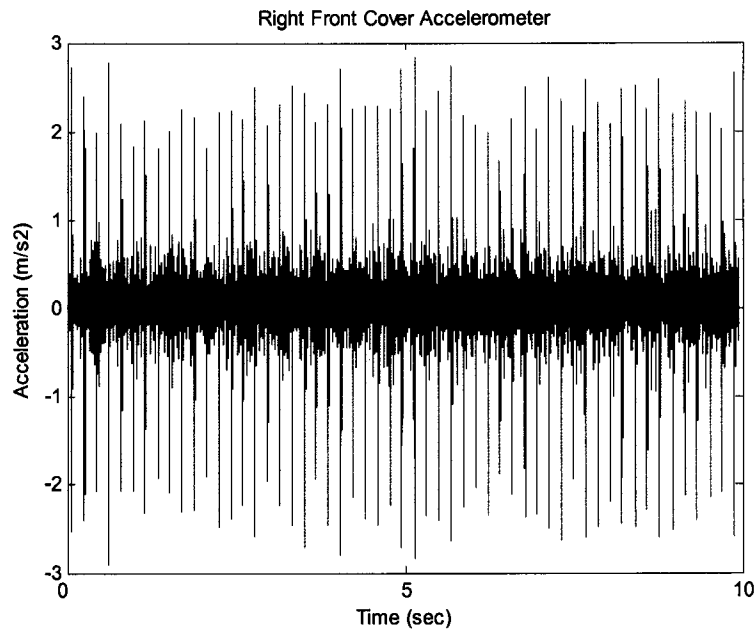


Figure 4.37: Vibrations recorded by FCR accelerometer

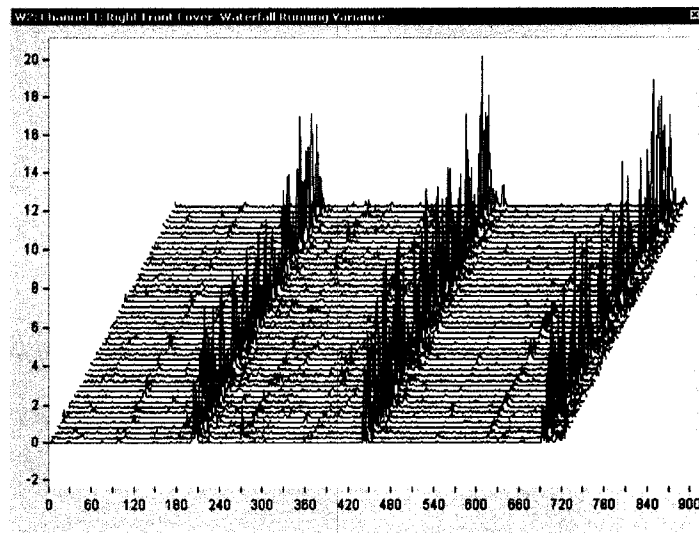


Figure 4.38: Running variance waterfall of FCR recorded vibrations for 40 engine cycles

We can see that the engine has a 3 vibration spikes occurring consistently for all engine cycles at approximately 200, 430 and 680 degrees crank angle. The engine cycle with the maximum energy content is chosen and decomposed using WPD. The plot of vibration amplitude from FCR for one engine cycle is shown in Figure 4.39.

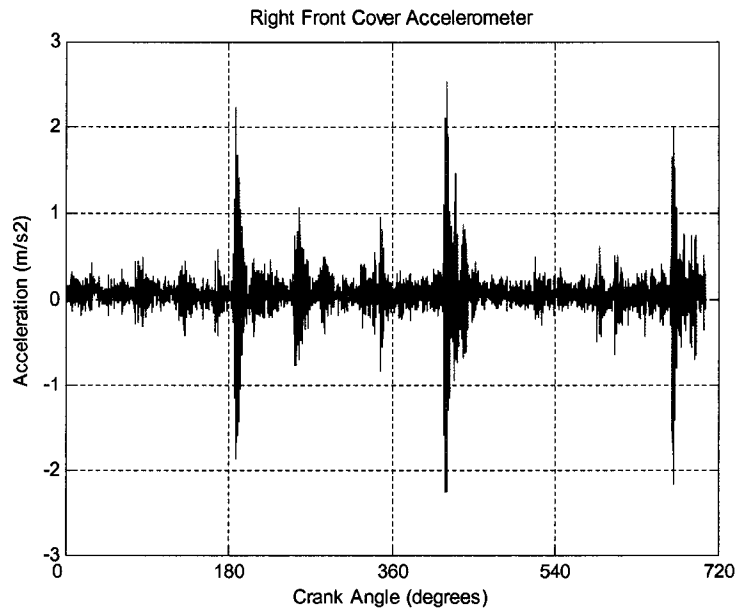


Figure 4.39: Vibration amplitudes for 1 engine cycle

The wavelet packet coefficients and packet energies for all packets at level 4 are shown in Figure 4.40 and Figure 4.41 respectively.

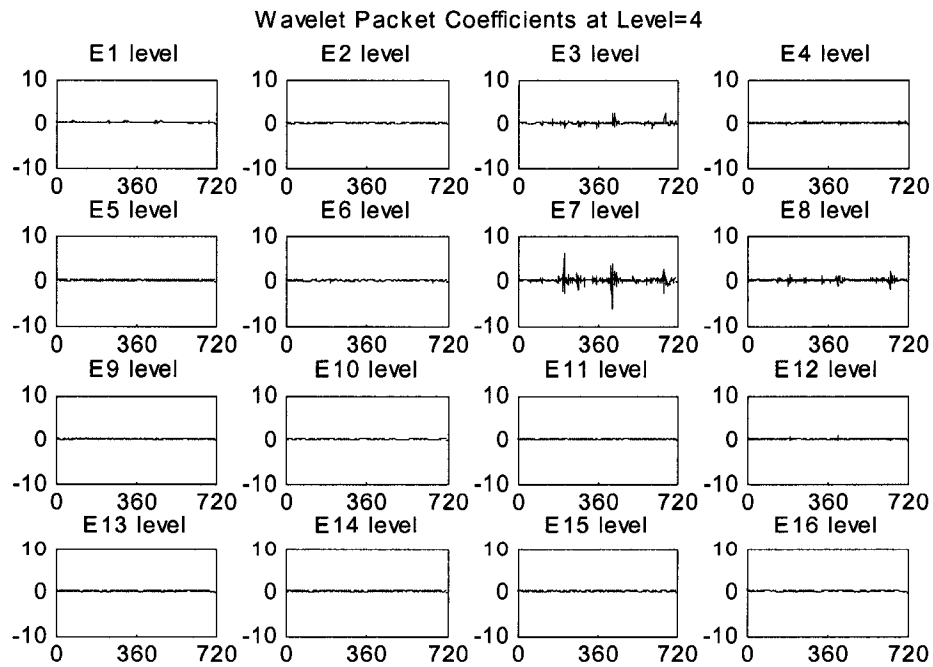


Figure 4.40: Wavelet packet coefficients

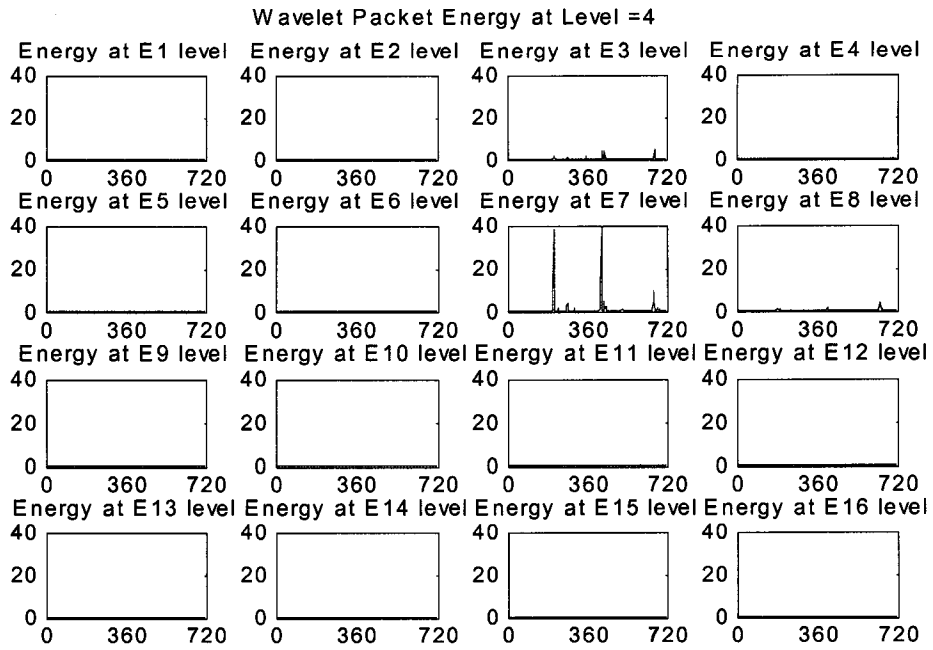


Figure 4.41: Wavelet packet energy

In this case, FCR is the most dominant accelerometer followed by LugRF. We can see from Figure 4.40 that most of the energy of the vibration generated by the fault is concentrated in the frequency bandwidth of E7 wavelet packet. The levels of energy are almost negligible in other frequency bands. The magnitude of E7 level exceeds the fault threshold. Furthermore, there are three vibration spikes that occur at 200, 430 and 680 degrees. Vibrations caused by faulty chain tensioner usually have 3 spikes that are separated by 240 ± 20 degrees. Therefore this matches the fault signature of a faulty right bank chain tensioner. Therefore the defect corresponds to Fault #27 (Right Bank Chain Tensioner) in the fault database (Table 4.8)

Right Bank Chain Tensioner	27	FCR	LugRF	-	-	E7	-	-
----------------------------	----	-----	-------	---	---	----	---	---

Table 4.8: Fault parameters for defective right bank chain tensioner

4.8.3 Case Study: Defective Cylinder #1 Intake Lash Adjuster

Vibrations from a defective Cylinder #1 intake lash adjuster is best detected by the HeadRF accelerometer due to its proximity. Hence it is the most dominant accelerometer followed by FCR accelerometer. The maximum variance values for all accelerometer for the engine in case study is given in Table 4.9.

Accelerometer	Maximum Variance
HeadRF	3
FCR	1.8
HeadRR	1.2
LugRF	1.2
LugRR	0.9
HeadLF	0.8
FCL	0.7
HeadLR	0.3
LugLR	0.3
LugLF	0.3

Table 4.9: Maximum variance for each accelerometer channels

The time domain data from HeadRF accelerometer and the waterfall plot of running variance for 40 engine cycles for the engine is shown in Figure 4.42 and Figure 4.43 respectively.

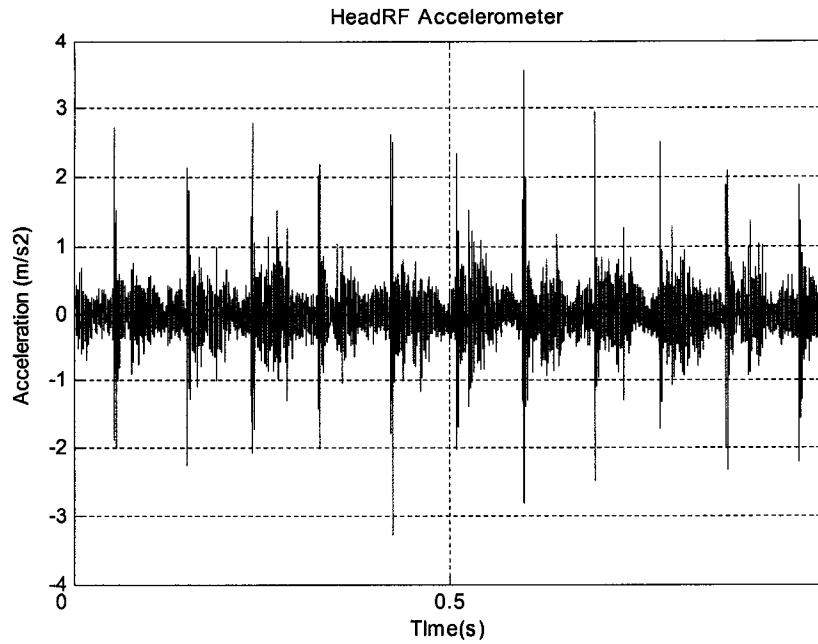


Figure 4.42: Vibrations recorded by HeadRF accelerometer

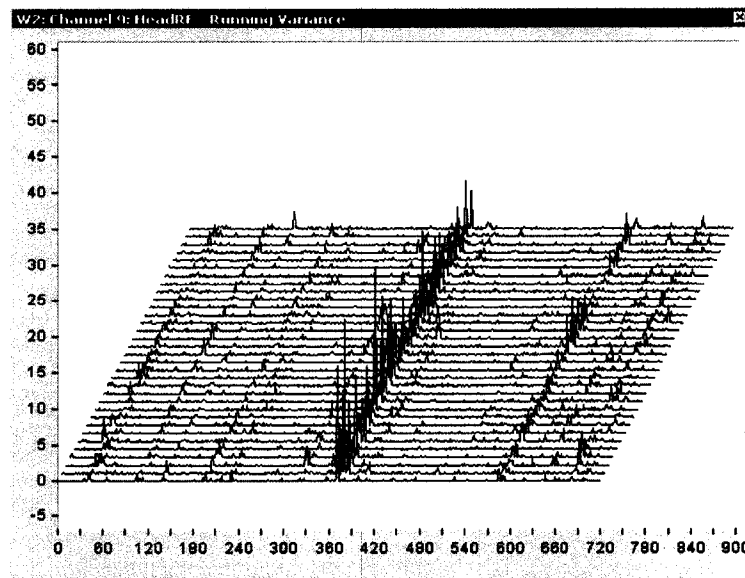


Figure 4.43: Running variance waterfall of HeadRF recorded vibrations for 40 engine cycles

We can see that the engine has a vibration spike occurring consistently for all engine cycles at approximately 365 degrees crank angle. The engine cycle with the maximum energy content (shown in Figure 4.44) is chosen and decomposed using WPD.

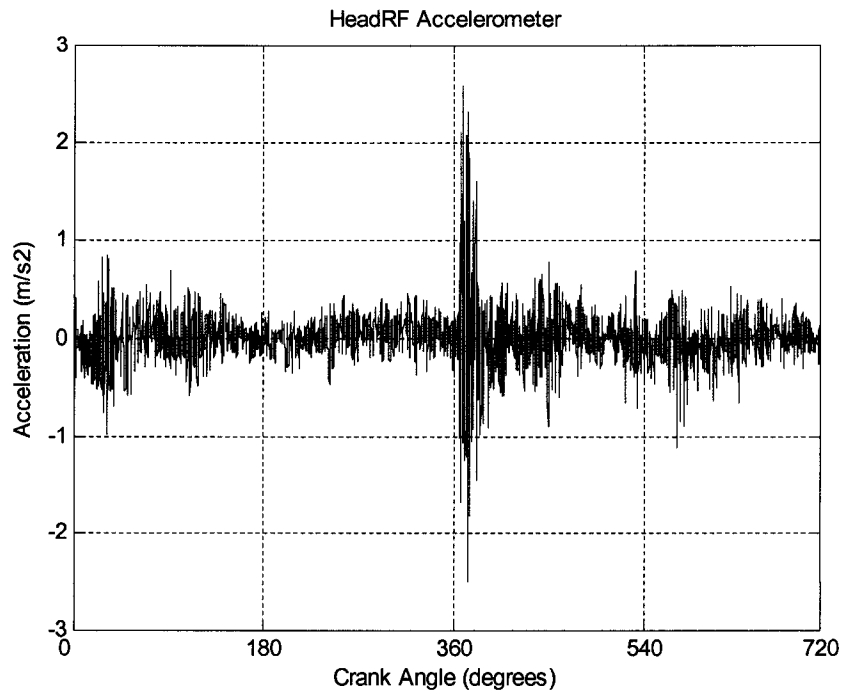


Figure 4.44: Vibration amplitudes for 1 engine cycle

The wavelet packet coefficients and packet energies for all packets at level 4 are shown in Figure 4.45 and Figure 4.46 respectively.

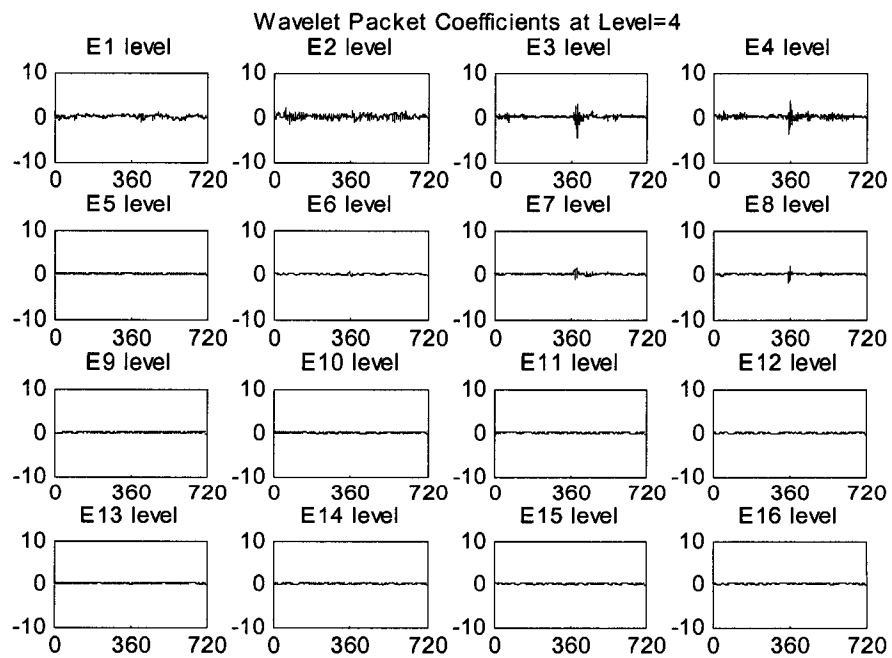


Figure 4.45: Wavelet packet coefficients

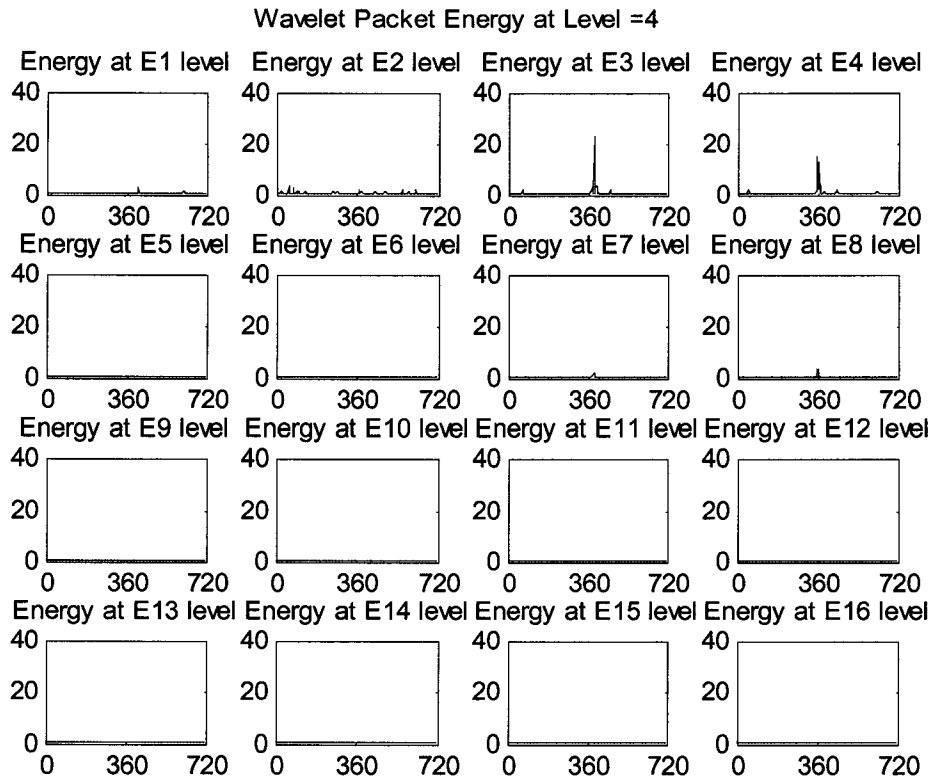


Figure 4.46: Wavelet packet energy

We can see from Figure 4.46 that most of the energy of the vibration generated by the fault is in the frequency bandwidth of E3 and E4 wavelet packet and these levels exceed the fault threshold. Furthermore, the vibration spike occurs at 360 degrees crank angle, Therefore, the defect corresponds to Fault #1 and #2 (Cylinder #1 intake front and rear lash adjusters) in the fault database (Table 4.10).

Cylinder#1 Intake Rear LA	1	HeadRF	FCR	580	360	E3	E4	-
Cylinder#1 Intake Front LA	2	HeadRF	FCR	580	360	E3	E4	-

Table 4.10: Fault parameters for defective Cylinder #1 Intake Lash Adjusters

In this case study, we can narrow down the defect to the Cylinder #1 Intake Lash Adjusters but are unable to distinguish between front and rear Lash Adjuster. If such a

defect were detected in an engine, the solution to repair would be to replace both intake lash adjusters. Replacing both components does not consume any extra repair time than if one were replace just one of them.

4.8.4 Case Study: Defective Cylinder #4 Exhaust Lash Adjuster

Vibrations from a defective Cylinder #4 exhaust lash adjuster is best detected by the HeadRR accelerometer due to its proximity. Hence it is the most dominant accelerometer followed by HeadRF accelerometer. The maximum variance values for all accelerometer for the engine in case study is given in Table 4.11.

Accelerometer	Maximum Variance
HeadRR	6
HeadRF	2.1
LugRR	1.1
FCR	0.9
LugRF	0.9
HeadLR	0.8
LugLF	0.7
HeadLF	0.6
LugLR	0.6
FCL	0.4

Table 4.11: Maximum variance for each accelerometer channels

The crank angle domain data from HeadRR accelerometer and the waterfall plot of running variance for 40 engine cycles for the engine is shown in Figure 4.47 and Figure 4.48 respectively.

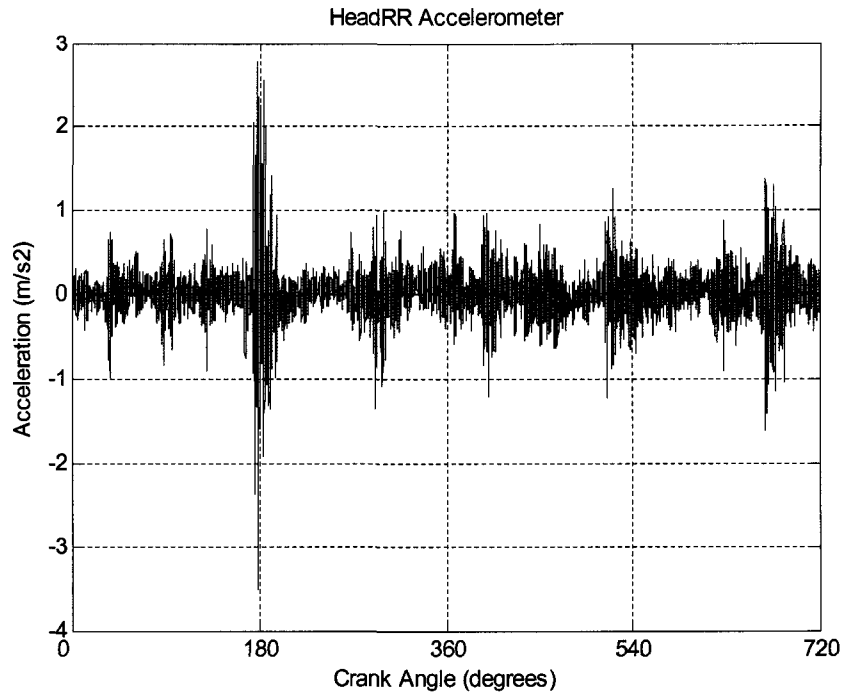


Figure 4.47: Vibrations recorded by HeadRR accelerometer

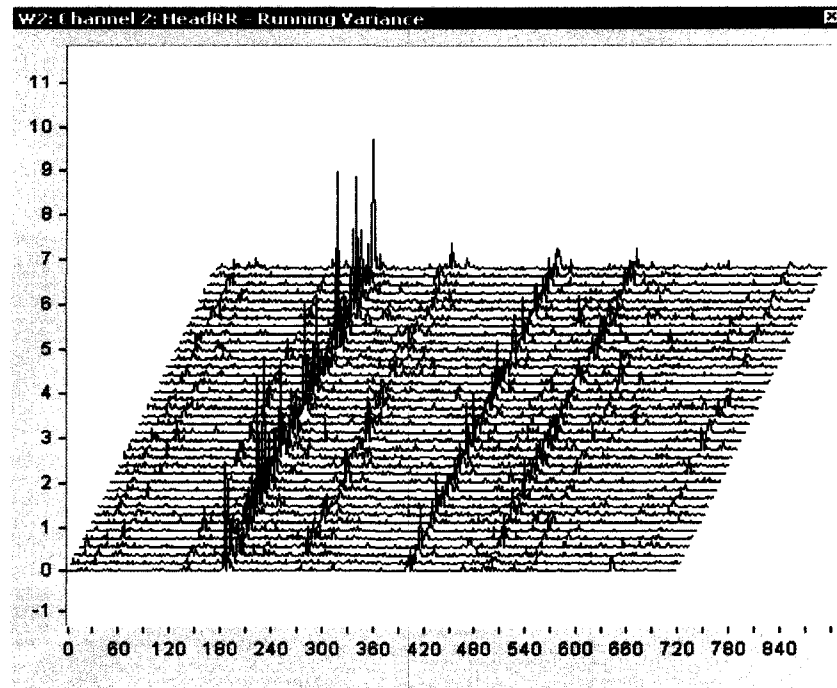


Figure 4.48: Running variance waterfall of HeadRR recorded vibrations for 40 engine cycles

We can see that the engine has a vibration spike occurring consistently for all engine cycles at approximately 180 degrees crank angle. The engine cycle with the maximum energy content is chosen and decomposed using WPD. The wavelet packet coefficients and packet energies for all packets at level 4 are shown in Figure 4.49 and Figure 4.50 respectively.

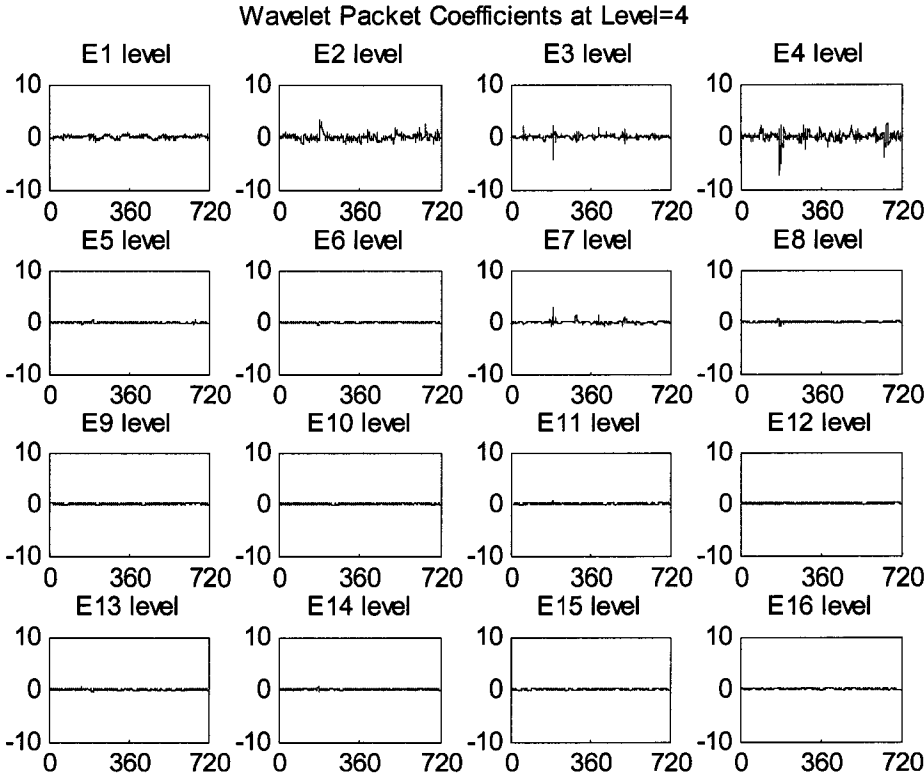


Figure 4.48: Wavelet packet coefficients

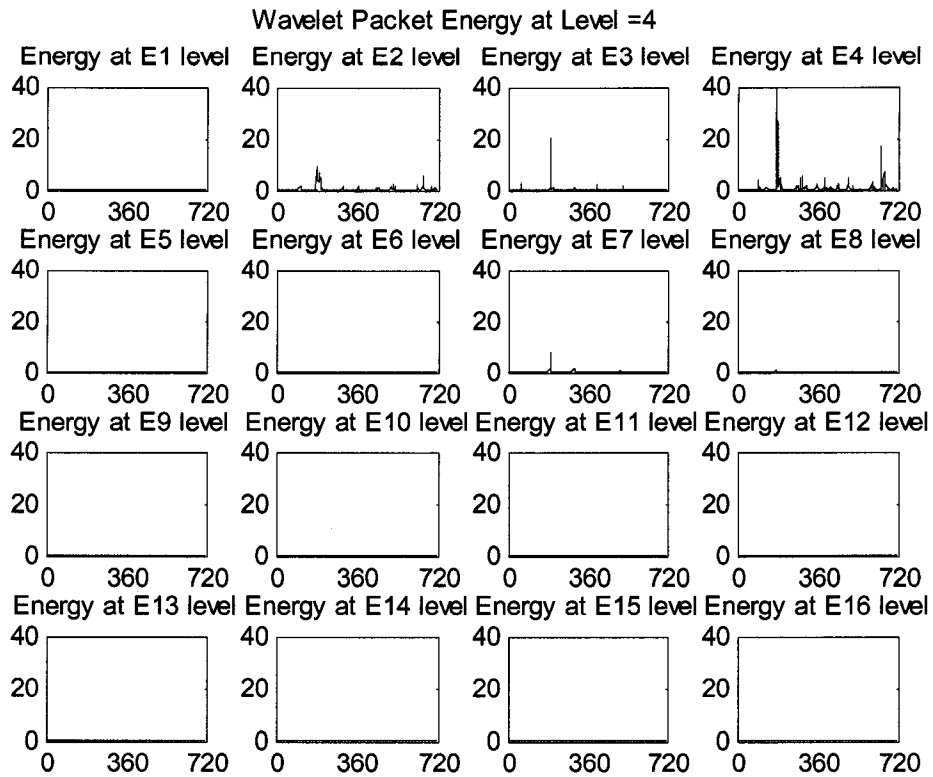


Figure 4.49: Wavelet packet energy

We can see from Figure 4.49 that most of the energy of the vibration generated by the fault is in the frequency bandwidth of E3 and E4 wavelet packet and these levels exceed the fault threshold. Furthermore, the vibration spike occurs at 180 degrees crank angle, which corresponds to Fault #10 and #11 (Cylinder #4 intake front and rear lash adjusters) in the fault database (Table 4.12).

Cylinder#4 Intake Rear LA	10	HeadRR	HeadRF	390	180	E3	E4	-
Cylinder#4 Intake Front LA	11	HeadRR	HeadRF	390	180	E3	E4	-

Table 4.12: Fault parameters for defective cylinder#4 intake lash adjuster

Again, as in the previous case study, we are unable to distinguish between front and rear Lash Adjuster. If such a defect were detected in an engine, the solution to repair would be to replace both intake lash adjusters, as it would require no addition time and energy.

4.8.5 Case Study: Cylinder #4 Bore Non cleanup

Non-cleanup of cylinder bore is a common machining defect, which results in rough surface of cylinder bore. The finish of the cylinder bore must be extremely smooth so that the friction between piston rings and bore is minimal. Rough surface would cause the piston ring to impact with non machined parts of the bore and would lead to ring degradation and wear. If such a defect is diagnosed, the engine is usually scrapped as changing the block means rebuilding the whole engine from bare block.

Figure 4.51 shows 40-engine cycle waterfall variance plot for LugRR accelerometer.

Figure 4.52 shows the average variance for over 40 engine cycles

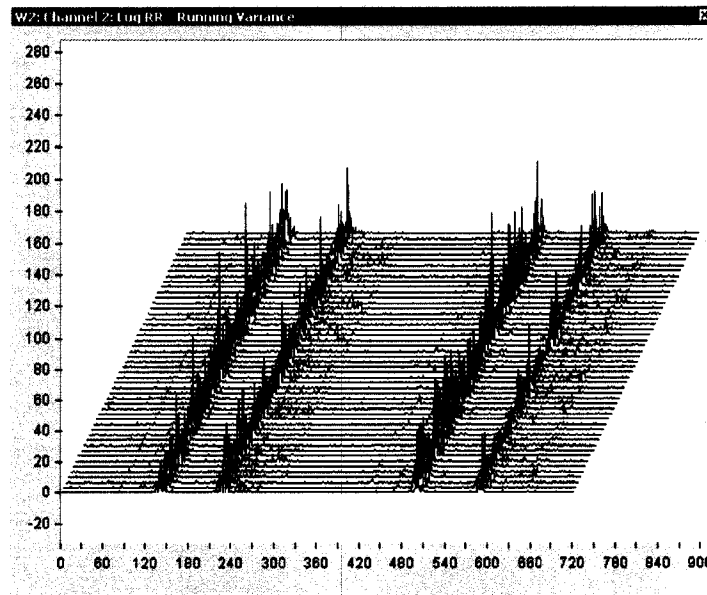


Figure 4.51: 40-Engine cycle waterfall plot for LugRR accelerometer

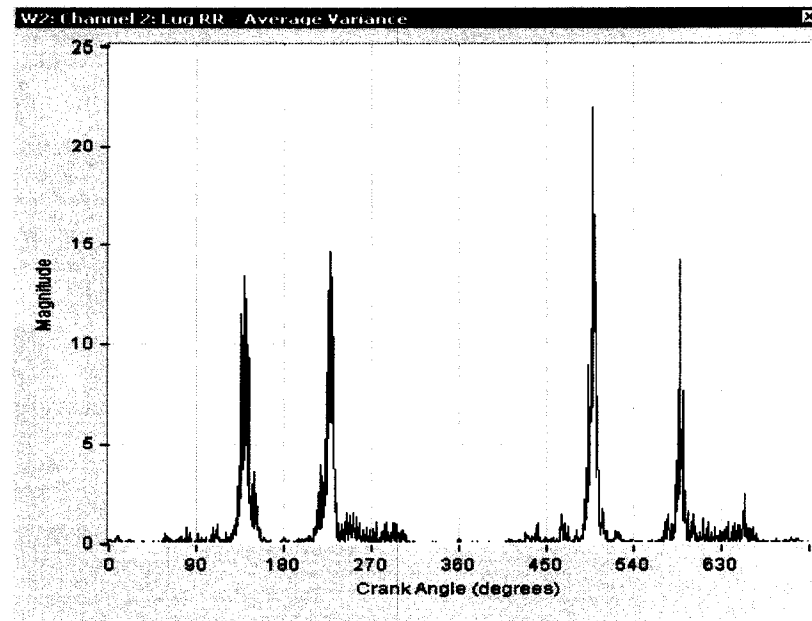


Figure 4.52: Average variance in crank angle domain

The proposed method is unable to identify these defects based on wavelet packets as the frequency content of the impact vibrations vary over a wide spectrum. This is largely due to variations in the severity of the defect. However these defects have a distinct vibration signature in the crank angle domain, which is, it has four vibration spikes per engine cycle. Although this is only true when the defect is present in a small portion of the bore such as presence of a groove. These spikes are symmetrically located in the angle domain with respect to either top-dead-center (TDC) or bottom-dead-center (BDC) of the cylinder where the defect is located. This is due to the fact the piston travels up twice and down, twice in an engine cycle and each time it passes by the non machined part of the cylinder bore, it causes vibration. Table 4.13 shows the positions of each piston at every 90 degrees interval of crank angle. Table 4.14 lists the fault database referred to when diagnosing this defect.

V-8 PISTON LOCATION vs. CRANK ANGLE

Firing Order: 1-3-7-2-6-5-4-8

Crank Angle	Cyl #1	Cyl #2	Cyl #3	Cyl #4	Cyl #5	Cyl #6	Cyl #7	Cyl #8
0	FIRE	↓	↑	BDC-EXH	↑	TDC-INT	BDC-CMP	↓
90	↓	BDC-CMP	FIRE	↑	TDC-INT	↓	↑	BDC-EXH
180	BDC-EXH	↑	↓	TDC-INT	↓	BDC-CMP	FIRE	↑
270	↑	FIRE	BDC-EXH	↓	BDC-CMP	↑	↓	TDC-INT
360	TDC-INT	↓	↑	BDC-CMP	↑	FIRE	BDC-EXH	↓
450	↓	BDC-EXH	TDC-INT	↑	FIRE	↓	↑	BDC-CMP
540	BDC-CMP	↑	↓	FIRE	↓	BDC-EXH	TDC-INT	↑
630	↑	TDC-INT	BDC-CMP	↓	BDC-EXH	↑	↓	FIRE

***NOTE: Crank angle of 0° corresponds to TDC of power stroke for cylinder #1

Table 4.13: Piston position during engine cycle

Cylinder No.	Dominant Accelerometer #1	TDC (firing) Crank Angle	TDC (intake) Crank Angle
Cylinder #1	LugRF	0	360
Cylinder #2	LugRF	270	630
Cylinder #3	LugRR	90	450
Cylinder #4	LugRR	540	180
Cylinder #5	LugLF	450	90
Cylinder #6	LugLF	360	0
Cylinder #7	LugLR	180	540
Cylinder #8	LugLR	630	270

Table 4.14: Fault Database for Cylinder Non-Cleanup Defects

Using this information, the fault detection program determines that the engine in question has spikes symmetric to 540 degrees CA and 180 degrees CA, a signature that is typical for any Cylinder #4 non-cleanup related defect. This coupled with the fact that the dominant accelerometer is LugRR. Hence the defect present matches the signature of Fault #40: Cylinder#4 Non Clean up.

4.9: Comparison of Wavelet Analysis with Variance and STFT

In section 2.5, we discussed the advantages of performing wavelet analysis of vibration data over variance analysis and STFT. The main advantage of wavelet analysis over variance analysis is that it retains both time and frequency domain information of the signals. Thus it has the advantage of having information about an extra dimension that variance analysis do not. As a result, while variance analysis of vibration data in crank angle domain can detect the vibration impulse occurring due to mechanical impacts of faulty components at particular crank angles (engine cycle position), it can not distinguish between two events if they can take place at the same time in a engine cycle. This is illustrated in the following example. Figure 4.53 and Figure 4.54 shows the crank angle domain data for 1-engine cycle recorded by HeadRF accelerometer location for defective Cylinder #1 intake and Cylinder #1 exhaust lash adjuster respectively. Figure 4.55 and Figure 4.56 shows the variance of the crank angle domain data for each case respectively. We can see that in both cases, the accelerometer recorded an abnormal event at roughly 360 degrees crank angle. Since the both spikes occur at the same time in the engine cycle, the variance plot is fails to identify the source of the defect. Figure 4.57 and Figure 4.58 shows the wavelet packet energies at level 4. We can see from the wavelet packets that even though both spikes occur at around the same crank angle, their dominant energies are concentrated in different frequency bands hence wavelet analysis is able to distinguish between the two events. Thus using variance analysis, we can only narrow down the possible causes of defects to cylinder #1 intake and exhaust lash adjuster but can not be definitive about the specific defect while wavelet analysis has the

added dimensionality and can precisely detect the source of defect. Table 4.15 shows the fault parameters for defective cylinder #1 intake and exhaust lash adjusters.

Fault Description	Fault #	Accelerometer		Fault Crank Angle +/- 10 Degrees		Dominant Wavelets Rackets in (A)			Fault Detected
		Most Dominant (A)	2nd Most Dominant (B)						
Cylinder#1 Intake LA	1	HeadRF	FCR	580	360	E3	E4	-	YES*
Cylinder#1 Exhaust LA	2	HeadRF	FCR	370	100	E13	E14	-	YES

Table 4.15: Fault parameters for defective cylinder #1 intake and exhaust lash adjuster

We can see from figure 4.57 and 4.58 that the dominant wavelet packet for the intake lash adjuster is E3 while the dominant wavelet packet for the exhaust lash adjuster is E13.

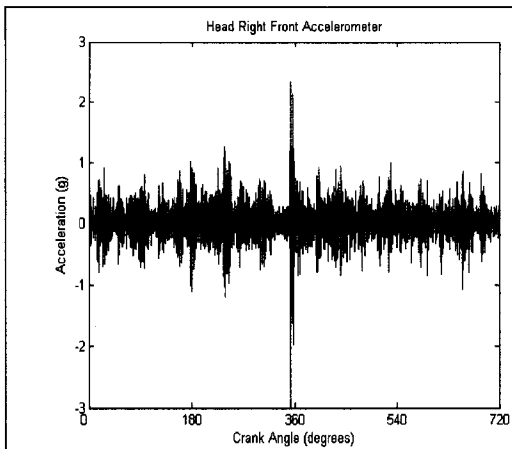


Figure 4.53: Defective Cylinder 1 intake Lash Adjuster. HeadRF Accelerometer position recorded a spike at 355 degrees CA.

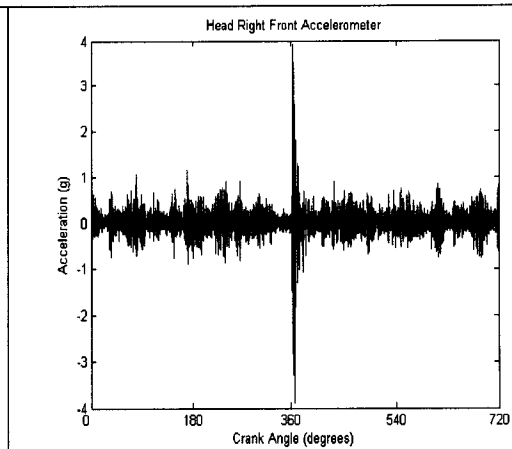


Figure 4.54: Defective Cylinder 1 exhaust Lash Adjuster. HeadRF Accelerometer position recorded a spike at 365 degrees CA.

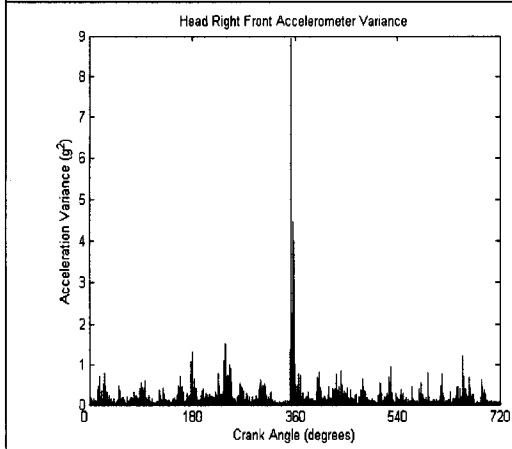


Figure 4.55: Defective Cylinder 1 intake Lash Adjuster. HeadRF Accelerometer position recorded a variance spike at 355 degrees CA.

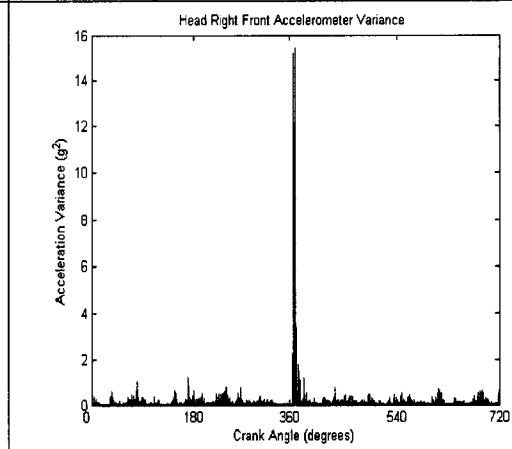


Figure 4.56: Defective Cylinder 1 exhaust Lash Adjuster. HeadRF Accelerometer position recorded a variance spike at 365 degrees CA.

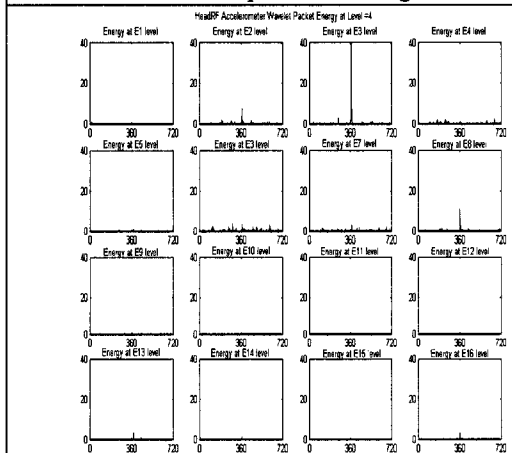


Figure 4.57: Wavelet Packet Energy at Level =4

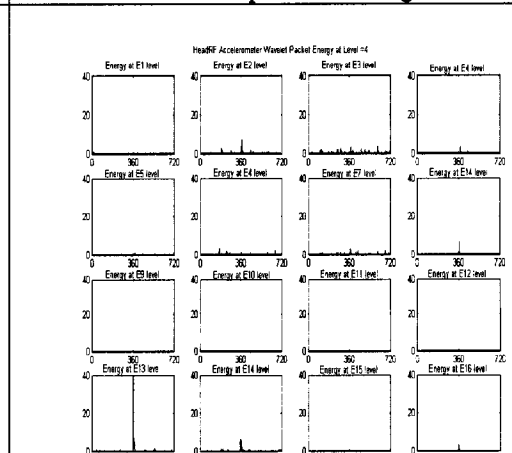


Figure 4.58: Wavelet Packet Energy at Level =4

Using Wavelet analysis can also be advantageous over Short-time Fourier transform. Figure 4.59 and Figure 4.60 shows the overlay plot of vibration data recorded by FCR accelerometer location in crank angle domain taken from a severely knocking phaser and a good phaser and a moderately knocking phaser and a good phaser respectively. We can see from the plots that there an abnormal event taking place at around 525 degrees crank angle. Figure 4.61 and Figure 4.62 shows frequency response over 1-engine cycle for each cases respectively. The plot was made using a Short-Time FFT with a frequency resolution of 2Hz with a Hanning Window. While little difference may be observed in the case of extremely severe case of defective phaser in Figure 4.61, no obvious difference can be seen in the frequency representation of the two signals for the case of the phaser with moderate knock (Figure 4.62). Figure 4.63 and Figure 4.64 shows the wavelet packet energies of the same signals and we can see that the dominant frequency content is both cases are located in a narrow band of frequency. Thus even though, we were unable to identify the faulty phaser from the frequency response, wavelet analysis can clearly identify the defect. Table 4.16 shows the fault parameters for defective right bank cam phaser.

Fault Description	Fault #	Accelerometer		Fault Crank Angle +/- 10 Degrees		Dominant Wavelets Packets in (A)		
		Most Dominant (A)	2nd Most Dominant (B)					
Right Bank Cam Phaser	25	FCR	HeadRF	520	45	E6	E8	-

Table 4.16: Fault parameters for defective right bank cam phaser

We can see from figure 4.63 and 4.64 that the dominant wavelet packet for the defective right bank cam phaser is E6.

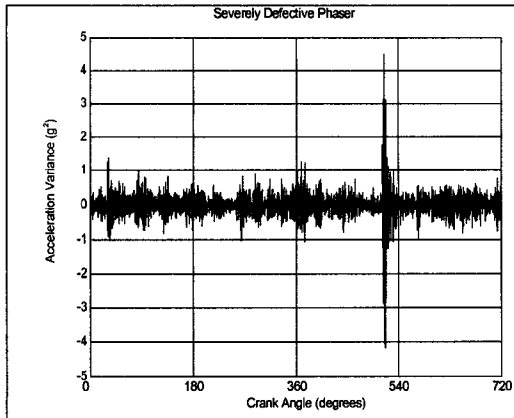


Figure 4.59: Severely defective right bank phaser. FCR accelerometer position recorded a spike at 525 degrees CA.

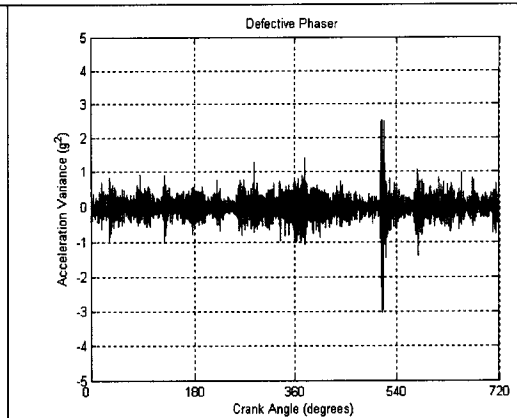


Figure 4.60: Defective right bank phaser. FCR accelerometer position recorded a spike at 525 degrees CA.

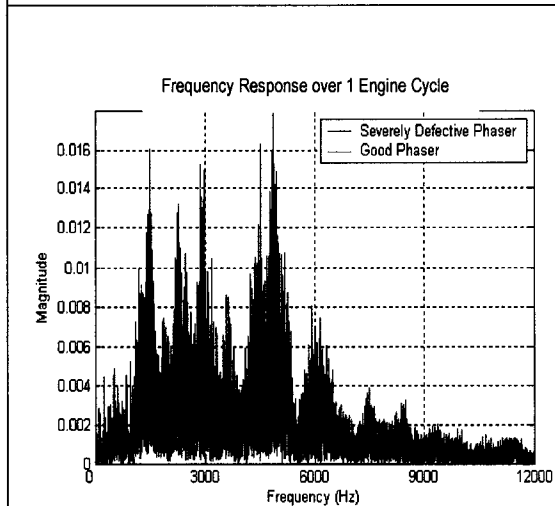


Figure 4.61: Frequency response over 1 Engine Cycle (Severely defective phaser and good phaser).

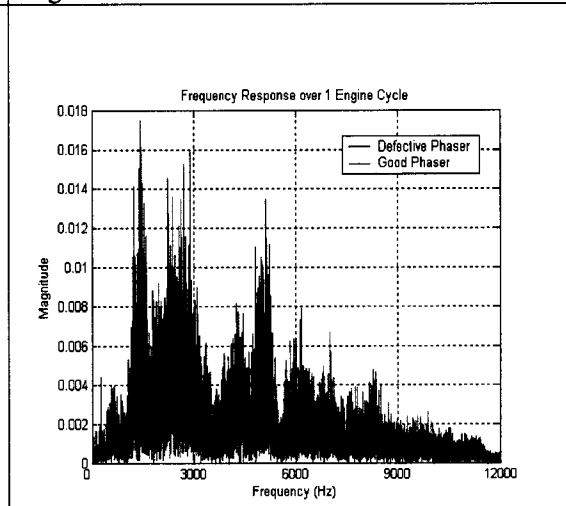


Figure 4.62: Frequency response over 1 Engine Cycle (Defective phaser and good phaser)

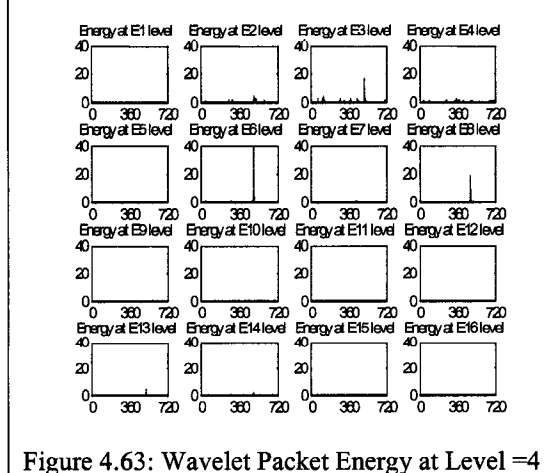


Figure 4.63: Wavelet Packet Energy at Level =4

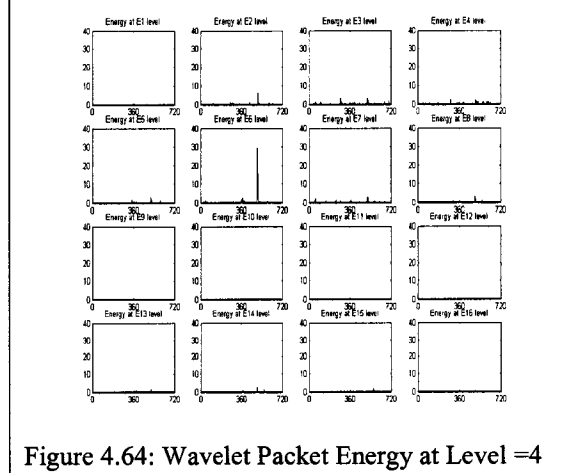


Figure 4.64: Wavelet Packet Energy at Level =4

4.10 Summary

In this chapter, we have discussed in detail the different steps of the proposed WPD based Engine Defect Detection System. The defect detection process is also illustrated using a flowchart. A brief overview of the user-friendly Matlab based software is given that was developed to implement the defect detection algorithm. Case studies are also provided for detection of each type of defective engine component. Table 4.17 provides a summary of all defects that can be detected using proposed WPD based engine defect diagnostic method. There are two drawbacks of this method. Firstly, it is unable to discriminate between the defective intake lash adjusters in the same cylinder. If such a defect is detected, it is advised that both lash adjusters in the cylinder be replaced to repair the engine since it does not take any extra effort to replace both instead of just one lash adjuster when they are located in the same cylinder. The other drawback is that features from WPD are unable to detect any machining related defect such as cylinder bore non-clean up. However these defects can still be detected in crank angle domain using symmetry of the vibration spikes in the angle domain when the defect is not too severe.

Fault Description	Fault #	Fault Detected	Fault Description	Fault #	Fault Detected
Cylinder#1 Intake Rear LA	1	YES*	Cylinder#8 Intake Front LA	23	YES*
Cylinder#1 Intake Front LA	2	YES*	Cylinder#8 Exhaust LA	24	YES
Cylinder#1 Exhaust LA	3	YES	Right Bank Cam Phaser	25	YES
Cylinder#2 Intake Rear LA	4	YES*	Left Bank Cam Phaser	26	YES
Cylinder#2 Intake Front LA	5	YES*	Right Bank Chain Tensioner	27	YES
Cylinder#2 Exhaust LA	6	YES	Left Bank Chain Tensioner	28	YES
Cylinder#3 Intake Rear LA	7	YES*	Cylinder #1 Piston/Rod	29	YES
Cylinder#3 Intake Front LA	8	YES*	Cylinder #2 Piston/Rod	30	YES
Cylinder#3 Exhaust LA	9	YES	Cylinder #3 Piston/Rod	31	YES
Cylinder#4 Intake Rear LA	10	YES*	Cylinder #4 Piston/Rod	32	YES
Cylinder#4 Intake Front LA	11	YES*	Cylinder #5 Piston/Rod	33	YES
Cylinder#4 Exhaust LA	12	YES	Cylinder #6 Piston/Rod	34	YES
Cylinder#5 Intake Rear LA	13	YES*	Cylinder #7 Piston/Rod	35	YES
Cylinder#5 Intake Front LA	14	YES*	Cylinder #8 Piston/Rod	36	YES
Cylinder#5 Exhaust LA	15	YES	Cylinder #1 Non Cleanup	37	NO
Cylinder#6 Intake Rear LA	16	YES*	Cylinder #2 Non Cleanup	38	NO
Cylinder#6 Intake Front LA	17	YES*	Cylinder #3 Non Cleanup	39	NO
Cylinder#6 Exhaust LA	18	YES	Cylinder #4 Non Cleanup	40	NO
Cylinder#7 Intake Rear LA	19	YES*	Cylinder #5 Non Cleanup	41	NO
Cylinder#7 Intake Front LA	20	YES*	Cylinder #6 Non Cleanup	42	NO
Cylinder#7 Exhaust LA	21	YES	Cylinder #7 Non Cleanup	43	NO
Cylinder#8 Intake Rear LA	22	YES*	Cylinder #8 Non Cleanup	44	NO

Table 4.17: Engine Fault Detection Summary

Due to these limitations the fault code database has been modified to reflect only the 28 classes of defects it is able to detect using features based on wavelet packets. Table 4.18 gives the new fault database.

Fault Description	Fault #	Accelerometer		Fault Crank		Dominant Wavelets		
		Most Dominant (A)	2nd Most Dominant (B)	Angle 1-10 Degrees	Angle 1-10 Degrees	Packets in (A)		
Cylinder#1 Intake LA	1	HeadRF	FCR	580	360	E3	E4	-
Cylinder#1 Exhaust LA	2	HeadRF	FCR	370	100	E13	E14	-
Cylinder#2 Intake LA	3	HeadRF	HeadRR	140	620	E2	E4	-
Cylinder#2 Exhaust LA	4	HeadRF	HeadRR	370	650	E13	E14	-
Cylinder#3 Intake LA	5	HeadRR	HeadRF	680	440	E2	E4	-
Cylinder#3 Exhaust LA	6	HeadRR	HeadRF	470	200	E13	E14	-
Cylinder#4 Intake LA	7	HeadRR	HeadRF	390	180	E3	E4	-
Cylinder#4 Exhaust LA	8	HeadRR	HeadRF	200	640	E13	E14	-
Cylinder#5 Intake LA	9	HeadLF	FCL	330	70	E3	E4	-
Cylinder#5 Exhaust LA	10	HeadLF	FCL	100	550	E5	E13	-
Cylinder#6 Intake LA	11	HeadLF	HeadLR	230	690	E3	E4	-
Cylinder#6 Exhaust LA	12	HeadLF	HeadLR	20	460	E13	E5	-
Cylinder#7 Intake LA	13	HeadLR	HeadLF	60	530	E2	E4	-
Cylinder#7 Exhaust LA	14	HeadLR	HeadLF	540	270	E14	E13	-
Cylinder#8 Intake LA	15	HeadLR	HeadLF	490	250	E3	E4	-
Cylinder#8 Exhaust LA	16	HeadLR	HeadLF	270	30	E13	E14	-
Right Bank Cam Phaser	17	FCR	HeadRF	520	45	E6	E8	-
Left Bank Cam Phaser	18	FCL	HeadRF	660	150	E6	E8	-
Right Bank Chain Tensioner	19	FCR	LugRF	-	-	E7	-	-
Left Bank Chain Tensioner	20	FCL	LugLF	-	-	E7	-	-
Cylinder #1 Piston/Rod	21	LugRF	LugRR	10	370	E5	E6	-
Cylinder #2 Piston/Rod	22	LugRF	LugRR	280	640	E5	E6	-
Cylinder #3 Piston/Rod	23	LugRR	LugRF	100	460	E7	E8	-
Cylinder #4 Piston/Rod	24	LugRR	LugRF	370	10	E7	E8	-
Cylinder #5 Piston/Rod	25	LugLF	LugLR	460	100	E5	E6	-
Cylinder #6 Piston/Rod	26	LugLF	LugLR	550	910	E5	E6	-
Cylinder #7 Piston/Rod	27	LugLR	LugLF	190	550	E7	E8	-
Cylinder #8 Piston/Rod	28	LugLR	LugLF	660	300	E7	E8	-

*LA = Lash Adjuster

Table 4.18: Modified Engine Fault Detection Table Summary

To validate the developed Engine Fault Detection System, engines with each type of defect were tested. Some of these engines include assembly plant and dealer returned engines with suspect unknown defect and others where known defective components were installed in engine in order to create a defect. Table 4.19 summarizes the cumulative success rate of this system for detecting engine defects by defective components.

Faults	Detected	Each Type of Fault Tested	Cumulative Success Rate
Lash Adjuster	Yes	10	89.38%
Phaser	Yes	30	100%
Chain Tensioner	Yes	10	100%
Piston Rod	Yes	10	88.75%
Bore Noncleanup	No		

Table 4.19: Summary of test engines and cumulative success rates

Therefore, during the course of this study, we have developed an algorithm that can detect and identify the fault type for several commonly occurring engine defects for the 5.4L 3V engine. Hence, our research goal is met.

CHAPTER 5

CONCLUSIONS AND RECOMMEDATIONS

5.1 Conclusions

After a detailed analysis of the experimental results obtained, the following conclusions have been reached:

- 1) Signature analysis using wavelet packet analysis provides an excellent indication of the engine condition in terms of presence of defects.
- 2) A fault diagnostic system is developed incorporating wavelet packets, crank angle and accelerometer location and was successful in detecting a number of commonly occurring and known defects such as defective lash adjuster, phaser, chain tensioner and piston rod knock. The designed system was also successful in identifying all engines that were defect free.
- 3) Engine defects can be identified using the proposed method with a high success rate. If such a system can be implemented at every dealership and assembly plant, it would considerably reduce warranty costs for the company.
- 4) The engine fault diagnostic system is customizable and can be used to detect new faults by building the reference table with the characteristics of the new fault such as wavelet packets, accelerometer location and crank angle. Also, the system is customizable such that, if a new fault is better detected at a different accelerometer location (for e.g. intake manifold), easy modifications can be made to add such new faults by adding the new accelerometer position in the fault

database and then creating its 2-D map of the defect comprising of frequency and crank angle information.

- 5) If the system detects any unusual vibration event that it cannot discriminate into a known fault, it will generate a warning message. This information can also be used to train the database with new engine faults.
- 6) The system is designed to be used at a dealership or assembly plants to detect defects in engines that have been already installed in the vehicle. The time to set up all ten accelerometer on an engine in a laboratory setting takes about 10 min. The data acquisition and fault detection can take another additional 10 minutes. Therefore the whole time would be up to 20 minute to complete diagnosis of the engine. However, in a vehicle the time to set up the accelerometer can take longer as not all accelerometer positions are easily accessible. The vehicle has to be put on a hoist to access the engine block lugs. Time to set up all ten channels of accelerometer in a vehicle can take up to 20 minutes with another additional 10 minutes to run diagnostics. For this reason, this system cannot be implemented as an online diagnosis system on the manufacturing lines.
- 7) This system is dependent on the manufacturing process and it may be sensitive to any change in it.
- 8) The engine operating conditions, data acquisition and processing has to be done the exact same way each time for proper comparison. Separate fault maps are needed for different running conditions such as speed, load and temperature.

5.2: Recommendations and Future Work

The following recommendations will provide possible future improvement to the engine fault detection system that was developed for this study

- 1) Investigate and add more faults to the fault database.
- 2) Create fault maps for same engine model but at different speed, load and temperatures.
- 3) Do fault mapping for other engine models.

REFERENCES

Alvey, A., Jay, G.C. (2005). "Application of NVH Techniques to Engine Production Line Test". Tecumseh Products Company, MTS Systems Corporation. *SAE Technical Paper #2005-01-2452*, 2005, 8 pages.

Beidl, C.V., Rust, A., Rasser, M. (1999). "Key Steps and Methods in the Design and Development of Low Noise Engines". AVL LIST GmbH. *SAE Technical Paper #1999-01-1745*, 1999, 11 pages.

Ben-Ari, J., deBotton, G., Itzhaki, R., Sher, E., "Vibration Signature Analysis as a Fault Detection Method for SI Engines" *SAE 1999-01-1223*, 1999, 9 pages.

Ben-Ari, J., deBotton, G., Itzhaki, R., Sher, E., "Fault Detection in Internal Combustion Engines by the Vibration Analysis Method" *SAE Paper 980115*, 1998, 8 pages.

Biqing Wu, Saxena, A., Khawaja, T.S., Patrick, R., Vachtsevanos, G., Sparis, P., "An Approach to Fault Diagnosis of Helicopter Planetary Gears", *IEEE AUTOTESTCON*, 2004, 7 pages.

Blough, J.R., Gwaltney, G.D. (1999). "Summary and Characteristics of Rotating Machinery Digital Signal Processing Methods". *Michigan Technological University. SAE Technical Paper #1999-01-2818*, 1999, 16 pages

Boggess, A., Narcowich, F., "A First Course in Wavelets with Fourier Analysis", Prentice Hall, 2001.

Boubal, O., "Knock Detection in Automobile Engines", *IEEE Instrumentation & Measurement Magazine*, September 2000, 5 pages.

Bryant, B., Marko, K. A., Soderborg, N., "Neural Network Application to Comprehensive Engine Diagnostics", *IEEE*, 1992, 10 pages.

Bruel & Kjaer (1982). "Measuring Vibration". *Bruel & Kjaer Technical Paper, Naerum, Denmark. Revision September 1982.*

Chandroth, G.O., Sharkey, A.J.C., Sharkey, N.E., "Vibration signatures, wavelets and principal components in diesel engine diagnostics", *Marine Technology*, Poland ODRA 1999, 10 pages, (1)

Chandroth, G.O., Sharkey, A.J.C., Sharkey, N.E., "Cylinder pressures and vibration in internal combustion engine condition monitoring", *Proceedings 'Comadem 99'*, Sunderland, UK, July, 1999, 11 pages, (2).

- Chandroth, G.O., Staszewski, W.J.**, "Fault detection in internal combustion engines using wavelet analysis", Proceedings 'Comadem 99', Sunderland, UK, July, 1999, pages 8, (3).
- Chung, J., Pope, J., Feldmaier, D.**, "Application of Acoustic Intensity Measurement to Engine Noise Evaluation, SAE Paper 890502, 1979, 12 pages.
- Cohen, L.**, "Time-Frequency Analysis, Prentice Hall, Englewood Cliffs, NJ, 1995.
- Daubechies, I.**, "Ten Lectures on Wavelets", SIAM, Philadelphia, 1992.
- Daws, M.C.**, "Assessment of the impact of camshaft machining inputs on valvetrain sound quality using vibration analysis". *University of Windsor, Masters Thesis, (M.A.Sc.)* 2002.
- Dimaggio S. J., Rubin S., Sako B.H.**, "Gear Fault Detection in Rocket Engine Turbomachinery ", *Journal of Propulsion and Power* 2001 0748-4658 vol.17 no.2, 2000, pp. 225-231.
- Djurovic, I., Stanovic, L.**, "A Virtual Instrument for Time-Frequency Analysis", *IEEE Transaction on Instrumentation and Measurements*, Vol. 48 No. 6. December 1999, pp. 1086-1092.
- Eren, L., Devaney, M. J.**, "Bearing Damage Detection via Wavelet Packet Decomposition of Stator Current". *IEEE Instrumentations and Measurements Technology Conference*, 2002, pp. 109-113.
- Eshelman, R. L.**, *Machinery Vibration Analysis I*. The Vibration Institute, VIPress, 1995.
- Ford Motor Company**, "Basic Order Tracking for NVH". *Ford Research & Vehicle Technology, Ford Powertrain NVH Design Guide, Ford Confidential Book. 5/21/2003.*
- Ghosh, B., Vora, K.C.**, "Vibrations Due to Piston Slap and Combustion in Gasoline and Diesel Engines", SAE Paper 911060, 1991, 11 pages.
- Goumas, Stefanos K., Zervakis, Michael E., Stavrakakis, G.S.**, "Classification of Washing Machines Vibration Signals Using Discrete Wavelet Analysis for Feature Extraction", *IEEE Transaction on Instrumentation and Measurements*, Vol. 51, No. 3. June 2002, pp 497-508.
- Heng, R.B.W., Nor, M. J.**, "Statistical Analysis of Sound and Vibration Signals for Monitoring Rolling Element Bearing Condition", *Applied Acoustics*, Vol. 53, No. 1-3, 6 pages, 1998.

Jonuscheit, H., “Acoustic Tests on Combustion Engines in Production”, MEDAV Technical Paper, 2000, 27 pages.

Konig, D., “Application of Time-Frequency Analysis for Optimum Non-Equidistant Sampling of automotive Signals Captured at Knock”, IEEE, 1996, pp. 2746-2749.

Leitzinger, E.R. "Development of In-process engine defect detection methods using NVH indicators". *University of Windsor, Masters Thesis, (M.A.Sc.)* 2002.

Licht, T.R., Serridge, M., “Piezoelectric Accelerometers and Vibration Preamplifier Handbook”, Bruel & Kjaer Publications, 1987, pages 12-37.

Martin, H.R., Honarvar, F., “Application of Statistical Moments to Bearing Failure Detection”, Applied Acoustics, Vol. 44, pp. 67-77, 1995.

Matlab Wavelet Toolbox Documentations,
<http://www.mathworks.com/access/helpdesk/help/toolbox/wavelet/>, 2007.

Mercer, C., “Frequency, Hertz & Orders: An Examination of the Relationships between Frequency and Orders”, <http://www.prosig.com/signal-processing/FrequencyHertzOrders.html>, 2007.

Miller, A. J., "A New Wavelet Basis for the Decomposition of Gear Motion Error Signals and its Application to Gearbox Diagnostics", Masters Thesis, Pennsylvania State University, 1999.

Mingzan, Wu, Qie Jie, Gu Qun, Shao Hongwen, “Wavelet Package-Neural Network based on Rough Set Diesel Engine Vibration Signal Identification Model”, IEEE, 2003, pp. 185-190.

Mitchell, S. J., Machinery Analysis and Monitoring. Pennwell Publishing Company, Oklahoma, 1981.

Modgil, G., Orsagh, R. F., Roemer, M. J., “Advanced Vibration Diagnostics for Engine Test Cells”, IEEE Aerospace Conference Proceedings, 2004, pp 3361-3371.

Molinaro, F., Castanie, F., “Knocking Recognition in Engine Vibration Signal Using the Wavelet Transform”, IEEE, 1992, pp. 353-356.

Nurhadi, I., Bagiasna, K., Wediyanto, “Signature Analysis of 4-Stroke 1-Cylinder Engine. SAE technical paper 932011. 1993.

Polikar, R., "The Engineers Ultimate guide to Wavelet Analysis: The Wavelet Tutorial", <http://users.rowan.edu/~polikar/WAVELETS/WTtutorial.html>, 1999.

- Politis, N.**, “Advanced Time-Frequency Analysis Applications in Earthquake Engineering”, Technical Paper, 2003, 7 pages.
- Priede, T.**, Noise and Vibration Control of the Internal Combustion Reciprocating Engine, *Noise and Vibration Control Engineering: Principles and Applications*, ed. L.L.Beranek and I.L. Ver, John Wiley & Sons, Inc.
- Rizzoni, G., Chen, X.**, “Detection of Internal Combustion Engine Knock Using Time-Frequency Distribution”, IEEE, 1993, pp. 360-363.
- Szczepanski, J.G.**, "New Equipment and Methodology to Perform High Speed Valvetrain Dynamics Testing and Analysis". *Ford Motor Company. SAE Technical Paper #2004-01-1720*, 2004, 13 pages.
- Seidlitz, S.**, "An Optimization Approach to Valvetrain Design", *SAE Technical Paper #901638*, 1990.
- Samimy, B., Rizzoni, G.**, "Time-Frequency Analysis For Improved Detection of Internal Combustion Engine Knock", IEEE, 1994, pp. 178-181.
- Samimy, B., Rizzoni, G.**, "Mechanical Signature Analysis Using Time-Frequency Signal Processing: Application to Internal Combustion Engine Knock Detection", IEEE, 1996, pp. 1330-1343.
- Sharkey, A.J.C., Chandroth, G.O., Sharkey, N.E.**, “Acoustic Emission, Cylinder Pressure and Vibration: A Multisensor Approach to Robust Fault Diagnosis”, IEEE, 2000, pp. 223-228.
- Staszewski, W. J., Ruotolo, R., Storer, D.M.**, "Fault Detection in Ball_Bearings Using Wavelet Variance, Proceedings of the 17th International Modal Analysis Conference (IMAC), Kissimmee, Florida, 1999, 9 pages.
- Suh, I.S.** "Application of Time-Frequency Representation Techniques to the Impact-Induced Noise and Vibration from Engines". *DiamlerChrysler. SAE Technical Paper #2002-01-0453*, 2002, 11 pages.
- Tafreshi, R., Ahmadi, H., Sassani, F., Dumont, G.**, “Informative Wavelet Algorithm in Diesel Engine Diagnosis”, IEEE, 2002, pp. 361-366.
- Tamaki, K., Matsuoka, Y., Uno, M., Kawana, T.**, “Wavelet transform based signal waveform identification: Inspection of rotary compressor,” in *Proc. IECON '94—20th Annual Conf. IEEE Ind. Electron.*, vol. 3, Bologna, Italy, Sept. 5–9, 1994, pp. 1931–1936.
- Thomas, J., Dubuison, B.**, "A Diagnostic Method using Wavelet Networks Application to Engine Knock Detection", IEEE, 1996, pp. 244-249.

Tjong, J., "Engine Dynamic Signal Monitoring and Diagnostics". University of Windsor, PhD Thesis, 1992.

Tjong, J., Reif, Z., "Development and Applications of Engine Dynamic Signal Monitoring and Diagnostic System", 1993, 5 pages.

Toshihiko Kato, Sadao Akishita, Ziyi Li "Engine Failure Diagnosis With Sound Signal Using Wavelet Transform", SAE 970034, 1997, 10 pages.

Tumer, I., Huff, E.M., "Principal Component Analysis of Triaxial Vibration Data from Helicopter Transmission", Proceedings of the 56th meeting of the Society of Machinery Failure and Prevention Technology, 2002, 10 pages.

Van Dyke, D.J., Watts, W.A., "Automated Rolling Contact Bearing Fault Detection Using Cepstrum Analysis", Technical Paper, DLI Engineering, 2001.
<http://www.dliengineering.com/downloads/Automated%20Rolling%20Contact%20Bearing.pdf>

Wang, W. J., McFadden P. D., "Application of wavelets in nonstationary signal analysis for early gear damage diagnosis," in *Proc. Int. Conf. Vibration Eng., ICVE'94*, Beijing, China, pp. 615–620.

Yazici, B., Kliman, G. "An Adaptive Statistical Time-Frequency Method for Detection of Broken Bars and Bearing using the Stator Current", IEEE Transaction on Industry Applications, Vol. 35, No. 2, 1999, pp.442-452.

Yen, G., Lin, Kuo-Chung, "Conditional Health Monitoring using Vibration Signatures", Proceedings of the 38th Conference on Decision and Control, IEEE, 1999, pp. 4493-4498 (1).

Yen, G., Lin, Kuo-Chung, "Wavelet Packet Feature Extraction for Vibration Monitoring", IEEE Proceedings on Control Applications, 1999, pp. 1573-1578 (2).

Yen, G., Lin, Kuo-Chung, "Wavelet Packet Feature Extraction for Vibration Monitoring", IEEE Transaction on Industrial Electronics, Vol. 47, No. 3. June 2000, pp. 650-667.

Yen, G., Wen Fung Leong, "Fault Classification on Vibration Data with Wavelet Based Feature Selection Scheme ", IEEE 2005 pp. 1644-1649.

Zheng, G.T., McFadden, P., "A Time Frequency Distribution for Analysis of Signal with Transient Components and its application to Vibration Analysis", ASME, Vol. 121, July 1999, pp. 328-333.

Zheng, G. T., Wang, W. J., “A New Cepstral Analysis Procedure of Recovering Excitations for Transient Components of Vibration Signals and Applications to Rotating Machinery Condition Monitoring”, *Journal of Vibration and Acoustics*, April 2001 -- Volume 123, Issue 2, ISSN 1048-9002, 2001, pp. 222-229.

APPENDICES

A: 5.4L 3V ENGINE SPECIFICATIONS

The specifications for the 5.4L 3V engine are given in *Table A.1: 5.4L 3V Engine Specifications*:

<i>Manufacturer / Assembly Plant</i>	Ford Motor Company, Windsor, Ontario, Canada
<i>Engine Type</i>	8-Cylinder, 90°V, Single Overhead Cam
<i>Block</i>	Cast Iron
<i>Head</i>	Aluminum
<i>Horsepower (@ rpm)</i>	300 @ 5000
<i>Torque (ft. lb. @ rpm)</i>	365 @ 3750
<i>Displacement</i>	5.4 litres
<i>Bore & Stroke (mm)</i>	90.2 x 105.8
<i>Compression Ratio</i>	9.8:1
<i>Engine Management</i>	EEC-V Powertrain Control Module
<i>Main Bearings</i>	5
<i>Valve Lifters</i>	Hydraulic Lash Adjuster with Roller Followers
<i>Valves per Cylinder</i>	3 (2 intake, 1 exhaust)
<i>Fuel Induction</i>	Sequential Multiport Fuel Injection
<i>Fuel Recommendation</i>	Regular Unleaded
<i>Exhaust</i>	Single Catalyst System
<i>Ignition System</i>	Coil on Plug
<i>Availability</i>	F-150, Super Duty, Navigator, Expedition

Table A.1: 5.4L 3V Engine Specifications

B: CELL#7 DYNAMOMETER SPECIFICATIONS

The specifications for the Cell #7 Dynamometer are given in *Table B.1: Cell #7 Dynamometer Specifications*:

<i>Location</i>	P.E.R.D.C., Cell #7
<i>Type</i>	FREC Dynamometer
<i>Manufacturer</i>	Meidensha Inc.
<i>Model</i>	FC95-355L
<i>Year Manufactured</i>	2001
<i>Base Speed</i>	2500/2647 rpm
<i>Maximum Mechanical Inertia</i>	3.0 kg ·m ² (inertia of Moment)
<i>Maximum Absorbing Power</i>	496 Hp
<i>Maximum Motoring Power (Continuous)</i>	355 Hp
<i>Maximum Absorbing Torque (Continuous)</i>	1413 N ·m
<i>Maximum Motoring Torque (Continuous)</i>	955 N ·m
<i>Maximum Speed</i>	8000 rpm

Table B.1: Cell#7 Dynamometer Specifications

C: CHARGE-TYPE ACCELEROMETER SPECIFICATIONS

The specifications for the charge-type accelerometers are given in *Table C.1: Charge-type Accelerometer Specifications*:

<i>Model & Serial Number</i>	Bruel & Kjaer Type 4366, #1105214
<i>Maximum Temperature</i>	250 °C; or 482°F
<i>Maximum Continuous Sinusoidal Acc. (Peak)</i>	20,000 m/s ² ; or 2000 g
<i>Typical Temperature Transient Sensitivity</i>	(Low Lim. Freq.: 3Hz) 0.1 m/s ² /°C; or 0.01 g/°C
<i>Typical Base Strain Sensitivity</i>	0.006 m/s ² /μstrain; or 0.0006 g/μstrain
<i>Reference Sensitivity at</i>	50 Hz at 23 °C
<i>Cable Capacitance</i>	115 pF
<i>Charge Sensitivity</i>	5.41 pC / m/s ² ; or 53.1 pC/g
<i>Voltage Sensitivity</i>	4.01 mV / m/s ² ; or 39.3 mV/g
<i>Capacitance (including cable)</i>	1351 pF
<i>Maximum Transverse Sensitivity</i>	2.2 %
<i>Weight</i>	30 grams
<i>Undamped Natural Frequency</i>	35 kHz
<i>Frequency Range</i>	1 to 10 kHz (+/- 1 dB)
<i>Polarity</i>	Is positive on the centre of the connector for an acceleration directed from the mounting surface into the body of the accelerometer.
<i>Resistance</i>	Minimum 20,000 MΩ at room temp.

Table C.1: Charge-type Accelerometer Specifications

D: ICP-TYPE ACCLEROMETER SPECIFICATIONS

The specifications for the ICP-type accelerometers are given in *Table D.1: ICP-type Accelerometer Specifications*:

<i>Model & Serial Number</i>	PCB Model#353B15, Serial#20455
<i>Temperature Range</i>	-65 / 250 °F
<i>Voltage Sensitivity</i>	9.72 mV/g
<i>Maximum Transverse Sensitivity</i>	1.9 %
<i>Undamped Natural Frequency</i>	80 kHz
<i>Frequency Range</i>	1 to 10,000 Hz (+/- 5%) 0.7 to 18,000 Hz (+/- 10%) 0.35 to 30,000 Hz (+/- 3 dB)
<i>Output Bias Level</i>	8.9 VDC
<i>Time Constant</i>	1.5 s
<i>Range</i>	+/- 500 g pk
<i>Broadband Resolution</i>	0.005 g RMS

Table D.1: ICP-type Accelerometer Specifications

E: ACCELEROMETER CALIBRATOR SPECIFICATIONS

The specifications for the calibration exciter are given in *Table E.1: Accelerometer Calibrator Specifications*:

<i>Make & Model</i>	Bruel & Kjaer Calibration Exciter Model #4294
<i>Frequency</i>	159.15 Hz +/- 0.02% (1000 rad/s)
<i>Acceleration</i>	10 m/s ² (RMS) +/- 3%
<i>Velocity</i>	10 mm/s (RMS) +/- 3%
<i>Displacement</i>	10µm (RMS) +/- 3%
<i>Warm-up time</i>	Less than 5 seconds
<i>Calibration Acceleration Result</i>	10.04 m/s ²

Table E.1: Accelerometer Calibrator Specifications

F: PROSIG ACQUISITION SYSTEM SPECIFICATIONS

The specifications for the PROSIG data acquisition system are given in *Table F.1:*

PROSIG System Specifications:

<i>Make & Model</i>	PROSIG Data Acquisition System, Model P5600
<i>Analog Inputs</i>	8
<i>Sampling Rate</i>	Up to 100 kHz per channel
<i>Internal Storage Capacity</i>	1,000,000 samples/channel
<i>Resolution</i>	16 bit
<i>Overall Accuracy</i>	+/- 0.10% full scale at gain < 1000
<i>Sensitivity</i>	+/- 300 μ V (gain = 1) +/- 0.3 μ V (gain = 1000)
<i>Input Voltage Range</i>	+/- 10 V to +/- 1.25 mV
<i>Input Impedance</i>	10 Mohm
<i>Communications</i>	High speed serial
<i>Signal Input</i>	Direct Voltage ICP
<i>Gain</i>	1 to 8000
<i>Anti-alias Filter</i>	Butterworth low pass, 48 dB/octave (160 dB/decade)
<i>Autozero</i>	Signal autozero and amplifier autozero
<i>Transducer Excitation</i>	10 V in 128 steps
<i>ADC</i>	16 bit ADC per channel
<i>Excitation Voltage</i>	Up to 10 VDC (30 mA)
<i>ICP</i>	4 mA @ 24 VDC
<i>Operating Temperature</i>	0 °C to 40 °C
<i>Control</i>	Mouse and keyboard from PC

Table F.1: PROSIG System Specifications

G: 8-CHANNEL CHARGE AMPLIFIER SPECIFICATIONS

The specifications for the charge amplifier / conditioner is given in *Table G.1: 8-Channel Charge Amplifier Specifications*:

<i>Make & Model</i>	Bruel & Kjaer, Model #5974 Charge Amp
<i>Input Type</i>	Grounded or Floating
<i>Maximum Input Level</i>	7 V RMS
<i>CMRR (100 Hz, floating inp. rel. to grnd.)</i>	> 40dB
<i>Input Sensitivity (+/-0.2 dB)</i> (output = 1 mv / 1 pC at 0 dB gain)	0.316 pC / m/s ² (30 dB gain) 1.00 pC / m/s ² (20 dB gain) 3.16 pC / m/s ² (10 dB gain) 10.00 pC / m/s ² (0 dB gain)
<i>High-Pass Filters (-1 dB)</i>	0.3, 1, 3, or 10 Hz
<i>Low-pass Filters (-1 dB)</i>	1, 5, or 10 kHz, or off (40 kHz)
<i>Integrator Gain (input sensitivity = 10 pC / m/s²)</i>	Velocity: 0 dB @ 16 Hz Displacement: 0 dB @ 4 Hz
<i>Integrator Lower Limiting Frequency</i>	1 Hz
<i>Fixed Output Calibration</i>	10 mV / m/s ²
<i>Output Impedance</i>	50Ω (100Ω with semi-floating output)
<i>Maximum Output Level</i>	7 V RMS
<i>Overload Level</i>	10.5 V Peak
<i>Channel Separation (10 kHz)</i>	> 80 dB
<i>Output Noise (0.3 Hz to 22 kHz, with shortened input)</i>	< 12 μV (0 dB gain) < 35 μV (10 dB gain) < 60 μV (20 dB gain) < 200 μV (30 dB gain)
<i>Accelerometer Input Connector</i>	TNC
<i>Signal Output Connector</i>	BNC

Table G.1: 8-Channel Charge Amplifier Specifications

VITA AUCTORIS

NAME: Bhaskar Ray
PLACE OF BIRTH: Oshawa, Ontario, Canada
YEAR OF BIRTH: 1976

EDUCATION: University of Windsor, Windsor, Canada
Bachelor of Applied Science (EE), 2002

University of Windsor, Windsor, Canada
Master of Applied Science (EE), 2007